M-AM-Sy1 CELLULAR RECOGNITION AND TRIGGERING BY MOBILE HAPTENS IN MODEL MEMBRANES. H. M. McConnell, J. W. Parce,* D. Hafeman,* J. T. Lewis,* and G. M. K. Humphries,* Dept. Chemistry, Stanford University, Stanford, CA 94305.

It has been known for a long time that a multiplicity of haptens, bound to a relatively rigid carrier such as a protein, can elicit a variety of immunoglobulin-dependent immune responses, whereas free haptens in solution do not. This has led to the view that multivalent hapten-mediated intermolecular cross-linked immunoglobulins provide unique efferent and afferent signals for the immune system. Our studies of complement and cellular immune responses to lipid bilayer membranes containing laterally mobile haptens provide another view of the critical molecular events involved in antibody-dependent immune responses. Thus, we have found that laterally mobile nitroxide spin-label lipid haptens in lipid vesicles and liposomes can trigger specific in vitro antibody-dependent immune responses of complement, neutrophils, and macrophages. (Dinitrophenyl-lipid haptens in liposomes can also stimulate a primary in vitro B cell response.) In these lipid systems the antibodies bound to mobile lipid haptens are randomly distributed on the vesicle membrane surface, and have effectively only intramolecular cross links. The antibodies are evidently "activated" by a conformational change upon binding to membrane-bound lipid haptens and then bind to and presumably activate Fc receptors on the neutrophils and macrophages. The trigger signal for cellular response may require subsequent lateral associations of activated Fc receptors as might be inferred from cellular triggering by insulin and Fc receptors in adipocytes, and mast cells[1,2].

1. C. R. Kahn, et al., Proc. Natl. Acad. Sci. USA 75, 4209-4213 (1978).
2. D. Segal, et al., Proc. Natl. Acad. Sci. USA 74, 2993-2997 (1977).
This work has been supported by the National Institutes of Health Grant 5R01 AI13587.

M-AM-Sy2 ENTRY OF SEMLIKI FOREST VIRUS INTO HOST CELLS. A. Helenius and K. Simons, European Molecular Biology Laboratory, Heidelberg, Federal Republic of Germany.

The initial event in the entry of viruses into cells is the attachment of the virus to the host cell surface. Animal viruses attach via an interaction of the viral surface proteins with specific receptors on the host cell membrane. Semliki Forest virus (SFV) is a simple membrane virus capable of infecting insect cells as well as most vertebrate cells in culture. The virus attaches to the cell surface by glycoprotein spikes (MW 110K) which extend 7-8 nm from the viral membrane. We have recently shown that SFV binds to the classical histocompatibility antigens on human and mouse cells (Proc. Nat. Acad. Sci. 75, 3846). These cell surface antigens present on the surface of nucleated cells (coded for by the H-2K and H2-D gene regions in mice and by the HLA-A and HLA-B regions in humans) show a high degree of homology in their amino acid sequences. It may well be that SFV recognizes a site common to all histocompatibility antigens. This would explain the wide host range of the virus. After binding to the host cell surface, the virus can be found attached to specialized coated indentations of the plasma membrane, coated pits which transform into coated endocytotic vesicles. The virus is rapidly internalized into coated vesicles at 37°. SFV seems to enter the cell mainly by this pathway. No evidence for entry through fusion with the cell surface has been found. Coated vesicles involved in receptor-mediated endocytosis are known to fuse with lysosomes. We are currently studying whether the coated vesicles with the virus follow this route and how the virus nucleocapsid is released into the cytoplasm of the cell to initiate infection.

M-AM-Sy3 ONE RHODOPSIN ACTIVATES MANY PHOTORECEPTOR ESTERASE MOLECULES BY LATERAL DIFFUSION. P. A. Liebman, University of Pennsylvania, Dept. of Anatomy, Philadelphia, PA 19104.

Rod "quantal vision" requires photon detection by one rhodopsin molecule followed by rapid amplification and communication between separate rod disk and plasma membrane through a soluble intracellular transmitter. Identification of light sensitive cyclic nucleotide phosphodiesterase (PDE) in rods by other laboratories led us to seek quantitative information that might implicate it in control of such a transmitter. We study kinetics of hydrolysis of substrate 3'-5' cyclic guanosine mononucleotide (cG) by PDE bound to suspensions of bovine rod disk membrane vesicles via H^+ recording methods. Our studies show that all PDE's on a vesicle can be activated by a single photon. The resultant cG turnover is so large that many PDE molecules must be activated per photon (Yee and Liebman, J.B.C., in press). Amplification from one light quantum to many enzyme quanta is associated with a time delay suggesting a mechanism whereby a single hit rhodopsin molecule laterally diffuses in the disk to serially carry its message to nearby PDE's while multiple light quanta yield quicker but no greater activation than one. These results are predicted (Liebman and Pugh, Vis. Res., in press) by calculations based on our previously published measurement of rhodopsin diffusion coefficient in disk membrane (Science 185:457-459). Activation also requires GTP cofactor. This seems to mediate a short lived (~1 sec) memory of activation which permits temporal summation of the serial molecular activations. Deactivation utilizes ATP cofactor via a phosphate transfer reminiscent of opsin kinase activity. The two stages of gain (PDE activation and fast cG turnover no.) provide enough sensitivity, gain, speed and control of a soluble "transmitter" to mediate visual excitation. Our molecular model of excitation, though far more complicated than previous ones and perhaps still incomplete, contains several important lessons in cell biology and suggests tests to mediate rapid self-correction. EY00012,EY01583.

M-AM-Sy4 MATING RECEPTORS FOR THE SEXUAL RESPONSE OF CHLAMYDOMONAS. U.W. Goodenough, W.S. Adair, E. Caligor, and J.L. Hoffman, Department of Biology, Washington University, St. Louis, Mo. 63130.

The sexual response of the unicellular eukaryote, Chlamydomonas reinhardi, is mediated by its two flagella. The flagellar membranes of the two mating types, mt^+ and mt^-, first recognize each other and agglutinate together. This agglutination transmits a "signal" to the cell body to initiate sexual fusion, and fusion is accompanied by a "reverse signal" which results in the disadhesion of the interacting flagella. The entire mating sequence can occur within 30 sec and appears independent of hormonal mediation; therefore, information is apparently conveyed via a sequence of precise membrane-membrane interactions. Experiments are described that probe the nature and mode of action of the membrane components involved in sexual recognition, sexual adhesion, and sexual signaling. Antibody cross-linking of surface components is shown to accurately mimic the sexual reaction in mutant strains lacking functional agglutinins, and tubulin-like membrane polypeptides appear to participate in the generation of the signal.

M-AM-A1 TRANSIENT ELECTRIC BIREFRINGENCE OF T7 PHAGE DNA. Donald C. Rau* and Victor A. Bloomfield (Intr. by R. K. Herman), Dept. of Biochemistry, Univ. of Minnesota, St. Paul, MN 55108.

We have examined the electric birefringence of T7 DNA in the Kerr region. The decay kinetics are consistent with a bead and spring model for a flexible polymer and an induced dipole orientation mechanism. In order to account satisfactorily for the observed differences in rise and decay kinetics, we postulate an electrically induced restoring force. The magnitude of the induced dipole is inversely porportional to the Debye-Hückel shielding parameter, κ, and proportional to the square of the net effective DNA charge density. These observations are consistent with an asymmetric ion atmosphere flow mechanism of orientation.

M-AM-A2 CATION-INDUCED COLLAPSE OF DNA. Robert Wilfred Wilson* and Victor A. Bloomfield, Dept. of Biochemistry, Univ. of Minnesota, St. Paul, MN 55108.

DNA from T7 bacteriophage can be transformed from an extended, random coil form to a compact form in the presence of multivalent cations. This transition can be monitored, at the low concentrations required for monomolecular collapse, using laser light scattering detected by photon counting. Collapse has been observed in aqueous solutions of the polyamines spermidine and spermine as a function of $[Na^+]$ and $[Mg^{++}]$, and in 50% methanol:water mixtures with Mg^{++} alone as well as with the polyamines and univalent cations. Examination of the cation concentrations required for collapse, in the light of Manning's theory of counterion condensation of linear polyelectrolytes, yields a striking regularity: DNA collapse occurs, regardless of the cation composition, whenever its linear charge density is about 80% neutralized. Electron microscopy and quasielastic light scattering determination of the diffusion coefficients of the collapsed DNA indicates that it generally has a radius comparable to the radius of the T7 phage head. However, larger structures are sometimes seen, and circular dichroism spectroscopy indicates that the specific structure of the particles depends on the cations that cause the collapse.

M-AM-A3 CIRCULAR DICHROISM AND DNA SECONDARY STRUCTURE. W. A. Baase* and W. C. Johnson, Jr. Department of Biochemistry and Biophysics, Oregon State University, Corvallis, OR 97331.

The change in average rotation of the DNA helix has been determined for the transfer from 0.05 M NaCl to 3.0 M CsCl, 6.2 M LiCl and 5.4 M NH_4Cl. This work, combined with data at lower salt from other laboratories, allows us to relate the intensity of the CD of DNA at 275 nm directly to the change in the number of base pairs per turn. The change in secondary structure for the transfer of DNA from 0.05 M NaCl (where it is presumably in the B-form) to high salt (where the characteristic CD has been interpreted as corresponding to C-form geometry) is found to be -0.22 (± 0.02) base pairs per turn. In the case of mononucleosomes, where the CD indicates the "C-form", the change in secondary structure (including temperature effects) would add -0.31 (± 0.03) turns about the histone core to the -1.25 turns estimated from work on SV40 chromatin.

M-AM-A4 THERMODYNAMIC PROPERTIES OF DNA AT INTRACELLULAR CONCENTRATIONS. A. A. Brian*, L. S. Lerman, and H. L. Frisch, Center for Biological Macromolecules, State University of New York, Albany, N.Y., 12222.

In order to determine the interaction between DNA molecules in solution at small distances we have examined the thermodynamic properties of solutions of DNA at intracellular concentrations, i.e., on the order of 10 volume per cent, by analysis of the sedimentation equilibrium of sonicated DNA. The behavior of such extremely concentrated solutions is non ideal. Rather than showing the usual exponential dependence on $\omega^2 r^2$, the distribution of molecules in the centrifugal field increases sharply with increasing radius then levels off. Where the concentration reaches a critical, temperature insensitive value, a phase transition occurs, seen in the centrifuge as an abrupt change in the optical properties of the solution. The calculated osmotic pressure rises steeply with DNA concentration in the pretransition region, and if a virial expansion is applied, higher order terms dominate, indicating a significant contribution by many-body interactions. We have modeled the solution of DNA molecules as a system of hard, rigid spherocylinders and have applied the scaled particle theory of fluids to the system below the critical concentration. The spherocylinder diameter is given by the van der Waals molecular diameter plus a contribution from the electrostatic potential, which is approximated by a hard core potential. The equation of state from scaled particle theory can be written solely in terms of the particle axial ratio and the second virial coefficient. Both can be determined in the same experiment. We attribute the phase transition to an order → disorder transition, similar to the one that occurs in concentrated solutions of tobacco mosaic virus.

M-AM-A5 LINEAR DICHROISM OF DRUG-DNA COMPLEXES. Patrick E. Lorenz* and Anne K. Krey, Department of Molecular Biology, Walter Reed Army Institute of Research, Washington, DC 20012

Binding of chemotherapeutic drugs and dyes to their bioreceptor DNA, customarily studied by a variety of conventional biophysical means, has in the present work additionally been investigated by an electro-optical technique. This technique orients DNA with the long axis of the double helix approximately parallel to the applied electric field. Bound drugs exhibit under such conditions characteristic dichroic effects. The effects observed for quinacrine and chloroquine suggest a direction of the drugs' 2 longest-wavelength absorption moments perpendicular to the DNA axis in agreement with the substances' intercalation between adjacent base pairs of DNA. In contrast, non-intercalative distamycin showed dichroism indicative of slightly different orientations for the transition moments of the antibiotic's 3 individual N-methylpyrrole chromophores with a composite moment directed more parallel to DNA's helix axis. Titrations, monitored by electric dichroism, yield the maximum stoichiometry of 1 quinacrine or chloroquine intercalated per approximately 2 base pairs of DNA; for distamycin, such titrations suggest a binding of 1 antibiotic molecule attached per approximately 6 A·T pairs. Finally, methylene blue exhibited, as single DNA-intercalated molecules, dichroic effects indicating 2 intra-chromophoric-ring-system transitions while effects for bound dye aggregates suggest an orientation of externally bound dye molecules that is different from the direction of methylene blue in the intercalation complex. The results of these dichroism studies provide a more definitive description of the structural and electronic properties of molecular drug-DNA complexes than do the conventional spectrophotometric and hydrodynamic techniques.

M-AM-A6 DIRECT RELATIONSHIP BETWEEN ACRIDINE ORANGE UPTAKE AND NUCLEAR MORPHOMETRY IN CYCLING VERSUS CONFLUENT HUMAN FIBROBLASTS. M. Grattarola, F. Beltrame, S. Lessin* and C. Nicolini, Division of Biophysics, Temple University, Philadelphia, PA 19140.

WI-38 human diploid fibroblasts have been grown up to 18 days into *"deep"* confluency with weekly changes of the medium. Two parameter flow microfluorimetry of WI-38 cells stained with Acridine Orange (Nicolini, et al., J. Histo. Cytochem. 1978) shows that one day after plating, we obtain a log-phase distribution for the green fluorescence with a population of cells having the same scatter (respect to G1) but quite lower chromatin primary sites (green fluorescence) and lower amount of RNA (red fluorescence). This subpopulation, likely relating to *non-cycling G0 cells* (that, after plating, even if adherent to the plastic, did not start growing), drastically reduces at 4 days (5%) and then progressively increases at 6 days (30%) and 18 days (up to 95%) at the expenses of progressively decreasing G1 peak. Nuclear morphometry, carried out by a Quantimet Image Analyzer, on Feulgen-stained smears from the same populations yield a fraction of cell (G0) having respect to G1 the same DNA (IOD) and quite larger chromatin condensation (larger average optical density) and more circular geometry (larger form factor), in striking agreement with AO uptake. These findings are compatible with previous observation using Ethidium Bromide, that the *transition* between a proliferating *G1* and non-proliferating *G0* cells is *not a continuum* change, but rather a reversible *quantum jump in chromatin organization.* In separate experiments we have maintained WI-38 for 7 days after confluency in medium, either with or without serum; nuclear morphometry and AO uptake studies of cells still adherent to the plastic indicate identical chromatin organization in situ both for *"starved"* unhealthy (irreversibly out of cycle) and *"deeply confluent"* healthy (reversibly out of cycle) WI-38 cells.

(This work was supported by NIH grants CA18258 and CA20034).

M-AM-A7 CHROMATIN STRUCTURE BY DIGITAL ANALYSIS OF LIGHT MICROSCOPY IMAGES. F. Beltrame* and C. Nicolini, Division of Biophysics, Temple University, Phila., PA 19140.

Monodimensional digital techniques are applied to analyze cross-sections of *nuclear images* from synchronized HeLa S3 cells, *Feulgen-stained* at 0 hr (Mitosis), 3 hrs (middle G1) and 8 hrs (early S) after selective mitotic detachment.

The image cross-sections are acquired through a Zeiss Ultraphot microscope on line with a Quantimet 720-D Image Analyzer interfaced to a PDP11/40.

We investigate chromatin-DNA morphometry by means of digital *cross-correlations*, implemented through the Fast Fourier Transform Algorithm, between different scan lines of the image either parallel or orthogonal to each other, each of these 256 picture points long and averaged 100 times in order to enhance the signal to noise ratio. We report the observation of correlation patterns, which are independent of cell-orientation, but quite different between cells in middle G1, early S and M phases.

Similar analysis conducted on peripheral and central scan lines of the same nuclei confirm the existence of *DNA patterns unique for each cell cycle phase* and compatible with the higher order chromatin structures appearent by "freeze-fracture" and "wet replica" electron microscopy. (See "Chromatin Structure and Function", editor, C. Nicolini, Plenum Publishing Co., NATO-ASI Series, 1978).

Complete images, acquired in two dimensions, reproduce also specific optical density patterns depending on cell cycle phases: i.e., middle G1 cells consistently show periodic spikes along the nuclear border, while mitotic cells do *not*.

Data is interpreted in terms of an ordered "*drapery-like*" quinternary structure for chromatin-DNA in situ, which modulates during the cell cycle.

(This work was supported in part by NIH Grant #CA20034).

M-AM-A8 A STUDY ON THE CONFORMATIONAL STATES OF CORE HISTONE COMPLEXES. A.W. Fulmer* and G.D. Fasman, Brandeis University, Waltham, MA 02154.

The core histone complex (H3:H4:H2A:H2B) and products of dissociation, H3:H4 tetramer and H2A:H2B dimer, were isolated from chicken erythrocyte chromatin by extraction with aqueous solutions of varying high ionic strength at pH 8. The conformational and oligomeric characteristics of these histone complexes were compared to analogous histone complexes prepared by renaturation of acid extracted histones by circular dichroism (CD) and analytical gel filtration chromatography. The salt extracted core histone complex and the purified dissociation products, H3:H4 tetramer and H2A:H2B dimer, differ in conformation to analogous histone complexes prepared by renaturation in 2 M NaCl, pH 7. The native core histone complex is isolated by 2 M NaCl extraction in a metastable state. Irreversible relaxation from this metastable state by cycling through solvents of low ionic strength or pH is triggered by the irreversible relaxation of salt extracted H3:H4 tetramer. Salt extracted H2A:H2B dimer spontaneously relaxes from the native state. The relaxation of salt extracted H2A:H2B is reversed in the presence of salt extracted H3:H4. The relaxed states of salt extracted histone complexes appear to be identical to the conformational states obtained upon renaturation of acid extracted histones. Quantitative analysis of CD changes upon conformational relaxation indicate a loss of β-sheet accompanied by an increase in α-helix. These estimates are in good agreement with regions of histone primary structure predicted to undergo α-helix⇄β-sheet interconversions. The relaxed α-helix rich conformational state of the core histone complex shows a decreased tendency to associate to higher oligomers (e.g., hexamers, octamers) than the metastable β-sheet rich conformational state. These two different conformational states of the core histone complex result in physically distinguishable nucleoprotein upon reconstitution with DNA. Supported by N.I.H., Amer. Cancer Soc., and D.O.E.

M-AM-A9 THERMAL DENATURATION OF CHICKEN ERTHYROCYTE CORE PARTICLES IN 1 mM CACODYLATE BUFFER. J.C. Kent,* B. Ramanathan,* and K.S. Schmitz, Department of Chemistry, University of Missouri-Kansas City, Kansas City, Missouri 64110.

Weischet et al. (Nucl. Acids Res. 5, 139 (1978)) reported circular dichroism (CD), optical absorbance, and excess heat capacity studies on chicken erythrocyte core particles in 1 mM cacodylate buffer. The results of this study indicate the thermal profiles of $\Delta h/\Delta T$ (h=hyperchromicity) and excess heat capacity suggest two transitions, a broad transition (5-10°) followed by a very sharp transition (T_m ~74°C). The CD data also exhibited two maxima, but the onset of $(\Delta\theta/\Delta T)_{273}$ (i.e. DNA contribution) occurs ~20°C before any change in optical absorbance. We have examined this "premelt" transition in the temperature range 30-49°C by the methods of conductivity, viscosity, quasielastic light scattering and fluorescence of bound proflavin. The following model appears to be consistent with the data: 1) below 35°C the core particle is in an apparent elongated shape; 2) in the region 35-45°C the DNA tertiary conformation changes and ions from the solution are absorbed resulting in a more compact or spherical shape for the core particle; 3) the broad melting region corresponds to denaturation of DNA and a release of counter ions; 4) finally the core particle structure completely dissociates in the sharp melting region. This research was supported in part by grants from NSF (PCM 7622073) and NIH (GM 24346).

M-AM-A10 ORGANIZATION OF INACTIVE CHROMATIN AND CHROMATIDS. S. Basu, Division of Laboratories and Research, New York State Department of Health, Albany, NY 12201.

The highest ordered structure of the nucleosome filament in wet, unstained and unfixed inactive chromatin (e.g. chicken erythrocytes and rat liver) is a second-order superhelical organization (supersolenoid) whose width, pitch and the DNA compaction ratio are respectively in the ranges of 0.15-0.2 μm, 50-150 nm and 1500-2000. This superstructure is preserved preferentially in non-ionic wetting solvents but decondenses in ionic solvents and under denaturing conditions into its lower-order form which is basically a solenoidal coil (width 30-35 nm) of the nucleosome filament. Owing to torsional convolutions (via sharp bends and kinks) the axial symmetry of the solenoidal coil is lost. The loosened solenoidal turns then resemble unstretched 'superbeads.' Strikingly, in dividing cells the chromatid structure of prometaphase and metaphase chromosomes (chinese hamster) is not represented by a further supercoiling of the 0.2 μm (diam.) supersolenoid. The chromatid arrangement primarily involves the decondensed forms, i.e. the 30-35 nm diam. solenoid and the nucleosome filament. The multiple number of 20-30 nm diam. fibrils at the chromosome constriction, the chromosome surface characteristics and the small degree of DNA orientation across each chromatid as determined by optical studies of the same chromosomes suggest that the unineme chromatid must have a distinctive arrangement of the nucleosome filament. The latter unravels at least twice or more while passing through the centromere and then quite unevenly up and down each chromatid. In both arms of the chromatid, the nucleosome filament describes alternate longitudinal orientations and extensive side-loops which then supercoil into the solenoidal form. This arrangement also reveals itself, but partially, in banded chromosomes and in transmission images of dried chromosomes.

M-AM-A11 LOCALIZATION OF CONCANAVALIN A BINDING SITES IN POLYTENE CHROMOSOMES. P. D. Kurth, E. N. Moudrianakis, and M. Bustin*. Laboratory of Molecular Carcinogenesis, National Cancer Institute, National Institutes of Health, Bethesda, Md. 20014.

It has recently been demonstrated that the plant lectin, concanavalin A, binds specifically to 3 non-histone chromosomal proteins found in rat liver chromatin (Rizzo and Bustin, J. Biol. Chem. 252, 7062, 1977). This suggested the feasibility of using concanavalin A in a manner analogous to antibodies as a specific reagent for localizing chromosomal glycoproteins in the polytene chromosomes of the midge, Chironomus thummi. Fluorescein- or ^{3}H-labelled concanavalin A were found to bind specifically and with a reproducible fluorescent pattern to chromosomes prepared by formaldehyde fixation, but not to chromosomes prepared by the standard acetic acid treatment. Specificity was ascertained by incubation with the appropriate sugars and with unlabelled concanavalin A. Concanavalin A binds specifically to selected bands of the chromosome, suggesting a possible functional role for the glycoprotein(s). Indeed, a correlation was found between the degree of puffing and the intensity of fluorescent staining in the Balbiani rings of the fourth chromosome--demonstrating that lectins can be used to study the correlation between functional and structural changes in polytene chromosomes.

M-AM-A12 DISSOCIATION OF ACTINOMYCIN D FROM POLY(dG-dC)·POLY(dG-dC) AND NATURAL DNA. J. W. Hook III,* M. Petersheim,* S. Lin, and T. R. Krugh, Department of Chemistry, University of Rochester, Rochester, N.Y. 14627.

The sodium dodecyl sulfate (SDS) induced dissociation of actinomycin D from poly(dG-dC)·poly(dG-dC) has been studied as a function of the nucleotide/actinomycin D ratio. At high ratios of nucleotide/actinomycin D (ie, in the presence of excess binding sites) the dissociation of actinomycin D is adequately described by a single exponential relaxation, with a lifetime of 950 sec. This result is in contrast to the multiple exponential decays observed for the dissociation of actinomycin D from DNA [W. Müller and D. M. Crothers J.Mol.Biol. 35, 251-290 (1968)]. The dissociation of actinomycin D from poly(dG)·poly(dC) is adequately described by two exponential relaxations. These results suggest that the multiple relaxation processes observed for the dissociation of actinomycin D from DNA are due to heterogeneity in the actinomycin D binding sites, and not to multiple decay pathways, as suggested by Müller and Crothers. In the kinetic experiments with poly(dG-dC)·poly(dG-dC) we have also observed that the apparent actinomycin D dissociation lifetime is a function of the nucleotide/actinomycin ratio. At saturation binding levels ($\sim$8 nucleotides/actinomycin) the lifetime of the bound actinomycin D molecules increases to approximately 2100 seconds. A detailed analysis of the relaxation curves for the dissociation of actinomycin D from poly (dG-dC)·poly(dG-dC) at or near saturation of the polymer provides evidence for the mutual interaction of actinomycins bound at adjacent sites on the polymer. (This work was supported by research grant CA-14103 from the National Cancer Institute).

M-AM-A13 KINETICS OF ISOTOPIC HYDROGEN EXCHANGE AT THE 8-C POSITION IN GUANINE NUCLEOTIDES DETERMINED BY RAMAN SPECTROSCOPY. M. Lane*and G.J. Thomas, Jr., Department of Chemistry, Southeastern Massachusetts University, North Dartmouth, MA 02747.

Pseudo-first-order rate constants (k_ψ) governing deuterium exchange of the 8-CH groups of guanosine-5'-monophosphate (5'-rGMP) and guanosine-3':5'-monophosphate (cGMP) were determined over the temperature range 30 to 90°C on neutral D_2O solutions of the nucleotides. Rate constants were evaluated from quantitative measurement of the intensity decay of the purine ring vibrational frequency ca. 1480 cm^{-1}. For both 5'-rGMP and cGMP the logarithm of the rate constant exhibits strictly linear dependence on reciprocal temperature. The activation energy, E_a, and frequency factor, A, in the expression $\ln k_\psi = \ln A - Ea/RT$ are, respectively, 24.6 kcal/mole and 9.25 x $10^{14}sec^{-1}$ for 5'-rGMP, and 24.2 kcal/mole and 3.52 x $10^{13}sec^{-1}$ for cGMP. Exchange is thus consistently more rapid in nucleotides of guanine than of adenine at the same experimental conditions [cf. Biochemistry 14, 5210 (1975)]. One interpretation of these results is that the electron charge distribution in the imidazole moiety of the purine ring is highly sensitive to the external substituents at the 2-C and 6-C ring positions. Spectral effects of the deuterium exchange (and hydrogen back-exchange) also suggest a number of new assignments for the guanine nucleotides.

Supported by Public Health Service Grant AI 11855-04.

M-AM-A14 ^{31}P-NUCLEAR MAGNETIC RESONANCE CHARACTERISTICS OF SOME ADENYLYL PHOSPHONATE ANALOGS. C.T. Burt, L.H. Schliselfeld, T. Myers* and R.J. Labotka*, University of Illinois Medical Center, Department of Biological Chemistry, 1853 W. Polk St., Chicago, Ill. 60612

Diphosphonate analogs of ATP and ADP are important tools in studies of muscle contraction and protein synthesis. We have employed ^{31}P-NMR to study the behavior and structure of α,β-methylene ADP ($Ap(CH_2)p$), α,β-methylene ATP ($Ap(CH_2)pp$), and β,γ-methylene ATP ($App(CH_2)p$). In the absence of divalent metal ions the chemical shifts of the two phosphorus atoms bound directly to the methylene group move during titration in opposite directions. This is in contrast to ATP and β,γ-imido ATP whose phosphorus chemical shifts move downfield or show no significant change as the pH rises from 3 to 11. Addition of Mg^{2+} to $App(CH_2)p$ at pH 7 causes an initial loss of peak height for the β- and γ-phosphorus atoms, but normal peak heights are restored at $[Mg^{2+}]$:$[App(CH_2)p]$ molar ratios of 0.50. Further titration of $App(CH_2)p$ with Mg^{2+} causes the chemical shift values to move for the β- and γ-phosphorus atoms, and suggests a maximum binding of 1.0 mole Mg^{2+} to 1.0 mole $App(CH_2)p$. Using the changes in chemical shift values with increasing pH, the pK'_a values of the phosphoryl groups can be determined. The table below summarizes some of the results:

Analog	Peak	Δδ	pK'_a	Direction change	Peak	Δδ	pK'_a	Direction Change
$Ap(CH_2)p$	α	4.02	8.31	downfield	β	3.59	8.27	upfield
$Ap(CH_2)pp$	α	1.09	7.56	downfield	β	1.00	7.68	upfield
$App(CH_2)pp$	β	5.68	8.27	downfield	γ	3.22	7.96	upfield
$App(CH_2)pp{\cdot}Mg^{2+}$	β	5.83	4.93	downfield	γ	4.47	4.35	upfield

(Sponsored by NIH-HL 18179-09 and the Chicago Heart Association).

M-AM-B1 EFFECTS OF THE ANTIBIOTIC BEAUVERICIN ON THE IONIC PERMEABILITY OF LIPID BILAYERS IN THE PRESENCE OF ALKALINE EARTH CATION ELECTROLYTES. S. Ciani and S. Pajong*, Physiol. Dept., UCLA Medical School, Los Angeles, CA 90024.

The cyclic antibiotic beauvericin increases the conductance of GMO bilayer membranes in the presence of the nitrate salts of Ca, Sr, Ba. The zero-voltage conductance, G(0), is a linear function of the salt concentration and a higher than second power function of the aqueous antibiotic concentration (e.g., in 0.1 M $Ca(NO_3)_2$, G(0) increases from 10^{-5} to $2.2 \cdot 10^{-4}$ ohm^{-1}cm^{-2} for a variation of the beauvericin concentration from 10^{-6} to $3 \cdot 10^{-6}$ M). This finding, along with similar ones when the antibiotic is dissolved in the membrane-forming solution, suggest that more than one beauvericin molecule is involved in the ion-carrier complex formation. The conductance, G(V), increases with voltage, and the conductance ratio, G(V)/G(0), can be described by the Nernst-Planck equation generalized to allow for a trapezoidal energy barrier. Dilution potentials for all the three salts show Nernst slopes for monovalent cations, suggesting that singly charged ion pairs (e.g., $CaNO_3^+$) are probably the charged species transported across the membrane. In mixtures of nitrates, the potential is described by the Goldman equation, again for univalent cations, with permeability ratios, $P_{Ba}:P_{Sr}:P_{Ca} = 1:1.1:40$. When the concentration of $CaCl_2$ is the same on both sides and $Ca(NO_3)_2$ is added to one side, potential measurements give a permeability ratio which increases proportionally to the $CaCl_2$ concentration (e.g., $P_{Ca(NO_3)_2}/P_{CaCl_2}$ varies from 3.3 to 40 for an increase of $CaCl_2$ from 10^{-2} to 10^{-1} M). This result can be accounted for considering that $Ca(NO_3)_2$ is partially associated in aqueous solutions ($K = [Ca^{++}][NO_3^-]/[CaNO_3^+] \simeq 0.5$ M), and assuming that beauvericin binds the ion pair $CaNO_3^+$.
Supported by USPHS (NS 13344).

M-AM-B2 ION TRACER FLUXES THROUGH GRAMICIDIN A MODIFIED LIPID BILAYERS. J. Procopio* and O. S. Andersen, (Intr. by C. M. Connelly), Dept. Physiology and Biophysics, Cornell University Medical College, New York, N. Y. 10021.

22-Na^+ and 137-Cs^+ fluxes have been measured in gramicidin A modified diphytanoylphosphatidylcholine/n-decane bilayers. Na^+ fluxes were determined in 0.1 M, 1.0 M, and 5.0 M NaCl. The correlation factor, f, the exponent, n, of the modified Ussing flux-ratio equation, and the transference number, t^+, were all within experimental accuracy, found to be equal to 1.0. (For technical reasons only f could be determined in 5.0 M NaCl.) That is, there are no detectable interactions among Na^+ moving through the channels. These results are consistent with the notion that at most one Na^+ can occupy the channel at attainable aqueous concentrations, but they cannot exclude the possibility of multiple ion occupancy in an "equilibrium" channel. Cs^+ fluxes have been determined in 0.1 M and 1.0 M CsCl. We find that t^+ again is equal to 1.0, within experimental accuracy, while both f and n differ significantly from unity. In 0.1 M CsCl $n \simeq 1.4$ and $f \simeq 0.7$, in 1.0 M CsCl, $n \simeq 1.6$ and $f \simeq 0.6$. There is thus, clear evidence for multiple ion occupancy with Cs^+, but our results do not at present allow us to distinguish between a 2-site channel and a 4-site channel. These results are qualitatively similar to those reported by Schagina et al. (Nature, vol. 273, p. 243, 1978) for Rb^+-fluxes.
Supported by NIH Grant #GM21342. J. P. is the recipient of a FAPESP Fellowship, O. S. A. is a N. Y. Heart Association Senior Investigator.

M-AM-B3 THE KINETICS OF NA^+ MOVEMENT THROUGH GRAMICIDIN A CHANNELS. O. S. Andersen and J. Procopio*, Dept. Physiology and Biophysics, Cornell University Medical College, New York, N. Y. 10021

I/V characteristics of gramicidin A (Gram A) single channels in diphytanoylphosphatidylcholine/n-decane bilayers have been studied at NaCl concentrations from 0.02 M to 5.0 M. At low salt concentrations the I/V characteristics tend to be saturating, at high salt concentrations ($\geq$ 1.0 M) they are superlinear. These results suggest that the rates of the association/dissociation reactions between Na^+ and Gram A are of the same order of magnitude as the rate of ion translocation through the channel. That is, the channel is not an "equilibrium" channel. As there are no detectable interactions among Na^+ in the channel (Procopio and Andersen), the data (for $C \leq 1.0$ M and $V \leq 300$ mV) have been analyzed in terms of a two-site-one-ion model with Eyring-type barriers. The activity for half-maximal conductance is 0.14 M at 25 mV and 0.36 M at 300 mV. The rate constant for ion entry into the channel is $\simeq 1 \times 10^{-16}$ liter/(channel x sec), the rate constant for ion exit is $\simeq 2 \times 10^7$ ions/(channel x sec), and the rate constant for translocation through the channel is $\simeq 1 \times 10^7$ ions/(channel x sec). About 80% of the applied potential falls across the middle barrier. It thus appears that the Gram A channel is not an "equilibrium" channel with respect to Na^+. I/V characteristics at NaCl concentrations above 1.0 M cannot be fitted satisfactorily to the present model. We do not believe that these deviations represent multiple ion binding to the channel.
Supported by NIH grant #GM21342. O. S. A. is a N. Y. Heart Association Senior Investigator, J. P. is the recipient of a FAPESP Fellowship.

M-AM-B4 MEASUREMENTS OF ELECTRICAL CAPACITANCE AND CONDUCTANCE OF LIPID BILAYER MEMBRANES IN THE PRESENCE OF TIME DEPENDENT IONIC CURRENT. S. Takashima, Department of Bioengineering D2, University of Pennsylvania, Philadelphia, PA 19104.

Capacitance and conductance of lipid bilayer membranes have been measured carefully by several investigators. However, in biological membranes, similar measurements often have to be performed in the presence of time dependent non-linear ionic currents. Results of admittance measurements indicate the presence of three components in nerve membranes, i.e., capacitive, conductive and inductive components. They are all frequency and voltage dependent. However, the origin of these components, in particular, inductive component is not well understood. In this experiment, capacitance and conductance of egg lecithin bilayer membrane were determined in the presence of alamethicin which induces a time dependent non-linear current. Without alamethicin, lecithin bilayers have a capacitance of 0.6-0.65 μF/cm^2 with an exceedingly high D.C. resistance. This capacitance is independent of frequency unlike that of squid axon membrane. If alamethicin is added at the concentration of about 10^{-7} mol/l on one side of the membrane in the bathing solution, and admittance measurements are performed during depolarizing square pulses, we observe a nonlinear increase in conductance as has been suggested by voltage clamp experiments with this system. In addition to the increase in conductance, we found a marked decrease in the apparent capacitive component. The decrease is strongly dependent on frequency and voltage and increased progressively as the frequency decreased. This behavior is quite similar to the inductive component found by Cole and Curtis in squid axon membrane. The inductive component was also observed even without depolarizing pulses if an excess amount of alamethicin was added in the bathing solution.

M-AM-B5 THE EFFECT OF DIELECTRIC CONSTANT ON THE CONDUCTANCE OF LIPID BILAYERS. James Dilger and Stuart McLaughlin, Dept. of Physiology and Biophysics, HSC, SUNY, Stony Brook, N.Y. 11794.

The weak acid DTFB (5,6-dichloro-2-trifluoromethylbenzimidazole) transports protons across artificial bilayers and, in accordance with the chemiosmotic hypothesis, acts as an uncoupler of oxidative phosphorylation in mitochondria. In bilayers containing decane, the charged permeant species is an HA_2^- complex formed between the neutral HA and anionic A^- forms of the weak acid. At physiological pH, the proton conductance increases quadratically with [DTFB]. In mitochondria, however, the rate of oxygen consumption increases linearly with [DTFB]. These observations can be reconciled with the chemiosmotic hypothesis by postulating that the proteins in the inner mitochondrial membrane raise the average dielectric constant of the lipid bilayer matrix. The Born energy for the A^- species to enter the membrane would thus be reduced by a greater amount than the Born energy for the HA_2^- species to enter the membrane. To demonstrate the effect of dielectric constant on ion permeability, phosphatidylcholine (PC) bilayers were formed with either decane or 1-chlorodecane, a more polar solvent. The specific capacitance of PC/decane bilayers is .39μF/cm^2, whereas the specific capacitance of PC/chlorodecane bilayers is significantly higher, .73μF/cm^2. This is presumably due to the higher dielectric constant of PC/chlorodecane bilayers. The proton conductance produced by DTFB in PC/chlorodecane bilayers is enhanced two orders of magnitude over that in PC/decane bilayers. Also, there is a linear relationship between proton conductance and [DTFB] with the PC/chlorodecane bilayers. Supported by NSF grant PCM76-04363 to S. McLaughlin.

M-AM-B6 MECHANISM OF THE COMPRESSION OF BLACK LIPID MEMBRANES BY AN ELECTRIC FIELD. Stephen H. White, Dept. of Physiology, Univ. of Calif., Irvine, CA 92717.

Transmembrane electric fields decrease the thickness of planar bilayer membranes (black films) by displacing alkane solvent from the bilayer into the annulus (torus) and microlenses [Requena et al (1975). Biophys. J. 15:77]. I report here the mechanism underlying this effect. The electric field produces an electrostrictive increase in the pressure (P) acting on the alkane molecules in the bilayer but not in the annulus. This raises the chemical potential of the alkane in the bilayer relative to the annulus. Since the bilayer alkane must remain in equilibrium with the annulus alkane, the bilayer alkane concentration decreases to reduce the chemical potential to the annulus value. The consequent decrease in bilayer thickness would be small if the alkane formed an ideal solution with the bilayer. However, the bilayer solution is highly non-ideal as can be found by controlling the activity of n-decane in the torus of glyceryl monooleate bilayers using squalene which is insoluble in the bilayer [White (1978). Biophys. J. 23:337]. The relation between torus decane mole fraction (X_{DEC}) and bilayer thickness is shown in the figure. This figure is equivalent to a vapor pressure-composition diagram for the black film. Note that large changes in thickness occur for relatively small changes in X_{DEC}. Thus, small changes in alkane chemical potential have large effects on thickness. Research supported by the NIH (NS-10837, NS-00146) and the NSF (PCM76-20691).

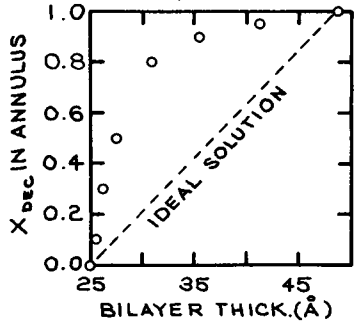

M-AM-B7 PHOTO-ISOMERIZATION INDUCED VOLTAGE TRANSIENTS IN BILAYER MEMBRANES. J.S. Huebner, J.R. Duchek*, D.L. Jonan*, R.J. Koftan*, L.A. Thompson*, and W.E. Varnadore*, Department of Natural Sciences, University of North Florida, Jacksonville, FL. 32216.

Azo and cyanine dyes, which are known to photo-isomerize, induce transmembrane voltage transients when added to one side of a bilayer membrane and illuminated, while cyanine dyes which are sterically hindered from isomerization do not. More than 120 dyes (mostly cyanine dyes) have been studied. A theory correlating the physical movement of membrane sorbed dye to the observed voltage variations has been published (Huebner, 1978; Baker et al, submitted). The time constants of light induced molecular events which displace electric charge in membranes can be measured directly from the voltage variations induced by brief light flashes. The experimental setups used employ either a zenon flashtube, which generates a 200 μJ, 7 μs white light flash, or a tunable pulsed dye laser, which generates a 10 to 50 μJ, 10 ns monochromatic light flash. The electronics used accurately follow membrane voltage variations into the 100 MHz (~10 ns risetime) range (Huebner, submitted).

The trans to cis isomerization of 3,3'bis(α-(trimethylammonium)methyl)azobenzene diiodide (or Bis-Q) in phosphatidyl ethanolamine-decane bilayer membranes in distilled water induces a positive photo-voltage with 80 to 100 μs risetime. The photo-voltages induced by 3,3'dimethyl-2,2'oxacarbocyanine chloride (or diO-C_1-3-Cl) are more thoroughly studied. They demonstrate that factors which modify bilayer membrane structure, such as the lipid and solvent composition, temperature and electrolytes (in the aqueous solution) also modify the photo-voltage waveforms. This suggests that dye induced photo-voltages may provide a useful new method for studying membrane structure.

J. S. Huebner, J. Memb. Biol. 39 (1978) 97-132. Supported by NIH grant GM 23250.

M-AM-B8 DETAILS OF ANESTHETIC-MEMBRANE INTERACTION AS REVEALED BY DEUTERIUM NMR OF SPECIFICALLY-LABELED ANESTHETICS AND LIPIDS. Y. Boulanger,* S. Schreier* and Ian C.P. Smith (Intr. by K.W. Butler) Div. Biol. Sci., NRC, Ottawa, Canada K1A 0R6.

Selectively deuterated local anesthetics procaine(PRC) and tetracaine(TTC) were synthesized and bound to membranes of either egg phosphatidylcholine(PC) or egg phosphatidylcholine-phosphatidylserine(PC-PS). Partition coefficients between water and lipid indicated stronger binding for the uncharged form of the anesthetic (pH 9.5), although TTC bound substantially in its charged form (pH 5.5). Two types of resonance are observed, a quadrupole splitting for the bound anesthetic and a single line for the free anesthetic. The results are consistent with two binding sites for anesthetic in the membranes, one in slow and the other in fast exchange with the external solution. The largest quadrupole splitting was obtained for the deuterons in the aromatic ring which are likely to be buried in the bilayer and therefore the most restricted. The presence of a relatively low quadrupole splitting for the other positions suggested that they remained in the highly disordered head group region of the bilayers. Stronger binding was usually observed in the presence of PS whose negative charge is thought to play a role in the interaction. The hydrophobic n-butyl chain of tetracaine is considered responsible for its binding more strongly than procaine. Phosphatidylcholine labeled in the N-methyl groups was also used; the variations in quadrupole splitting upon addition of anesthetic were consistent with the conclusions drawn from the deuterated anesthetics.

M-AM-B9 THE EFFECT OF n-ALKANES ON LIPID BILAYER STRUCTURE. T.J. McIntosh and S.A. Simon, Depts. of Anatomy, Anesthesiology, and Physiology, Duke Univ. School of Medicine, Durham, N.C. 27710.

We have studied the effects of n-alkane solvents on lipid bilayer organization, both above and below lipid phase transition temperatures. The lipids used in these studies were DML, DPL, DOL, and egg lecithin, while the n-alkanes varied in number of carbons from n=6 to n=12. Long chain alkanes (12 to 16) exhibit different effects on the bilayers than the shorter alkanes. Calorimetry and light scattering data show that the longer alkanes increase the phase transition temperature of DPL bilayers, while shorter alkanes decrease the temperature and broaden the transition. X-ray diffraction experiments show that the shorter alkanes increase the width of the bilayer far more than the long chain alkanes. Electron density profiles indicate that the longer alkanes align themselves parallel to the lipid hydrocarbon chains and increase the width of the bilayer solely by straightening the lipid chains. The shorter alkanes, however, increase the bilayer width to a dimension greater than the width expected from completely extended hydrocarbon chains. This means that the long alkanes are confined to each monolayer of the bilayer, while in the case of the shorter alkanes some of the solvent molecules may reside in the center of the bilayer, between opposing lipid monolayers.

M-AM-B10 THE EFFECTS OF ANIONIC DETERGENTS ON A BLACK LIPID MEMBRANE. Jonathan J. Abramson and Adil E. Shamoo. University of Rochester, School of Med. & Dent., Rochester, NY 14642.

Three ionic detergents:SDS, cholate, and DOC are shown to act as divalent cation ionophores when incorporated into black lipid membranes made from either oxidized cholesterol or a mixture of phosphatidylcholine and cholesterol (PC:Cholesterol = 5 mg:1mg). At a concentration greater than or equal to 1 μM, SDS shows large selectivity differences between cations and anions, and between the different cations tested (Ba^{2+}, Ca^{2+}, Sr^{2+}, Mg^{2+} and Mn^{2+}). Deoxycholate and cholate at concentrations greater than 4 x 10^{-4}M and 10^{-3}M respectively also act as divalent cation ionophores. The selectivity sequence measured for these two detergents is evidence for a strong ionic interaction between the divalent cation and the anionic charged groups on the detergent. In the case of cholate, the conductance depends on the third or fourth power of the cholate concentration and shows a linear dependence on $CaCl_2$ concentration. The conductance for deoxycholate depends on the sixth or seventh power of the DOC concentration and is also linearly dependent on the $CaCl_2$ concentration. Small concentrations of $LaCl_3$ (<1μM) inhibit the Ca^{2+} conductivity ($(CaCl_2)$= 5 mM) for each of the detergents tested. This suggests that $LaCl_3$ can very effectively replace Ca^{2+} at the ionophoric site in many transport systems. Investigators reconstituting membrane bound transport proteins which have been solubilized with detergents should be careful to remove sufficient detergent so as not to be measuring the transport properties of the detergent instead of the reconstituted protein.

Supported by NIH and U.S. DOE Contract and assigned Report No. Uk-3490-1498. Dr. Abramson is a fellow of MDA of America.

M-AM-B11 DIPICRYLAMINE (DpA^-) AS A PROBE OF VARIATION OF THE BILAYER MEMBRANE POTENTIAL PROFILE. D. D. Lee* and L. J. Bruner. Department of Physics, University of California, Riverside, CA 92521.

The surface density, σ_s, of adsorbed DpA^- and the relaxation time, τ_o, for membrane translocation of the anion have been measured using combined high and low amplitude voltage-step techniques. Black membranes are formed from dioleylphosphatidylcholine in decane, using unbuffered 0.1M NaCℓ solutions as the surrounding aqueous phases. The measurements employ a fixed aqueous phase concentration (e.g., 2x10^{-8}M) of DpA^- and varying concentrations of 4,5,6,7 tetrachloro-2-methylbenzimidazole (TMB) or of 2,3,5,6 tetrachlorophenoxyacetic acid (TPA). Increasing TPA concentration from zero to 2x10^{-4}M decreases τ_o by a factor of three while increasing σ_s by 20%. TMB at a concentration of 10^{-5}M increases τ_o by a factor of 2 while increasing σ_s by 15%. Neither compound by itself contributes to membrane conductance. The increase (decrease) of τ_o is presumed to result from an increase (decrease) of the positive potential energy difference between the center of the membrane and the DpA^- adsorption planes, and will be discussed in terms of possible dipole field effects introduced by TMB and TPA. The relatively small observed variation of σ_s suggests, on the other hand, that the electrostatic potential difference between the bulk aqueous phases and the DpA^- adsorption plane is not significantly affected by added TMB or TPA.

This work was supported by the U.S. Army Research Office.

M-AM-B12 MEMBRANES FROM PURE LIPIDS.
R. C. Waldbillig and G. Szabo, Department of Physiology, University of Texas Medical Branch, Galveston, Texas 77550.

Black lipid membranes have been formed from pure lipids in the absence of solvents. An adaptation of the Muller-Rudin method was used to make planar bilayers from mixtures of pure (> 99%) monoglycerides and triglycerides. The bilayers are large (1.3 mm^2), stable and have specific capacitance values similar to cell membranes.

Three lines of evidence indicate that the thin bilayer contains only monoglyceride. First, membranes were formed from mixtures in which the length (i.e., molar volume) of the monoglyceride acyl tail was changed. It was found that the bilayer specific capacitance varies inversely with the number of tail carbons (C16 = 957; C18 = 858; C20 = 701; C22 = 622 nF/cm^2). Second, bilayers were formed from mixtures in which the length of the triglyceride acyl tail was varied. It was found that the bilayer capacitance is independent of the triglyceride molar volume over a wide range of acyl carbon numbers (C11, C14, C16, C18, C20, C22). Third, bilayers were formed from mixtures in which the concentration of the triglyceride was varied. It was found that the bilayer capacitance is independent of the mole fraction (0.2 - 0.9) of triglyceride in the bulk mixture. The combined results suggest that the bilayer is composed of pure monoglyceride and consequently may be regarded as the electrophysiological equivalent of the thermodynamic standard state. Squalene and other solvents thicken the bilayer. The available evidence indicates that as many as two carbons/chain may be 'outside' the low dielectric region of the bilayer.

Supported by NIH Grant DEW-R01-NS-14247. Submitted Nov. 1, 1978.

M-AM-B13 MEMBRANE PROTEIN FILMS AND THE LIMIT OF SUPERFICIALITY. M. Blank, Dept. of Physiology, Columbia University, College of Physicians and Surgeons, New York, NY 10032.

The question—how thick is an interface?--is important in biological systems, since many structures appear too small to be considered bulk systems but too large to be considered surface layers. Of particular interest to us is the natural membrane, an 80 Å thick structure that contains several layers of molecules, e.g., a lipid bilayer with an adjacent layer of protein (approximately two monolayers in the red cell). We have studied the problem of the transition from film to bulk phase by measuring several surface properties of red cell membrane endofacial proteins, spectrin-actin (S+A). The surface viscosity and surface elastic modulus of S+A layers from about 3.5 to 30 thicknesses show a parabolic dependence on the thickness, with a minimum at about 80 Å. The equivalent bulk properties become independent of thickness after about 80 Å (four monolayers), indicating negligible surface effects above this point. On the other hand, the two-dimensional residual yield and the equivalent three dimensional value vary with thickness over the entire range. The bulk yield is highest at the lowest values of thickness studied, suggesting that the molecular interactions become less effective within a layer as the number of layers and the interactions between layers increase. Measurements of the permeability of these layers to ions show that the diffusion coefficient increases with the thickness of the S+A film, supporting the view that succeeding layers do not pack as well as the initial layer. All of the properties studied are in the range of significant surface effects for the in vivo thickness of S+A layers. The role of surface water appears to be particularly important in determining the magnitudes of these properties. (Supported by NSF-PCM 76-11676.)

M-AM-B14 MONAZOMYCIN DETECTION OF THE BINDING OF DIVALENT AND MONOVALENT CATIONS TO PLANAR BILAYER LIPID MEMBRANES. J.A. Cohen and M.M. Moronne*, Laboratory of Physiology and Biophysics, University of the Pacific, San Francisco, California 94115.

The antibiotic monazomycin has been used as a conductance probe to monitor the electrostatic surface potentials of planar bilayer lipid membranes (BLMs). A current-clamp technique permits continuous, on-line detection of changes in BLM surface potentials, with 1 mV sensitivity. Monazomycin-treated BLMs of phosphatidylserine-phosphatidylethanolamine (PS-PE) mixtures, in monovalent-electrolyte solution, were titrated with repetitive additions of $MgSO_4$ or $CaCl_2$ to the aqueous chambers. In all cases the resultant surface-potential shifts exceeded the shifts predicted by the Gouy-Chapman theory (Grahame equation). Thus, in addition to screening the negative PS-PE BLM surface charge, the divalent cations appear to bind to the BLMs, altering their surface-charge densities. Simple Stern analysis, employing a single effective divalent-ion binding constant for each type of BLM, does not give consistent results for the whole PS-PE series. Distinct binding constants for the PS and the PE are required. Moreover, the magnitude of the observed shifts depends on the type of monovalent electrolyte present, indicating that monovalent cations also bind to the BLMs. Analysis of the full binding problem requires information on the divalent and monovalent binding stoichiometries as well as assumptions regarding the statistics of binding to the membrane lattice. Within this framework, monovalent- and divalent-ion binding constants have been determined.

Supported by NSF (PCM 76-11950) and NIH (HL 16607).

M-AM-C1 THE MOTIONS OF LARGE MOLECULES WITH DIPOLES AS A MECHANISM FOR CHANNEL GATING IN SQUID GIANT AXON. Michael E. Starzak, State University of New York at Binghamton, Binghamton, NY 13901

The ramifications of a physical model for gating in the K^+ channels of squid giant axon are explored. The model postulates a tetrahedral configuration of gating molecules which are stabilized by intermolecular interactions when the four molecules are present in a "closed" configuration. The transition to an "open" configuration and the concomitant ion flow are precipitated by the motion of a dipole which is an intrinsic part of the large gating molecule. The dipole motion is constrained by the remainder of the gating molecule and the intermolecular interactions. The fraction of open channels for this model is computed as a function of potential and the results are compared with the steady state fraction of open channels computed from K^+ currents observed for the squid giant axon. For this model, the change in the constrained dipole must occur on a millisecond time scale. This constraint is used to deduce physical information for the gating molecule and its environment. The configurational change is described using molecular parameters such as the dipole moment and molecular size and environmental parameters such as the viscosity of the lipid "medium" in which the changes occur.

M-AM-C2 PERFUSION AND SUPERFUSION OF GIANT AXONS WITH POTENTIOMETRIC PROBES - FAST OPTICAL SIGNALS. B.M. Salzberg, University of Pennsylvania, Philadelphia, PA. 19104

Changes in extrinsic absorption, fluorescence, or birefringence in response to voltage clamp steps were measured from squid axons following the addition of various dyes either by superfusion or by internal perfusion. Potentiometric probes may be used to detect electrical activity of intracellular membrane systems, e.g., skeletal muscle, and might also be used, following microinjection in the manner of Procion or Lucifer Yellow, to indicate electrical events in the plasma membranes of fine axonal or dendritic processes. In squid, no potential dependent fluorescence signal was detected following perfusion with Lucifer Yellow CH (0.1 %) itself. However, the presence of this intracellular marker did not block the potential dependent absorption signal exhibited by axons perfused with a Merocyanine-rhodanine dye (WW 375). As in the absence of Lucifer, and consistent with its fixed negative charge rendering WW 375 membrane impermeant, the optical signal was opposite in sign, though similar in size to that obtained following addition extracellularly. A different result was obtained following perfusion with Nile Blue A. Axolemma stained with this dye exhibits an increase in fluorescence upon depolarization, whether it is stained from the outside or by internal perfusion, as though the dye were membrane permeant. It has been reported by Valenzeno and Pooler (Biophys. J. 21, 43a, 1978) that 2,4,6-trinitrobenzene sulfonic acid (TNBS) blocks the photodynamic damage produced by the potentiometric probe Merocyanine 540. We found that 5 mM TNBS (pH 7.3) blocks 90 % of the M540 phototoxicity, but also reduces the size of the optical signal by a factor of four or five. Many of these experiments were done in collaboration with Alan Fine. Supported in part by National Science Foundation grant BNS-7705025 and a Steps Toward Independence Fellowship from the Marine Biological Laboratory, Woods Hole, Massachusetts.

M-AM-C3 DARK EFFECTS OF DYES IN PERFUSED SQUID AXONS. Robert S. Croop* and Clay M. Armstrong, Dept. Physiology, University of Pennsylvania, Philadelphia, Pa. 19104.

In recent years dyes have been utilized in axons as indicators of membrane potential and as photodynamic agents to alter the structure of the ionic channels. We have investigated the actions of many dyes (concentration 0.1-0.5 mM) on the ionic currents in perfused squid axons and have found that nearly all have significant effects when applied internally in darkness. Members of the thiazin, azin, oxazin, safranin, acridine, xanthine, indamin, and triphenylmethane families were screened. Of particular interest were the following. 1) The azin dye Neutral Red, and other dyes, cause 'inactivation' of I_K, reminiscent of TEA derivatives. 2) The safranin Amethyst Violet (0.5 mM) strongly decreases I_{Na} and I_K. 3) The xanthene Pyronin Y greatly reduces I_K and causes rapid decay of I_{Na} following a voltage step. 4) The thiazin Azure A (0.1-0.5 mM), like the drug Pancuronium, simulates inactivation after normal inactivation has been destroyed by Pronase. Azure A does not affect opening kinetics of Na channels, or ON gating current that is generated as the channels open. I_{Na} tails recorded as the channels close are rounded, greatly reduced in amplitude, and prolonged. OFF gating current, recorded as the channels are closing, is also reduced and slowed. These effects are reversible. Like Pancuronium, Azure A interferes with closing of the activation gate and prevents the movement of the gating charge that is linked to closing and opening of the gate.

Our results suggest that a highly specific interaction between dye and channel may be the basis for the photodynamic effects seen by others.

M-AM-C4 IMPROVED INTERNAL PERFUSION IN MYXICOLA. J.L. Kenyon* and L. Goldman, Dept. of Physiology, School of Medicine, Univ. of Maryland, Baltimore, Md. 21201.

We now routinely obtain voltage-clamped, internally perfused Myxicola giant axons showing long term survival and stable electrical properties. In experiments in which current-voltage characteristics were determined every 30 min, 9 out of the 12 preparations attempted showed initial action potential amplitudes of 110mV or greater, and conducted action potentials for a mean period of 5½hr (range 2½ to > 10hr). Mean initial action potential amplitude of these 9 preparations was 118mV (range 111 to 128mV). Resting membrane potential (mean initial value -68mV, range -57 to -74mV, corrected for liquid junction potentials) held stable for hours. Mean initial peak inward current was 3.62 ma/cm^2 (range 1.88 to 5.15 ma/cm^2), and mean resting membrane resistance was about 75% of that in similar control experiments on three intact axons. The standard internal perfusate used was modified from Narahashi and Seyama (J. Physiol. 242:471, 1974) and contained Na 1mM, K 398mM, F 51mM, Glutamate 320mM, H_2PO_4 15mM, EGTA 4mM, Sucrose 180mM, pH 7.3±0.05. Identical results were obtained if HEPES was substituted for the phosphate buffer. The most significant improvement over the previous procedure was obtained by liquefying the axoplasm in KCl perfusate (K 515mM, Cl 450mM, F 50mM, EGTA 4mM H_2PO_4 15mM, pH 7.3±0.05) rather than the 1mg/ml papain used previously. 1mg/ml pronase was also deleterious. Long term survival was not promoted if the 50mM KF in the liquefying perfusate was replaced with KCl, and reducing the KF in the standard perfusate from 50 to 20mM was deleterious. Increasing the KF in the liquefying perfusate to 100 or 150mM, by substitution for KCl did not further promote survival, and 500mM KF would not liquefy. Introduction of Cl^- internally increases the leak conductance, but the effect is reversible. This improved preparation was used for studies on the selectivity properties of the Na channel. (Supported by USPHS Grant NS-07734)

M-AM-C5 TESTS OF A SIMPLE METHOD FOR CONTINUOUSLY MONITORING MEMBRANE SLOPE CONDUCTANCE DURING A VOLTAGE CLAMP. William J. Adelman Jr., Laboratory of Biophysics, IRP, NINCDS, NIH, MBL, Woods Hole, MA 02543.

When membrane potassium currents are corrected for ion accumulation in the periaxonal space, larger maximal conductances and slower turn-on kinetics are obtained than those obtained using simple chord conductance relations with constant reversal potentials (Adelman et al., J. Memb. Biol. 13: 387). G_K kinetics were also obtained by superposing a small jump voltage, ΔE, on the larger voltage pulse. In this case, $g_K = \Delta I/\Delta E$, ΔI being the corresponding small step in current (a method suggested by Richard FitzHugh in 1958 and applied by Cole and Moore with equivocal success as their slower voltage clamp obscured ΔI with large capacity currents). It is now possible to continuously monitor the slope conductance during a clamp pulse by superposing a small amplitude continuous square wave of constant frequency on the voltage pulse. In TTX-treated squid axons, we compared results obtained with this method with results from both conventional currents and two-pulse instantaneous currents. As the square wave duration (100-250 µsec) was significantly less than the time constants of g_K (1-10 msec) and significantly greater than the voltage clamp settling time (10 µsec), and as the amplitude of the continuous wave was small (5 mV), one could superpose a curve of the mean current between the discrete jumps (correcting for I capacity) on the equivalent unperturbed I_K curve. Using the continuous square wave monitor, g(t) for a series of E_m were obtained uncontaminated by K^+ accumulation. Tail current g_K kinetics were separated from K^+ wash-out kinetics. In addition, the times and voltages at which instantaneous I/E relations had zero slopes ($\Delta I=0$) and negative slopes (phase reversal in ΔI jumps) were readily determined with an economy of measurements as compared to the two-pulse method.

M-AM-C6 STUDIES ON CARDIAC-LIKE ACTION POTENTIALS FROM SQUID AXONS. F. Ramón, S.A. Simon* and J. W. Moore (Intr. by T. J. McManus), Dept. Physiol., Duke Univ. Med. Ctr., Durham, N.C. 27710.

Squid axons internally perfused with TEA produce long duration action potentials similar in shape to those recorded from cardiac muscle. We are trying to determine similarities between these two preparations insofar as action potential behavior. We have performed axial wire voltage and current clamp experiments as well as studied propagated action potentials (PAP's). We found that: a) During the phase of sustained depolarization of membrane action potentials (MAP's) input resistance increases continuously without reaching resting values. In contrast, for PAP's input resistance remains at resting values and does not change during the plateau. Both MAP's and PAP's show repolarization in response to hyperpolarizing current pulses. During the plateau of MAP's, measurements of current resulting from voltage clamp pulses to sodium and potassium equilibrium potentials demonstrate a decrease in sodium and an increase in potassium conductance. b) External application of cardioactive drugs (-)Norepinephrine (5×10^{-5} M), Octanol (3×10^{-5} M), (+) & (-)Alprenolol (5×10^{-5} M) and (-)Propranolol (5×10^{-5} M), shows that (-)Norepinephrine increases the duration of MAP's whereas the other drugs shorten the duration of MAP's and also reverse the effect of (-)Norepinephrine. Voltage clamp studies indicate that (-)Norepinephrine's primary effect is to increase the magnitude of sodium currents. The other drugs act by decreasing sodium currents shifting inactivation and sodium conductance curves in the hyperpolarizing direction. This latter effect can be rationalized, in part, by shifts in the electrostatic potential energy barrier across the membrane as ascertained by measurements on monolayers and bilayers. (Supported by NIH Grants HL22767 and NS03437).

M-AM-C7 CONTROL OF REPETITIVE FIRING IN SQUID AXON MEMBRANE AS A MODEL FOR A NEURON OSCILLATOR. R. Guttman, S. Lewis* and J. Rinzel*, Brooklyn College of CUNY, Brooklyn, N.Y. 11201; Marine Biological Laboratory, Woods Hole, Mass., 02543 and Mathematical Research Branch, NIAMDD, NIH, Bethesda, Md. 20014.

Repetitive firing in space-clamped squid axons bathed in low calcium and stimulated by a just suprathreshold step of current can be annihilated by a brief depolarizing or hyperpolarizing pulse of the proper magnitude applied at the proper phase. In response to such perturbations, membrane potential and ionic currents show damped oscillations toward a steady state. For other, non-annihilating, perturbations, repetitive firing resumes with unaltered frequency but with phase resetting. Experimental findings are compared with calculations for the space and current-clamped Hodgkin-Huxley equations. Annihilation of repetitive firing to a steady state corresponds to a solution trajectory perturbed off of a stable limit cycle and into the domain of attraction of a coexistent stable singular point. Experimentally and theoretically the nerve exhibits hysteresis with two different stable modes of operation for a just suprathreshold range of bias current: the oscillatory repetitive firing state and the time-independent steady state. Analogy is made to a brief synaptic input (excitatory or inhibitory) which may start or stop a biological pacemaker.

Supported in part by NIH grant ROl NS 12272-03 awarded to RG.

M-AM-C8 HYDROSTATIC PRESSURE INCREASES THE STEADY STATE CONDUCTANCE IN THE SQUID GIANT AXON. B.B. Shrivastav, J.L. Parmentier* and P.B. Bennett*, Dept. of Anesthesiology, Duke University Medical Center, Durham, North Carolina 27710.

It is well known that increased hydrostatic pressure results in increased whole animal excitability (Hunter and Bennett, Undersea Biomed. Res. 1, 1-28, 1974). These experiments investigated the effects of pressure on specific ionic currents in single nerve membranes. Intact squid axons were voltaged clamped inside a high pressure chamber using the "piggy-back" electrode system with an Ag-AgCl reference electrode. Series resistance was compensated and leakage currents were subtracted from the steady state values. 300 nM TTX was added to the artificial sea water to suppress sodium currents. Ten axons were smoothly compressed at 6 psi/sec to 1000 or 2000 psig using helium gas. Cooling coils maintained the temperature of the bathing solution at 5.5°C and data was taken after 15 minutes at pressure. A pressure of 2000 psig caused an average increase of 10.9% in the steady state conductance at each membrane potential tested (10 mV steps between -40 and +80 mV) and caused a slight decrease in the time constant t_n. It is most likely that pressure increases the probability "n" of the open potassium channels; causing an increase in the steady state conductance. Leakage conductance was slightly increased and no apparent changes were seen in the membrane potential.

M-AM-C9 EFFECTS OF RAPID LONGITUDINAL STRETCH ON SQUID GIANT AXONS. Jay B. Wells and David E. Goldman, Laboratory of Biophysics, IRP, NINCDS, NIH, MBL, Woods Hole, MA 02543.

Myelinated nerve and lobster giant axons can be excited by mechanical distortion which stretches their membranes. The mode, degree and rate of change of this distortion is applied differently to these axons but result in membrane depolarization which can lead to the generation of an action potential. We have prepared squid giant axons for recording in a conventional voltage clamp with internal electrodes. A voice coil is attached to one end for applying stretch at varying rates, degrees and durations and a stress transducer is attached to the other end. Application of stretch produces a depolarization roughly proportional to the rate and amplitude of the stretch. The depolarization lasts for a few milliseconds and is followed by a short duration hyperpolarization. Rapid, short duration stretches amounting to 6-8% of the specimen length trigger subthreshold responses and 10% generally produces action potentials. The depolarizations produced by electrical and by mechanical stimuli are additive. Records from the tension transducer show marked stress relaxation with major time constants of a few milliseconds. All of these phenomena are entirely reversible. Earlier work has shown that rapid longitudinal stretch of myelinated frog fibers is ineffective (Gray and Ritchie, 1954) but transverse compression produces depolarization of a few milliseconds duration (Rosenblueth et al., 1953). In the lobster giant axon, the depolarization produced by transverse compression requires a few seconds for recovery whether or not an action potential has occurred (Julian and Goldman, 1962). Limitations in suitability of specimens and in apparatus have limited the availability of results for quantitative analysis. However, further developments for application to squid axons will permit access to underlying mechanisms of mechanotransduction.

M-AM-C10 A NON-PROPAGATED POTENTIAL IN MAMMALIAN PERIPHERAL NERVE. S. Yeandle, Naval Medical Research Institute, Bethesda, Maryland 20014.

For many years the complex wave form recorded from vertebrate peripheral nerve has been interpreted as the superposition of propagated axonal action potentials of different conduction velocities and shapes. Such considerations have led to the well known classification of vertebrate peripheral axons based upon conduction velocities into A, B, and C classes. We report that in recordings from exised rat sciatic nerves placed on a grid of electrodes in a moist chamber there is component that is not propagated and occurs over a few centimeters of the nerve. This component, although variable in shape from preparation to preparation, appears to require that a propagated potential immediately preceed it since TTX and KCl in concentrations sufficient to block conduction also abolish the non-propagated component. The occurrence of non-propagated potentials is independent of the direction of the conducted action potentials.

Naval Medical Research and Development Command, Research Work Unit No. MF51.524.013-1018.

M-AM-C11 MEASUREMENTS OF THE TIME INTEGRAL OF AN INHIBITORY SYNAPTIC CONDUCTANCE IN THE BUCCAL GANGLIA OF APLYSIA CALIFORNICA. Daniel Gardner, Dept. of Physiology, Cornell Univ. Medical College, New York, N.Y. 10021.

Studies in synaptic biophysics have generally used the peak membrane voltage or current change of a postsynaptic potential (PSP) or current (PSC) as a convenient measurement of the size of the response. In a few cases, area rather than peak of the PSP or PSC has been measured or advocated. Recording inhibitory PSC (IPSC) under voltage-clamp from neurons of Aplysia buccal ganglia, I have approximated by numerical integration the time integral of the synaptic current. Resulting values for the synaptic charge, Q, transferred by each IPSC ranged from -100 to -500 pC for typical IPSC recorded near resting potential. Most of the charge is transferred during the interval between the peak and a time one time constant of decay later. In order to provide an alternate measure of synaptic efficacy, the slope of the Q vs. membrane potential curve was calculated and defined as the time integral of synaptic conductance, b. Values of b ranged from 2.6 to 51 pC/mV, averaging 14 pC/mV. For IPSCs recorded in 31 cells at room temperature, b was well correlated with g_{peak}, the peak synaptic conductance (r=0.86). Time integral of conductance is thus a useful and well-behaved alternate measure of synaptic size, especially appropriate where charge transfer is of interest. When temperature, T, was varied from 9-22°C, I found: 1) b was well correlated with the product of g_{peak} and IPSC decay time constant (r=0.96, n=51). 2) While g_{peak} decreased with lowered T, b was roughly constant, with slight peak at 12-17°C. I speculate that lengthening average postsynaptic channel lifetime, and therefore time constant of PSC decay, may have adaptive significance in maintaining synaptic response size invariant with changing temperature and consequent decreased transmitter release.

Supported by NIH-NINCDS grants NS11555 and RCDA NS00003.

M-AM-C12 MECHANISM OF END-PLATE CHANNEL BLOCK BY N-ALKYL GUANIDINE DERIVATIVES. J.M. FARLEY*, S. WATANABE*, J.Z. YEH, AND T. NARAHASHI (Intr. by E. Margoliash), Dept. Pharmacol., Northwestern Univ. Med. Sch., Chicago, IL 60611.

A number of compounds affect the kinetics and the I-V relationship of end-plate current (EPC). One mechanism that has been proposed to explain these effects is that open end-plate channels are blocked in a voltage dependent manner. We have previously found that guanidine is permeant to the end-plate channels whereas some derivatives of guanidine block the channels. In the present study a series of n-alkyl guanidine derivatives have been used to characterize the kinetics of channel block in the frog end-plate membrane. All these compounds altered the EPC kinetics and changed the I-V relation, and some exhibited stimulus-dependent block. Methyl-, ethyl- and propylguanidine shortened the inward EPC and prolonged the outward EPC. Amylguanidine caused a biphasic inward current and a prolonged monophasic outward current. Octylguanidine caused both the inward and outward EPC to decay faster. These compounds blocked inward current more effectively than outward current resulting in a non-linear I-V relation. The block of inward EPC caused by methyl- or ethylguanidine could be relieved by repetitive outward EPC's. The rate of recovery from block was dependent on the number of stimuli but independent of the frequency of stimulation (e.g., 0.1 Hz, 0.05 Hz, 0.033 Hz). These data suggest that blocked channel-receptor complex can return to a resting state and that only open channels can unblock. The simple sequential model with linear voltage-dependent blocking kinetics cannot account for our observations. It is proposed that these guanidine compounds block open channels in a current-dependent manner.

Supported by NIH grant NS 14145.

M-AM-C13 CONTROL OF THE MUSCLE ENDPLATE MEMBRANE POTENTIAL WITH CHANGES OF $[Cl^-]_o$.
D.M. Yahn,* L.S. Reynolds,* and E.G. Henderson, Dept. of Pharmacol. Univ. of Conn. Health Center, Farmington, CT 06032.

The endplate membrane of frog cutaneous pectoris like other striated muscle membranes (Hodgkin, A.L. and Horowicz, P., J. Physiol. 148, 1959; Adrian, R.H., Circul. 26, 1962) can be controlled by the chloride concentration ratio when the muscles have been loaded with extra K^+ and Cl^-. Muscles soaked for 3 hours in Ringer's solution with 100mM KCl had resting E_m's of -18.3±.69mV and positive going MEPP's. Substitution of an impermeable anion for Cl^- caused a rapid (within 2 minutes) change of E_m to +22.5±2.5mV which did not change further within 1 hour. The reversal potential of the MEPP's could be determined by continuous monitoring during the potential shift caused by Cl^- removal and was found to be between -5 and 0mV. A similar E_m shift to +28.8±1.87mV was found to occur if the $[K^+]_o$ was reduced to 2.5mM and $[Na]_o$ elevated to 218mM in the Cl^--free solution. The reversal potential of the MEPP's under these conditions was almost identical to that in 100mM $[K^+]_o$. Readmission of $[Cl^-]_o$ in the high Na^+, low K^+ solution caused the E_m to shift back to -55.4±3.8mV and the reversal potential estimated under these conditions was again between -5 and 0mV. The reversal potential measured with MEPP's by Cl^- shifts was confirmed by voltage clamping and measuring MEPC's as a function of clamping potential in each solution. These results indicate that the muscle endplate reversal potential is unaffected by significant elevations of either $[K^+]_i$ or $[K^+]_o$. E_m control of whole muscle bundles by varying $[Cl^-]_o$ should prove very useful in determining post-synaptic permeability changes with radioactive tracers.
(Supported by NIH NS 12563).

M-AM-C14 SPATIOTEMPORAL SIMULATION OF MINIATURE ENDPLATE CURRENT GENERATION.
Howard Krausz* and Paul Adams, Intr. by F. W. Banks, Department of Physiology and Biophysics, University of Texas Medical Branch, Galveston, Texas 77550.

Recent kinetic experiments have revealed that ACh triggers endplate channel opening by rapid binding to 2 independent sites on a receptor which then undergoes a rate limiting conformational change to an active form. We have based a computer simulation of mepc generation on this scheme, after scaling the isomerization rate constants to room temperature assuming a Q_{10} of 3. Ten thousand ACh molecules are dumped as a 50 nm diameter disk into a very thin homogeneous synaptic cleft of infinite extent at time zero. ACh diffuses out radially from the release point, binding to receptors, triggering channel opening and suffering hydrolysis as it spreads. Values for single channel current, receptor and esterase density, ACh diffusion constant and hydrolysis rate were taken from the literature. The simulations show that mepc generation occurs in 2 stages. In the initial "loading" stage ACh diffuses rapidly (< 40 μsec) out to a limiting perimeter which bounds about 10,000 binding sites. Thus within this area receptors are biliganded, whereas outside it they are unliganded. At the perimeter a small monoliganded fringe exists. The diffusion is rapid because during the loading stage most of the ACh is unbound. During the second "generative" stage diffusion beyond the limiting perimeter is halted by the Katz-Miledi rebinding effect. Within the limiting perimeter, biliganded receptors are either flipping to the active state, or reverting to monoliganded and then unliganded forms. The risetime, amplitude and decay time of the simulated mepc agree well with those of real mepcs.
Supported by NIH Grant NS-05665 to H. Krausz

M-AM-C15 ISOLATION OF A FRACTION OF SOYBEAN LIPOSOMES ENREACHED IN SODIUM CHANNELS INCORPORATED FROM LOBSTER NERVE.
Raimundo Villegas and Gloria M. Villegas*, Centro de Biofísica y Bioquímica, Instituto Venezolano de Investigaciones Científicas, (IVIC), Apartado 1827, Caracas 101, Venezuela.

The tetrodotoxin-sensitive ^{22}Na flux into different fractions of reconstituted vesicles was measured. Reconstituted vesicles were prepared by the freeze-thaw-sonication procedure (Biochim.Biophys.Res.Comm., 79: 210, 1977). Na^+ channels from lobster nerve membrane (1-2 mg of membrane protein/ml) were incorporated into soybean liposomes (50 mg of lipids/ml) prepared in a sulfate solution containing Cs^+ (0.5 Eq/l) and Tris buffer (10 mEq/l), pH 7.5, in the presence of veratridine (0.5 mM). After reconstitution, the vesicles were transferred and kept for 60-75 min in a similar solution in which Cs^+ was replaced by Na^+. At the end of this period, the vesicles were fractionated by centrifugation on a discontinuous sucrose density gradient and the tetrodotoxin-sensitive ^{22}Na flux into the vesicles of the different fractions was measured. All procedures were performed in the presence of veratridine (0.5 mM) at temperatures close to 0°C. The drug-sensitive ^{22}Na influx per mg of protein measured in the lighter fraction, collected on top of 10% sucrose, was about 4.5 to 5-fold higher than that found in the whole population of reconstituted vesicles.
Partially supported by Grant 31.26.S1-0702 of CONICIT, Venezuela.

M-AM-D1 ROLE OF OSMOTIC FORCES IN MYOFILAMENT LATTICE STABILITY IN STRIATED MUSCLE E.W. April and J. Schreder*. Department of Anatomy, College of Physicians & Surgeons of Columbia University, New York City, 10032.

A-band lattice stability in intact muscle fibers has been shown to be functions of van der Waal's (attractive), long-range electrostatic (repulsive), and Donnan-osmotic (compressive) forces (April & Wong. J.Mol.Biol. 101:107,1976). Exclusion of water across the intact sarcolemma places the A-band lattice in a volume-constrained liquid-crystalline form. Upon removal of the sarcolemma, the thick filament lattice expands to an electrically-balanced liquid-crystalline condition. While myosin filament separation within the intact fiber does not vary significantly during generation of tension (Elliott, et.al., J.Mol.Biol. 25:31, 1967), low-angle X-ray diffraction studies of the skinned fiber reveals an 11% decrease in filament separation upon induction of low-tension rigor by the method of Kawai & Brandt (J.Gen.Physiol. 68:267,1976). These results confirm a perpendicular component of contractle force. The A-band lattice of the skinned fiber can be osmotically volume-constrained with PVP-10 (polyvinylpyrrolidone, M.W.≅10,000). At an osmotic pressure of approximately 64 Torr (5 mM PVP), where the interaxial separation between the thick filaments of the skinned fiber approximates that of the intact fiber, the lattice spacing decreases by only 4% upon induction of low-tension rigor. Further shrinking of the A-band (120 Torr, 10 mM PVP) so stabilizes the lattice that induction of rigor does not affect interaxial separation. Enhanced electrostatic repulsive forces of the volume-constrained condition plausibly counterbalance the inwardly directed vector of contractile force. Since rigor-induced changes in the dimensions of the electrically-balanced A-band lattice diminish upon introduction of volume-constraint, Donnan-osmotic forces acting across a functional sarcolemma contribute to lattice stability. (Supported by grants from NIAMD and MDAA.)

M-AM-D2 X-RAY DIFFRACTION OF SKINNED MUSCLE FIBERS. Paul J. Shapiro*, Katsuhisa Tawada*, and Richard J. Podolsky, NIAMDD, NIH, Bethesda, MD 20014.

Equatorial X-ray diffraction patterns from chemically skinned rabbit and frog skeletal muscle fibers were recorded with an electronic position-sensitive X-ray detector as a function of sarcomere length, temperature, and degree of activation. Sarcomere length, s, and force were continuously monitored during the X-ray exposure. The X-ray signal-to-noise ratio was enhanced with a digital background subtraction technique, and d_{10}, the spacing of the 10 reflection planes, and I_{10}/I_{11}, the intensity ratio of the 10 and 11 reflections, were measured. As described previously (Rome, J. Mol. Biol. 37, 331 (1968); Matsubara & Elliott, J. Mol. Biol. 72, 657 (1972)), d_{10} in relaxed fibers decreased when s was increased. However in our experiments the decrease in d_{10} with s was very small until a definite 'break point' was reached (at about 2.5 μ in rabbit and 3.0 μ in frog) which appeared to coincide with the sarcomere length at which resting tension became measurable. The influence of activation was examined in rabbit fibers. At sarcomere lengths between 2.0 and 2.5 μ, activation (pCa 5) caused d_{10} to decrease by about 15%; d_{10} changed much less upon activation at longer sarcomere lengths. As in the case of intact fibers, activation caused I_{10}/I_{11} to decrease. The intensity ratio in the relaxed state increased with temperature and appeared to be more sensitive to temperature than that in the active state. The change in intensity ratio of the relaxed state with temperature reflects changes in filament structure which may be related to the strong influence of temperature on the ability of rabbit fibers to develop force.

M-AM-D3 PROPERTIES OF FROG MYOFIBRILS PREPARED BY A NOVEL METHOD. Alan Magid* and Michael Mumma*, (Intro. by M.K. Reedy). Dept. of Anatomy, Duke Univ. Med. Ctr. Durham, NC 27710

During force transducer studies of the relax-rigor transition in glycerinated insect flight muscle made to identify conditions which minimize force development, it was observed that 50% glycerol blocked virtually all tension development (M.K. Reedy, pers. comm.). By modifying solution composition somewhat, we found that the same behavior could be obtained in mechanically skinned frog fibers. Laser diffraction studies showed that no sarcomere shortening occurred during MgATP washout, although the characteristic rigor stiffness slowly developed. Using this glycerol-rigor approach, a new method for isolating myofibrils from frog muscle was developed. We proceed as follows: hindlimbs are dissected from Rana pipiens, soaked at 4°C overnight in a depolarizing saline (120 mM KCl, 5 mM EGTA, 20 mM MOPS, pH 7.0 = basal buffer), and dissected into individual muscles. They are then minced with scissors and razor blade and 1--2 g stirred for 0.5 h in 50 ml of 300 mM Kacetate, 1mM Mgacetate, 1 mM EGTA, 20 mM MOPS, 50% glycerol, pH 7.0 which is then made 0.5% in Triton X-100, stirred for 0.5 h more, and the glycerol-detergent mixture decanted. 50 ml of basal buffer is added, the mince briefly homogenized in a Sorvall Omnimixer, strained thru cheese cloth, and washed twice in basal buffer + 5 mM Mg^{++}. Light microscopy shows that this method gives fibrils with excellent sarcomeric order, which respond to relaxing solution by returning to normal in vivo equilibrium sarcomere length (2.0--2.2 μ), and briskly contract when calcium-activated. Preliminary measurements (4 mM MgATP) indicate a very low resting ATPase rate (0.006 μmol/mg/min) which increases 40--60 fold at pCa 4.6. X-ray diffraction patterns obtained from frog sartorius muscle treated with glycerol-Triton solution show a well-developed rigor pattern. (Supported by NIH grant AM 14317 to M.K. Reedy; A.M. is an MDA postdoctoral fellow.)

M-AM-D4 REGULATION BY CALCIUM IONS OF CROSS-BRIDGE ATTACHMENT IN MYOFIBRILS STUDIED BY SATURATION TRANSFER EPR SPECTROSCOPY. S. Ishiwata,* J. Seidel and J. Gergely, Dept. of Muscle Research, Boston Biomedical Research Institute, Boston, MA, 02114.

As previously shown by saturation transfer (ST) EPR measurements all cross-bridges are attached in the absence of ATP (τ_2, rotational correlation time, $\approx 10^{-3}$ sec) and are detached in the presence of 5 mM ATP ($\tau_2 \approx 10^{-5}$ sec) regardless of the Ca^{2+} concentration (Thomas et al., Biophys. J., 1978). We studied the effects of non-hydrolyzable ATP analogs (PPi and AMPPNP), Ca^{2+}, ionic strength and temperature on the rotational motion of myosin heads on glycerinated myofibrils from rabbit skeletal muscle, in which about 25% of myosin heads were selectively labeled with N-(1-oxyl-2,2,6,6-tetramethyl-4-piperidinyl)-maleimide (MSL). In the presence of 5 mM PPi or AMPPNP, the ST-EPR spectra were intermediate between those of ATP- and rigor-myofibrils. These spectra were sensitive to Ca^{2+} in the micromolar range and were interpreted by assuming a mixture of cross-bridges whose motion was determined by whether they were attached or detached. The fraction of attached cross-bridges derived from the ST-EPR spectra agreed with estimates obtained from sedimentation of mixtures of unlabeled myofibrils and MSL-labeled subfragment-1. The spectra were consistent with an increase in the fraction of attached cross-bridges with increasing Ca^{2+} concentration. The Ca^{2+} dependence of cross-bridge attachment did not show cooperativity. Upon increasing the ionic strength or decreasing the temperature, the fraction of attached cross-bridges in the presence of ATP analogs decreased, whereas in the absence of ATP analogs the cross-bridges remained attached. These experiments show that in myofibrils in the presence of ATP analogs there exists an association-dissociation equilibrium between myosin and actin which is regulated by Ca^{2+}. (Supported by grants from NIH (HL-5949, HL15391), the National Science Foundation, and the Muscular Dystrophy Association of America, Inc.)

M-AM-D5 THE MEASUREMENT OF MYOSIN HEAD ORIENTATION IN MUSCLE FIBERS USING NITROXIDE SPIN LABELS. David D. Thomas, and Roger Cooke, (Intr. by R. Crooks), Dept. of Structural Biology, Stanford School of Medicine, Stanford, CA, and Dept. of Biochem/Biophys. and CVRI, Univ. of California, San Francisco, CA 94143.

Nitroxide spin labels were attached selectively and rigidly to myosin heads in glycerinated rabbit muscle fibers. The angular distribution of the principle axis of the spin label relative to the fiber axis was determined from EPR spectra of oriented fibers. In rigor, the angular distribution has a sharp maximum, with a full width at half maximum of 15-20 degrees. The angular distribution for spin labels on myosin in labeled fibers was virtually identical to that for spin-labeled myosin subfragment-1 or heavy meromyosin diffused into the fibers and bound to thin filaments. Thus, all of the myosin heads in a rigor fiber appear to have very nearly the same orientation with respect to the fiber axis, an orientation that is identical to that for myosin subfragments bound to thin filaments. Two different spin labels (iodoacetamide and maleimide derivatives) gave the same results. In relaxed fibers the orientation distribution is almost completely randomized with a full width at half maximum of at least 90 degrees. AMPPNP, an unsplittable analog of ATP, partially randomizes the distribution. Attachment of spin labels to myosin inhibited the K^+-activated ATPase activity of the myosin but did not inhibit the actin-activated ATPase activity. Spin-labeled fibers retain the ability to exert isometric and isotonic tensions.

Work supported by grants from NSF BMS75-14793, AHA 78-845, USPHS AM00497,and D.D.T. is a Helen Hay Whitne fellow.

M-AM-D6 FLUCTUATIONS IN POLARIZED FLUORESCENCE FROM RESTING AND ACTIVE SINGLE MUSCLE FIBERS. J. Borejdo*and S. Putnam*(Intr. by M. F. Morales), CVRI, UCSF, San Francisco, Ca, 94143.

We investigate whether sustained active tension in a fiber results from repeated impulsions by myosin cross-bridges (S-1 pieces). If so, fluctuations in S-1 rotational attitude during activity should be composed of the frequencies that constitute cross-bridge motion, while fluctuations during rest or rigor should be just noise. Attitude fluctuations are recorded as fluctuations in (number-independent) ratios of orthogonally-polarized components of fluorescence emitted from iodoacetyl fluoresceine molecules uniquely (verified by subsequent gel electrophoresis) fixed to the SH_1 thiols of the cross-bridges. The fluorophores are illuminated at 488 nm by an argon laser; photobleaching is adequately compensated by subtraction of slow drift. Steady tension of specially glycerinated single fibers lasts at least 15 m and is unaffected by labelling. Fluctuations are processed to yield power density spectrum or autocorrelation function, $G(\tau)$. In rest or rigor $G(\tau)$ is zero everywhere (noise), but during activity $G(\tau)$ is always obviously non-zero at small τ. Several tests rule out simple number fluctuation as the origin of these results, so we believe that the results authentically suggest repetitive S-1 rotation during activity. But improvements remain to be done. Mean delay times are still too long (10^2 ms), partly because photobleaching forces low illumination-prolonged counting, partly because events (e.g., ATPase) in glycerinated fibers are slow (see R. Takashi & S. Putnam, Anal. Biochem., in press). Research supported by NHLBI, NSF, AHA.

M-AM-D7 THE MECHANISM OF THE ACTOMYOSIN ATPase. Leonard Stein,* Richard P. Schwarz, and Evan Eisenberg, Laboratory of Cell Biology, NHLBI, NIH, Bethesda, Maryland 20014.

In the present study, we investigated the nature of the rate-limiting step in the actomyosin ATPase cycle. We first find that, at 15°, the forward rate constant of the initial P_i burst is about 5 times faster than the maximum actin-activated ATPase (V_{max}). Thus another step in the cycle must be rate-limiting. If this rate-limiting step occurs only when the S-1 is complexed with actin, as originally predicted by the Lymn-Taylor model, the ATPase and S-1 binding to actin should increase in parallel as the actin concentration is increased. Using turbidity determined in the stopped-flow apparatus as a measure of binding at 15° we find that, like the ATPase, the binding shows a hyperbolic dependence on actin concentration, approaching 100% assymptotically. However, the actin concentration required for half-maximal binding is 3 to 4 times greater than that required for half maximal ATPase. Thus, as at 0°, at 15° much of the S-1 is dissociated from actin when the ATPase is close to V_{max} showing that the transition from the refractory to the non-refractory state is the rate-limiting step. Our stopped-flow studies also reveal that after the S-1, actin, and ATP are mixed, regardless of the order of mixing, the steady-state turbidity level is reached almost instantaneously. Thus the steady-state binding is due to incomplete dissociation of the acto-S-1 complex by ATP. Both $M^*\cdot T$ and $M^{**}\cdot D\cdot P_i$ have the same binding constant to actin, and at high actin concentration are in rapid equilibrium with their respective actin complexes, $AM^*\cdot T$ and $AM^{**}\cdot D\cdot P_i$. Although, at very high actin concentration almost complete binding of S-1 to actin occurs, there is no evidence of any inhibition of the ATPase. This shows that both the initial P_i burst and the rate-limiting transition from the refractory to the non-refractory state occur at about the same rates whether the S-1 is bound to, or dissociated from, actin. Therefore, S-1 does not have to dissociate from actin each time an ATP is hydrolyzed.

M-AM-D8 A REEVALUATION OF THE MOLECULAR WEIGHTS AND HOMOGENEITY OF MYOSIN SUBFRAGMENTS. S.S. Margossian and W.F. Stafford III, Rosenstiel Center, Brandeis Univ., Waltham, MA. 02154.

In recent years, a number of methods have been reported for obtaining proteolytic subfragments of rabbit skeletal muscle myosin. In view of their extensive use in kinetic and structural analysis of muscle proteins, it was of interest to establish the homogeneity of these subfragments. Since SDS gel electrophoresis usually reveals multiple bands in the heavy chain region of papain S1 or tryptic HMM, it was decided to determine the extent of heterogeneity of these preparations under non-denaturing conditions by equilibrium ultracentrifugation. The plates were scanned using a flat bed densitometer. Fringe displacements were determined by the Fourier transform method of DeRosier *et al.* (1972) and subsequently analyzed using the computer programs of Roark and Yphantis (1969) and Johnson and Yphantis (1971). In a buffer containing 0.3 mM EGTA all three molecular weight averages: Mn, Mw, and Mz, were superimposable over the observable extent of the solution column for all S1 and HMM species, indicating a high degree of homogeneity. In the case of S1·A1 and S1·A2 fractionated on an ion exchange column, it was found that it is essential to include one more step of purification by gel permeation chromatography to remove traces of lower molecular weight contaminants. These determinations give a molecular weight of $(3.54\pm0.08)\times10^5$ for tryptic HMM, and a value of $(1.15\pm0.02)\times10^5$ for S1·A1 and $(1.11\pm0.02)\times10^5$ for S1·A2. The corresponding values for Mg·S1 and EDTA·S1 are $(1.31\pm0.04)\times10^5$ and $(1.13\pm0.03)\times10^5$, respectively, the difference accounting for the absence of DTNB l.c. in EDTA·S1. Experiments are underway to determine the molecular weights of LMM and the rod. Supported by grants from NIH (AM17350), NSF (PCM75-14790) to S. Lowey, NIH (HL21488) to W.F.S. S.S.M. is an Established Investigator of the American Heart Association.

M-AM-D9 THE SHAPE OF MYOSIN S-1 FROM X-RAY SOLUTION SCATTERING. R. A. Mendelson and K. M. Kretzschmar*, CVRI, University of California at San Francisco. CA 94143

Fluorescence depolarization measurements of S1 rotational correlation time suggested that S-1 might be more elongate then generally thought (Mendelson, Morales and Botts, Biochem. 12, 2250, 1973). We have investigated this and other features of S1 shape in more detail by low angle X-ray scattering of S1 solutions, using highly collimated x-radiation available at the Stanford storage ring (S.S.R.L.). From 8 to 18 mg/ml the S1 scattering showed no concentration dependence and the S1 ATPase was unaffected. Previously we reported (Kretzschmar, Mendelson and Botts, Biochem. 17, 2314, 1978) that the radius of gyration (R_G) is 32.5Å showing that S1 must be quite asymmetric. New, higher angle data, corresponding to 20Å resolution allowed modeling by various uniform density objects with (R_G) and volume ($140,000Å^3$) constraints. Using the Debye equation (evaluated using a fast subroutine by O. Glatter) we found that neither ellipsoids of revolution nor rods, rods bent at various angles, cones, cones plus hemispheres, spherical segments nor shapes suggested by electron microscopy fit the data well. A model consisting of a ball at the end of a cylinder, overall length ca. 130Å, fits significantly better indicating the mass distribution is highly skewed toward one end. Offer and Elliott (Nature 271, 325, 1978) considered a similiar model; however neither our (R_G) nor our scattering curve is compatible with their more detailed treatment of S1 (J.M.B., 123, 505, 1978). Preliminary Fourier model-refinement results (Chambers, Agard, Mendelson and Stroud, in preparation) will be presented. Supported by HS-06285, HL-16683, PCM 75-22698, PCM 76-11491, AHA CI8 and DMR 73-07692 (SSRP). K.M.K. was a Visiting Scientist of the AHA.

M-AM-D10 COMPARISON OF THE BINDING OF HEAVY MEROMYOSIN AND SUBFRAGMENT-ONE TO ACTIN. Lois E. Greene* and Evan Eisenberg, Section on Cellular Physiology, Laboratory of Cell Biology, NHLBI, NIH, Bethesda, Maryland 20014.

The binding to actin of the two soluble fragments of myosin, subfragment-one (S-1), a single-headed fragment, and heavy meromyosin (HMM), a double-headed fragment, was examined at μ = 0.22M, 22°. Previously, in several direct binding studies (Takeuchi, K. and Tonomura, Y., J. Biochem. (Tokyo) 70, 1011 (1971), Margossian, S., Lowey, S., and Barshop, B., Nature 258, 163 (1975), and Highsmith, S., Biochemistry 17, 22 (1978)), it was found that HMM binds to actin only about 10 times more strongly than S-1, suggesting that the binding of one HMM head to actin has a marked negative effect on the binding of the second head. In the present study the acto•HMM association constant was determined by having HMM and S-1 compete for binding sites on F-actin; the acto•S-1 association constant was obtained by studying the formation of the actin•S-1•nucleotide complex using three different ATP analogs: AMP-PNP, ADP, and PPi. In the competition experiments F-actin, along with the myosin fragments bound to it, was sedimented and the concentration of unbound myosin fragments was then determined. The data were analyzed using a set of theoretical equations proposed by T. L. Hill (Nature 274, 825 (1978)) that provide a simple way of analyzing the relative binding of one and two headed ligands. Using these equations, the acto•HMM association constant was determined to be 3×10^9 M^{-1}, while under the same conditions the acto•S-1 association constant is 5×10^6 M^{-1}. Therefore, we find a 600-fold difference between the binding constant of HMM and S-1 to actin. This indicates that the second head of myosin contributes significantly to the free energy of binding, which in turn opens up the possibility that the two HMM heads may bind independently to actin.

M-AM-D11 KINETICS OF ADP AND AMP-PNP BINDING TO SF-1. K. M. Trybus* and E. W. Taylor, The University of Chicago, Chicago, Illinois 60637.

The kinetics of binding of ADP and AMP-PNP as monitored by increases in intrinsic protein fluorescence were reinvestigated. Both nucleotides were found to bind in 3 steps with 2 fluorescence transitions, consistent with the mechanism $M+L \overset{K_1}{\rightleftharpoons} ML \overset{k_2}{\rightleftharpoons} ML^* \overset{k_3}{\rightleftharpoons} ML^{**}$. The total amplitude of the fluorescence change upon ADP binding to SF-1 is 10±2%. The observed amplitude decreases to 5% at high ADP concentrations due to a fast phase at the beginning of the transient which is completed within the instrument dead time. The graph of rate versus ADP concentration deviates from a hyperbola, and reaches a maximum rate of 100±20 sec^{-1} which is a measure of k_3 (20°, pH 7, 0.1M KCl). At 3° C, the fluorescence transient is markedly biphasic, with a fast phase of ∿150-200 sec^{-1} and a slower phase which reaches a maximum rate of 15±5 sec^{-1}. The maximum rate of ADP binding to SF-1 (k_3) has a distinctly different ionic strength dependence from the third step of ATP binding, which is presumably the hydrolysis step. The amplitude of the fluorescence signal when AMP-PNP binds to SF-1 is dependent on ionic strength, increasing from 15±3% at 0.1M KCl to 24±3% at 0.6M KCl. At both ionic strengths, the fluorescence associated with step 2 is ∿3/4 of the total signal. At 20° C, 0.1M KCl, pH 7 the maximum rate of the fast phase is ∿300 sec^{-1} and that of the slow transition (k_3) is ∿20 sec^{-1}. Dissociation of acto SF-1 by AMP-PNP (0.6M KCl, 20°, pH 7) showed 2 fluorescence transitions, one at a rate faster than dissociation, and the other at about the same rate as dissociation. This provides evidence for a conformational change before dissociation, i.e. an AM•L* state which could not be shown directly with ATP. (This work was supported by N.I.H. GM20592 and a grant from the Muscular Dystrophy Assn. of America, Inc.).

M-AM-D12 ON THE QUESTION OF COOPERATIVE INTERACTION OF MYOSIN HEADS WITH F-ACTIN IN THE PRESENCE OF ATP. E. Reisler, Dept. of Chemistry and Molec. Biol. Inst., UCLA, Los Angeles, CA 90024.

Modification of myosin heads with a bifunctional thiol reagent p-phenylenedimaleimide (pPDM) to bridge the reactive SH_1-SH_2 groups on myosin proceeds at identical rates with SI (A1) and SI (A2) fragments. The modified, inactivated heads do not bind actin. These features were utilized to characterize the populations of HMM solutions partially modified with pPDM. Enzymatic assays of partially modified HMM solutions combined with the analysis of their sedimentation in the presence of F-actin verified that the two heads of HMM react at random with pPDM. Partially reacted HMM systems with varying fractions of zero, one and two inactivated heads were then compared to a control HMM system for their interaction with F-actin and ATP. Vmax was found to be linearly dependent on the total fraction of unmodified heads and insensitive to the relative proportions of the zero and one inactivated heads of HMM. K_M values decreased with the relative decrease of the zero inactivated HMM species. The observed results are interpreted in terms of independent binding of myosin heads to actin in the presence of ATP. (Supported by NIH Grant AM 22031 and Grant 3386 of the Academic Senate, L.A. Division, UC.)

M-AM-D13 THE THIOLS OF MYOSIN S-1: EFFECTS OF THEIR LIGATION ON ATPase, ACTIN-AFFINITY, AND CONFORMATION. J. Botts, K. Ue*, J. Samet*, and T. Hozumi*, CVRI, UCSF, San Francisco Ca 94143.

We report the effects of labelling the thiols of myosin S-1 with one equivalent of 1, 5 IAEDANS and increasing methyl methane thiosulfonate (MMTS), a small sulfhydryl reagent. We monitored ATPases, actin-affinity and conformational changes of S-1. Titration using radioactive MMTS showed that only 8 of the 12 thiols of native S-1 are accessible; the remaining 4 are thought to reside in the interior of the S-1 head. With progressive labelling, the ATPase activities and the actin affinity of S-1 are significantly reduced. Yet even after 120-168 hr incubation with [MMTS]/[S-1] up to 25, perceptible non-zero levels of both actin-activated Mg^{2+} ATPase and S-1 - actin affinity were found. These results confirm others' conclusions (Wiedner, H., et al.; Barany, M., et al.) that the thiols of S-1 are not intrinsically catalytic. Also we show that cysteine residues are inessential in the binding of S-1 to actin. Three conformational probes monitored effects of blocking groups on thiols. First, the extent to which anilino-1,8 naphthalene sulfonate (ANS) penetrates and binds to S-1 was followed by fluorescence of bound ANS. However, the kinetics of this effect did not correlate well with activity and affinity loss. The second and third methods depended on properties of the (SH_1)-attached 1,5 IAEDANS, viz., Φ (rotational correlation time) and τ (excited state lifetime). The way that Φ and τ depend on reaction with MMTS is very similar to the way the S-1 functions depend on reaction with MMTS, suggesting that decreases of ATPase and actin affinity due to thiol blockage result from structural changes. We acknowledge NHLBI, NSF, and AHA support. T.H. is a Fellow of the AHA.

M-AM-D14 INACTIVATION OF MYOSIN SUBFRAGMENT 1 ATPASE BY COBALT CHELATION OF SH_1-SH_2. James A. Wells, M. M. Werber* and R. G. Yount, Washington State Univ., Pullman, WA 99164.

Treatment of 0.01 mM rabbit skeletal muscle myosin chymotryptic subfragment one (SF-1) with 0.1 mM $CoCl_2$, 0.1 mM 1,10 phenanthroline, 1.0 mM $Co(III)(phen)_2CO_3$ in the presence of 0.1 mM MgADP at 0° rapidly inactivates the NH_4^+ EDTA, Mg^{2+} and Ca^{2+}-ATPase activities. Studies correlating the loss of ATPase with cobalts/SF-1 show that while as many as 1.7 to 2.0 cobalts can be incorporated, the addition of only 1.2 to 1.3 cobalts/SF-1 correlates with the loss of 100% activity. Short treatment of cobalt-modified SF-1 with reducing agents $Co(II)(CN)_6^{4-}$ or Fe(II)EDTA restores 80 to 100 percent enzymatic activity and removes .8 to 1.0 enzyme bound cobalt(III). Following cobalt modification, three thiol groups are no longer titratable by DTNB analysis performed in 9 M urea. Two of these thiol groups are correlated with the loss of enzyme activity. Fe(II)EDTA treatment of cobalt-modified SF-1 regenerates two of three SH groups. Pretreatment of SF-1 with a 2.3 molar excess of N-ethyl maleimide (NEM) (believed to modify the cysteine, SH_1) or 1.3 molar excess p-phenylene N,N',dimaleimide (PPDM) in the presence of MgADP (believed to cross-link the cysteines, SH_1 and SH_2) prevents the incorporation of 1.0-1.3 cobalts/SF-1 and prevents further modification of all except .5 to .6 thiol groups. Treatment of SF-1 after cobalt modification with NEM or PPDM results in an enzyme which can be reactivated up to 70 percent of the original activity by Fe(II)EDTA treatment. Fe(II)EDTA will not restore activity to NEM or PPDM pretreated SF-1. These studies strongly suggest that the loss of enzyme activity is due to a simultaneous chelation of SH_1 and SH_2 by a single cobalt. Supported by grants from MDA, AHA of Washington and NIH (AM-05195).

M-AM-E1 ...ACE CHARGE DENSITIES OF LIGHT AND HEAVY DENSITY SARCOPLASMIC RETICULUM. Vincent C.K. Chiu, Donald R. Mouring*, and Duncan H. Haynes, Department of Pharmacology, University of Miami, Miami, Florida 33101

1-anilino-8-naphthalene sulfonate (ANS^-) was used as a surface potential probe for pre-existing surface charge on skeletal sarcoplasmic reticulum (SR) membrane surfaces. ANS^- shows no fluorescence in aqueous medium, but it is strongly fluorescent when it is bound to membrane surfaces. Binding of ANS^- on the outer and inner membrane surfaces can be distinguished based on their rates of fluorescent increase upon ANS^- addition to the medium. Binding of ANS^- on the outer membrane surface (A_o) is very rapid ($t_{\frac{1}{2}}$=100 μsec) and on the inner membrane surface (A_i) is slow ($t_{\frac{1}{2}}$=8 sec). An increase in K^+ concentration results in an increase in both A_o and A_i. This is due to the screening effect of K^+ on the pre-existing negative charge on the membrane surfaces allowing more ANS^- to bind. Using Guoy-Chapman theory, relating surface charge density, ionic strength and surface potential, we arrive at the following surface charge densities σ (charge/# of lipids):

	σ outer	σ inner
light SR	1/22	1/39
heavy SR	1/32	1/13

Our result indicates a higher charge density on the outer membrane surface of the light SR and a proportionally higher charge density on the inner membrane surface of the heavy SR. (Supported by NIH grants 1R01 GM 23990-01A1 and 1-PO-HL 16117, and Florida Heart Association)

M-AM-E2 SEPARATION OF THE CA^{2+}-ATPase FROM THE BASAL ATPase OF SARCOPLASMIC RETICULUM VESICLES. C. Hidalgo, M. Rosemblatt, J.L. Fernandez* and N. Ikemoto, Dept. Muscle Research, Boston Biomedical Research Institute and Dept. Neurology, Harvard Med. School, Boston, MA.

Freshly isolated sarcoplasmic reticulum (SR) vesicles were fractionated by sedimentation in sucrose density gradients into three groups: heavy, intermediate and light. Each fraction was incubated with calcium phosphate in the presence of ATP and heavier vesicles loaded with calcium phosphate were separated from the unloaded lighter vesicles by gradient sedimentation. About 35 to 50% of the vesicles in the heavy fraction, 10 to 25% of the intermediate, and less than 9% in the light fraction were loaded with calcium phosphate. After removal of the accumulated calcium phosphate by dilution and sedimentation all of them display high calcium uptake in the presence of oxalate. The vesicles so isolated from the heavy fraction display little or no Ca^{2+}-independent Mg^{2+}-ATPase (basal) activity. The corresponding vesicles from the intermediate and light fraction display basal ATPase activity indicating that the loading process does not produce inactivation. These results show that the basal ATPase is absent in a heavy fraction of SR vesicles which is the most efficient in transporting calcium. On solubilization of unfractionated SR vesicles with Triton X-100, Ca^{2+}-ATPase activity is selectively extracted while the basal ATPase remains in the Triton-insoluble residue. The insoluble residue does not contain the 100,000 dalton band characteristic of the Ca^{2+}-ATPase polypeptide as shown by SDS-gel electrophoresis. These results suggest that the Ca^{2+}-ATPase and the basal ATPase of SR are two different enzymes. (Supported by grants from NIH (AM-16922; HL-05811), NSF, the American Heart Association, and the Muscular Dystrophy Association of America.)

M-AM-E3 CALCIUM ATP CAN BE A SUBSTRATE FOR THE PHOSPHORYLATION OF THE CALCIUM-ATPASE REACTION OF SARCOPLASMIC RETICULUM. Shinpei Yamada and Noriaki Ikemoto, Dept. of Muscle Research, Boston Biomedical Research Institute; and Dept. of Neurology, Harvard Medical School, Boston, MA.

Previous work has shown that either ATP or Mg-ATP can serve as substrate in the phosphorylation of the ATPase enzyme of SR. The possibility of CaATP's being the substrate has previously not been considered. We have studied the effect of various forms of ATP (Ca-ATP, Mg-ATP and free ATP) on the reaction steps of purified Ca^{2+}-ATPase in which phosphoenzyme (EP) formation takes place under conditions that prevent EP decomposition (viz. high $[Ca^{2+}]$, low $[Mg^{2+}]$ and low [ATP]. The rate of EP formation (kf) depends strictly upon [Ca-ATP] as determined by plots of kf^{-1} versus $[(Me)\text{-}ATP]^{-1}$. The Km is 0.5μM and is independent of $[Ca^{2+}]$. Both the forward and reverse rates of EP formation are inhibited as the ionic strength increases from 0.08 to 0.4. The rate of the reverse reaction of the EP formation step is dependent upon the concentration of [ADP] but not on that of its metal complexes. The EP can be converted to the ADP-insensitive form of EP (Shigekawa and Dougherty, J. Biol. Chem. 253, 1458, 1978) by adding Mg^{2+} in the absence of KCl, and is subsequently decomposed as in the ATPase reaction that is carried out in a relatively high $[Mg^{2+}]$ range. These results suggest that Ca-ATP can replace Mg-ATP or ATP in the reaction steps in which EP-formation takes place. However, it appears that Mg^{2+} is required in order to proceed to the subsequent reaction steps via the ADP-insensitive EP. (Supported by grants from NIH (AM16922), NSF (PCM84124), the American Heart Association, and the Muscular Dystrophy Associations of America, Inc.)

M-AM-E4 KINETIC EVIDENCE FOR THE OLIGOMERIC INTERACTION OF THE CALCIUM ATPASE OF SARCOPLASMIC RETICULUM. Shinpei Yamada and Noriaki Ikemoto, Dept. of Muscle Research, Boston Biomedical Research Institute; and Dept. of Neurology, Harvard Medical School, Boston, MA.

Recent morphological and physicochemical evidence has suggested that the functional unit of the Ca^{2+}-ATPase of sarcoplasmic reticulum (SR) is made up of several 10^5 dalton subunits. We have studied the formation of the phosphorylated intermediate (EP) of the purified Ca^{2+}-ATPase of SR at high $[Ca^{2+}]$ (10-20 mM) and at low $[Mg^{2+}]$ ($\lesssim$ 0.2 mM) with [ATP] $\simeq$ 1/10 Km (Km = 0.5 μM) at 0°. Under these conditions the decomposition of EP is completely prevented. However, it was found that some Pi is liberated almost in parallel with the EP formation (transient Pi liberation). Direct determination of EP formation by means of the Millipore filtration method (without acid quenching) has indicated that this Pi is not derived from the acid-labile EP. The amounts of the liberated Pi are dependent upon the [enzyme]:[ATP] ratio. At [enzyme] $\lesssim$ [ATP], [Pi] $\simeq$ [EP] $\simeq$ 1/2[enzyme]. If the [enzyme] is in excess of the [ATP], the amount of transient Pi liberation approaches zero. The maximal [EP] does not exceed 1/2[enzyme] even at high [ATP]. Upon solubilization of the enzyme with high concentrations of Triton X-100 and Ca^{2+},which favors the monomerization of the ATPase molecules (Hidalgo, Thomas and Ikemoto, J. Biol. Chem. 253, 6879, 1978), [EP] exceeds 1/2 [enzyme], and concomitantly the transient Pi liberation decreases. These results can be best explained by a dimer model in which the EP of one subunit is stable, but that of the other subunit is destabilized as the result of subunit-subunit interaction. (Supported by grants from NIH (AM16922), NSF (PCM 84124), the American Heart Association and the Muscular Dystrophy Association of America, Inc.)

M-AM-E5 STUDIES ON THE CONFORMATION OF THE CALCIUM ATPASE OF SARCOPLASMIC RETICULUM WITH THE USE OF INTERACTION BETWEEN TWO ADJACENT THIOL GROUPS. Terrence L. Scott, Mario S. Rosemblatt and Noriaki Ikemoto, Dept. Muscle Research, Boston Biomedical Research Institute; and Dept. of Neurology, Harvard Medical School, Boston, MA.

The fluorescent thiol reagent S-mercuric N-dansyl cysteine (Dns.Cys.Hg) has been used previously for stoichiometric labeling of the thiol groups of the purified Ca^{2+}-ATPase of sarcoplasmic reticulum. The 12 reactive thiols may be grouped into three kinetically distinguishable classes which are,in order of decreasing reactivity; class A, 1 SH; class B, 5 SH; class C, 6 SH. The time course of the fluorescence change when one mol Dns.Cys.Hg reacts with one mol ATPase is biphasic; an initial rapid ($k = 2 \times 10^6 M^{-1}s^{-1}$) increase corresponding to the reaction with SH is followed by a slow ($k = 0.5\text{-}3 \times 10^{-3}s^{-1}$) decay. Upon separation of the protein from the reaction mixture by Millipore filtration, increasing amounts of Dns.Cys.SH are found in the filtrate. This indicates that the decay phase is the result of detachment of the Dns.Cys.SH moiety from Hg(II), the latter remaining bound to the protein, presumably in the form of an S-Hg-S bridge between SH_A and a second thiol in close proximity. Hg is linked to a second thiol, which appears to be in class B, as supported by the following facts. The Ca^{2+} dependence of the rate of bridge formation is similar to that of the reactivity of class B thiols; addition of a second mol of mercurial reagent at the peak of the fluorescence increase prevents the bridge formation. Various factors such as $[Ca^{2+}]$, $[K^+]$, ATP, ADP and pH affect the rate of bridge formation. Experiments are in progress to localize the bridge and the involved thiols within the ATPase peptide structure. (TLS is a Postdoctoral Fellow of MDA. Supported by grants from NIH (AM16922), NSF (PCM78-13008), MDA and the American Heart Association)

M-AM-E6 CYCLIC AMP-DEPENDENT PHOSPHORYLATION OF A 6,000 AND A 22,000 DALTON PROTEIN IN CARDIAC SARCOPLASMIC RETICULUM VESICLES. Jean M. Bidlack and Adil E. Shamoo. University of Rochester, School of Med. & Dent., Rochester, NY 14642.

Canine cardiac sarcoplasmic reticulum vesicles were phosphorylated at 25° at various time intervals in 40 mM histidine (pH 6.8), 2.5 mM EGTA, 0.5 mM $MgCl_2$, 25 mM NaF, and 20 μM (γ-^{32}P) ATP with and without the addition of cyclic AMP and cyclic AMP-dependent protein kinase. ^{32}P-phosphoproteins were determined by SDS-gel elctrophoresis and autoradiography. A 22,000 dalton protein, phospholamban, and a 6,000 dalton protein are dependent on cyclic AMP and protein kinase for maximal phosphorylation. Phosphorylation of the 22,000 dalton protein can be detected in less than 5 sec. after the initiation of the reaction, while the 6,000 dalton protein does not show any detectable phosphorylation until after about 1 min. of incubation with cyclic AMP and protein kinase. Both proteins reach steady state levels of phosphorylation within 10 min. Prior to phosphorylation both proteins are easily solubilized by DOC. After phosphorylation neither are solubilized by DOC. Trypsin attacks both proteins prior to phosphorylation and inhibits phosphorylation. After phosphorylation both proteins are resistant to trypsin. Both are hydroxylamine resistant. Phosphorylating the SR, then treating it successively with 90% methanol, chloroform:methanol (2:1), followed by chloroform:methanol:HCl (2:1:10 mM), will separate the 22K and 6K proteins. While the 6K protein is insoluble in acidified chloroform:methanol, the 22K is soluble, indicating the possibility of lipid being bound to the 22K protein. The individual properties of the 6,000 and the 22,000 dalton proteins are currently being investigated.

This research is supported by DOE contract and the Genesee Valley Heart Assoc. and is assigned Report No. UR-3490-1501

M-AM-E7 ON THE ROLE OF A TRANSMEMBRANE POTENTIAL OR pH GRADIENT IN SPONTANEOUS TIME-DEPENDENT CHANGES OF CALCIUM CONTENT OF SARCOPLASMIC RETICULUM VESICLES. C.F. LOUIS*, P. NASH-ADLER*, G.FUDYMA*, M.SHIGEKAWA* and A.M.KATZ. Dept. of Medicine, Univ. of Conn. Health Center, Farmington, Conn. 06032 (Intro. by R.L. Volle).

Various monovalent cation ionophores were used to examine a possible role for changing transmembrane potentials or proton gradients in controlling spontaneous time-dependent changes in Ca uptake by rabbit skeletal muscle sarcoplasmic reticulum vesicles (SR). These spontaneous changes, which were due to changing unidirectional Ca influx and efflux rates, were measured with 6 µg/ml SR at 25°C in 50 mM phosphate, 40 mM histidine buffer (pH 6.8), > 35 µM $^{45}CaCl_2$, and various concentrations of KCl. Addition of the monovalent cation ionophore Gramicidin delayed, but did not abolish, spontaneous Ca release that normally occured after approx. 6 min. in such reactions; Ca efflux rate was inhibited. This increased Ca uptake occured irrespective of the presence or direction of a K^+ gradient across the SR membrane. Valinomycin also stimulated Ca uptake in a similar manner in both KCl and NaCl (K-free) medium. Thus dissipation of a transmembrane potential due to a K^+ gradient is unlikely to account for these effects of monovalent cation ionophores. Because the spontaneous changes in Ca uptake are not abolished under conditions where these phosphate-permeant membrane also become readily permeable to cations, it is unlikely that these spontaneous changes are determined primarily by changing transmembrane potentials. Combinations of ionophores that would facilitate transmembrane proton fluxes modify the spontaneous changes in a manner similar to that observed in the presence of ionophores that would not abolish proton gradients. Thus the spontaneous time-dependent changes in Ca fluxes appear also to be independent of changing transmembrane proton gradients. (Supported by MDA, Conn. Heart Assoc., HL-21812 and HL-22135).

M-AM-E8 CHANGES IN SARCOPLASMIC RETICULUM COMPOSITION IN ACTIVATED FROG SKELETAL MUSCLE. A.V. Somlyo,*H. Gonzales-Serratos,*H. Shuman,*G. McClellan,*and A.P.Somlyo. Pennsylvania Muscle Institute and the Depts. of Physiology and Pathology of the University of Pennsylvania.

Bundles of 20 or less frog semitendinosus fibers were frozen during or after a 1.2 sec tetanus of 40 shocks/sec of 5msec duration or during a K contracture. Twitch and tetanic tension were monitored. A paired resting muscle bundle from the same animal was frozen under identical conditions. Frozen thin sections were cut at -130°C. and electron probe analysis utilizing 50-100nm probe diameter was used to measure the elemental composition of the terminal cisternae (TC) and adjacent cytoplasm (1,2,3) as well as mitochondria.

In 4 muscle bundles frozen during peak tetanic tension the [Ca] of the terminal cisternae was 53% of the paired control. A similar change in [Ca] was observed in muscles frozen during a K contracture. This approximately 40mmoles/Kg dry TC wt. was not accompanied by an equivalent uptake of Mg. Current studies are directed towards determining ion movements accompanying Ca release and uptake in the TC. The mitochondrial [Ca] in the contracted muscles was not significantly different from that in the paired resting muscles.

(1) Somlyo, A.V., Shuman, H. & Somlyo, A.P. Elemental distribution in striated muscle and effects of hypertonicity: electron probe analysis of cryo sections. J. Cell Biol. 74:828-857, 1977. (2) Somlyo, A.V., Shuman, H. & Somlyo, A.P. The composition of the sarcoplasmic reticulum in situ: electron probe x-ray microanalysis of cryo sections. Nature 268:556-558, 1977. (3) Shuman, H., Somlyo, A.V. & Somlyo, A.P. Quantitative electron probe microanalysis of biological thin sections: methods and validity. Ultramicroscopy. 1:317-339, 1976.

Supported by HL15835 to the Pennsylvania Muscle Institute.

M-AM-E9 MONOVALENT CATION CHANNEL OF SR: PRONASE REMOVES THE VOLTAGE-DEPENDENT GATE. C. Miller and R. Rosenberg*, Brandeis U., Waltham, Ma. 02154

A voltage-gated monovalent cation channel from SR may be detected by incorporating SR vesicles into a planar phospholipid bilayer by a process resembling membrane fusion. The K^+ conductance of bilayers containing many channels is low at -50mV and high at +50mV.(The "trans" side of the bilayer, to which SR vesicles are not added, is defined as ground.) Pronase added to the trans side (0.5mg/ml) causes a rapid reduction in the channel's voltage-dependence by raising the -50mV conductance more than the +50mV conductance. The channel's ion selectivity is unchanged by pronase treatment. The rate of the pronase reaction depends upon the voltage at which the reaction is run in a way suggesting that only the open state of the channel can react with pronase. Single-channel fluctuation experiments show that pronase affects the channel's probability of existing in the open state, not its open-state conductance. The pronase was fractionated, and the enzyme responsible for its action is shown to be alkaline proteinase b, a highly specific lysine/arginine endopeptidase. The purified enzyme gives the same effect at 10-20 µgm/ml that pronase does at 0.5 mg/ml. The effect of the enzyme upon SR-doped bilayers is abolished by N-tosyl-L-lysine chloromethyl ketone. The action of the enzyme, as analyzed by a two-state thermodynamic model for the channel, is to reduce the effective gating charge from 1.1 to less than 0.15, and hence to cause a given channel to exist in the open state about 50% of the time, regardless of voltage. Pronase added on the cis side of the bilayer had no effect on K^+ conductance.

M-AM-E10 STUDIES ON THE INCORPORATION AND THE FLUORESCENCE PROPERTIES OF DANSYL PHOSPHATIDYLETHANOLAMINE IN ISOLATED SARCOPLASMIC RETICULUM VESICLES. Cecilia Hidalgo, Department of Muscle Research, Boston Biomedical Research Institute, 20 Staniford St., Boston, MA 02114.

Incubation of isolated sarcoplasmic reticulum (SR) vesicles with dansyl phosphatidylethanolamine (PE) amounting to 1-5% of the SR phospholipids results in the incorporation of 90-95% of the dansyl PE in the SR membrane. At 22° the incorporation takes place as soon as dansyl PE is added to the SR vesicles. The fluorescence spectrum of dansyl PE incorporated into the SR membrane, measured in 0.1M Hepes buffer, pH 7.0, has an emission maximum at 505 nm at 25°. The excitation spectrum (λ_{em}=505 nm) reveals three peaks with maxima at 280, 290 and 330 nm, indicating that there is fluorescence energy transfer from tyrosine (presumably via tryptophan) and from tryptophan to dansyl PE. Addition of Triton X-100 to SR vesicles containing dansyl PE does not abolish the fluorescence energy transfer, even at high Triton X-100 concentrations that produce complete membrane solubilization. In contrast, gradual addition of sodium dodecyl sulfate, which produces progressive membrane solubilization, decreases energy transfer, which reaches a non-detectable level at the detergent concentration at which the membrane is completely solubilized. The fluorescence energy transfer between the membrane tyrosine and tryptophan residues and dansyl PE is only slightly decreased by addition of 0.5M NaI or KI indicating that neither donor nor acceptor chromophores are accessible to water-soluble quenching agents. The above results suggest that the fluorescence energy transfer takes place in the hydrophobic domain of the SR membrane, making dansyl PE a suitable probe to investigate conformational changes in the segment of the Ca^{2+}-ATPase buried in the lipid domain. (Supported by grants from NIH (AM-16922), the American Heart Association, and MDAA).

M-AM-E11 DEUTERIUM-NMR STUDIES OF FUNCTIONAL RECONSTITUTED SARCOPLASMIC RETICULUM MEMBRANE VESICLES. Sidney Fleischer and Cheng-Teh Wang*, Dept. of Molecular Biology, Vanderbilt University, Nashville TN 37235 and Joachim Seelig* and Michael Brown*, The Biocenter, University of Basel, Basel, Switzerland.

Reconstituted functional sarcoplasmic reticulum membrane vesicles (R-SR) were prepared with 1,2[9,10,d_2] dioleoyl phosphatidylcholine (DOPC) and measurements of quadrupole splitting and T_1 relaxation times made using a Bruker 360 MHZ Spectrometer. Quadrupole splittings were used as a measure of the ordering of the lipids. Protein-lipid recombinants (R-SR) are less ordered than are the DOPC vesicles devoid of protein. Seelig and coworkers also find similar results for E. coli and cytochrome oxidase membranes. The T_1 relaxation time is shorter in R-SR than in DOPC. Thus, the incorporation of protein reduces the rate of segmental reorientation and the membrane appears to be less fluid. We observed only a quadrupole splitting characteristic of a fluid environment. No immobilized signal was detected. (Supported by NIH grant AM14632, Muscular Dystrophy Association of America, Inc. and The Swiss National Science Foundation.)

M-AM-E12 MECHANISM OF CHLOROTETRACYCLINE TRANSPORT IN ATP-ASE RICH SARCOPLASMIC RETICULUM. Marshall S. Millman and Duncan H. Haynes, Univ. of Miami, Dept. Pharmacol., Miami, Fl. 33101

Active Ca transport by ATPase-rich SR in the presence of CTC produces a large fluorescence enhancement dependent on CTC uptake. We report the following observations on the CTC permeation rate:(1)In the absence of ATP, the CTC transport rate decreased with increasing [Ca], suggesting better permeation of the uncomplexed form.(2)Elevating the pH from 6 to 8 reduced the transport rate, indicating the neutral species as the major permeant (pK_a=6.8).(3)However, in the presence of sufficient Ca to chelate 10% of the CTC, the transport rate increased with increasing pH. The mechanism is therefore altered by small amounts of Ca, and involves greater $CaCTC^+$ binding to the more negative outer membrane surface at higher pH.(4)In the presence of ATP, CTC was added during Ca efflux induced by EDTA. Results indicate CTC and Ca move in opposite directions, and that CTC moves toward Ca^i rather than following Ca flux per se. CTC flux therefore does not involve obligatory coupling to Ca transport in active conditions. (5)However, the CTC rate constant decreased continuously with time of CTC addition after ATP. Its value when added just after ATP was twice that when added at the maximum of Ca accumulation ($t_{1/2}$=30 sec). This suggests that there is a significant cotransport of CTC with Ca at high rates of pump turnover. Analysis of the data indicates 1 CTC cotransported for every 30 Ca at 10^{-5}M CTC.(6)Addition of CTC to Ca-containing PC vesicles (which do not bind Ca) resulted in a large fluorescence increase ($t_{1/2}$=8 min). Therefore, the major mechanism for SR is $CTC^i + Ca^i(aq) \rightarrow CaCTC^i(aq) \rightarrow CaCTC^i_b$, rather than $CTC^i + Ca^i_b \rightarrow CaCTC^i_b$.(7)CTC flux upon addition at steady state of Ca accumulation is modelled to be proportional to $[SR][CTC_{tot}][Ca^i]$. The model is verified for [SR] and $[CTC_{tot}]$ and therefore predicts Ca^i to act as a trap for CTC through the complexation and membrane-binding reactions. Supported by NIH HL16117, AM20086, GM23990, HL23392 and HL071883.

M-AM-E13 COUPLED SODIUM, POTASSIUM AND CHLORIDE TRANSPORT IN ISOLATED TRANSVERSE-TUBULES OF RABBIT SKELETAL MUSCLE. Y. H. Lau*, A. H. Caswell*, M. Garcia* and L. Letellier* (Intr. by R. Robinson), Dept. of Pharmacology, Univ. of Miami, Miami, Fl. 33101.

A method for isolating transverse-tubules (T-tubules) from skeletal muscle has been established (Lau et al. J. Biol. Chem. 252, 5565, 1977). The existence of a Na^+ pump in the T-tubular vesicles was demonstrated by radioisotopes and millipore filtration techniques. In the presence of ATP and K^+, there is an initial fast phase of Na^+ uptake lasting 2-3 mins and a subsequent slow phase which continued for at least 40 mins. The active Na^+ accumulation could be inhibited by monensin but not by valinomycin; suggesting that in resting state, the Na^+ gradient across the T-tubular membrane is maintained by a Na^+ pump and intrinsic low membrane permeability to Na^+. $^{86}Rb^+$, when used as a tracer for K^+, showed a 1:1 coupling of K^+ release in the fast phase of Na^+ uptake. K^+ was then reaccumulated while Na^+ influx continued in the slow phase. Net Cl^- influx was also observed in this process. This indicated that ATP initiated an exchange of Na^+ for K^+ followed by uptake of K^+ accompanied by Cl^-. (This work was supported by MDA and NATO fellowships and research grants from NIH (1P01HLB 16117) and American Heart Association).

M-AM-F1 CHANGES IN THE ACTIVATION ENERGY OF ACTIVELY TRANSPORTED IONS DUE TO VOLTAGE CLAMP. Mumtaz A. Dinno. Physics Dept., VPI & SU, Blacksburg, VA 24061, and the Dept. of Pharmacology and Toxicology, Univ. of Louisville School of Medicine, Louisville, KY 40232.

On the basis of a simplified electrochemical model representing frog skin, the short circuit technique was introduced to distinguish between active and passive ion movement (Ussing & Zerahn. Acta Physiol. Scand. 23:110, 1951). This investigation demonstrates that while short circuiting blocks the passive components it brings about important changes on the actively transported ions. The temperature dependence of the electrophysiological parameters of frog gastric mucosa (Rana Pipiens), bathed in chloride solutions, were investigated under both open and short circuit conditions. In the open circuit (OC) experiments the hydrogen secretory rate (I_H) and membrane conductance (G) decreased with decreasing temperatures (20°C-10°C). However, the membrane potential, while consistently dropping to values below controls, exhibited changes of a relatively complicated nature. Similarly the short circuit current, hydrogen rate and the chloride current ($I_{C\ell}=I_{SC}+I_H$) decreased with temperature in the short circuited preparations. Arrhenius plots provided the activation energies for these parameters. It was found that short circuiting caused a decrease in the activation energy for H^+ and $C\ell^-$ secretion by 30% and 45% respectively. The new activation energies of $E^{I_H}_{A(SC)}$ = 8.15 KCal/mole and $E^{I_{C\ell}}_{A(OC)}$ = 6.3 KCal/mole presents clear evidence for changes in the membrane energy barrier upon short circuiting. This could be explained by changes in the polarized nature of the transepethelial shunt and/or some conformational changes in the carrier mechanisms for these ions due to the presence of the external electric field.

M-AM-F2 EFFECTS OF REAGENTS FOR AMINO GROUPS ON THE ANION CONDUCTANCE OF THE FROG SKIN D. Erlij* and I. Geld* (Intr. by E.B. McGowan) Dept. of Physiol., SUNY Downstate Med. Ctr. Brooklyn, N.Y. 11203

We have found that after blocking the Na movements across the frog skin by using either amiloride or Na-free solutions the transepithelial conductance becomes extremely sensitive to the replacement of Cl^- by other anions. Thus the conductance of 12 skins was .09 mmhos/cm^2, in Cl solution and was reduced to .04 mmhos/cm^2 when transferred to NO_3 Ringer and to .03 mmhos/cm^2 in SO_4 Ringer. In skins immersed in Cl solutions, conductance is also very sensitive to treatment with substances that react preferentially with amino groups. Addition of Trinitrobenzene sulfonate (5 mM), 2-methoxy-5-nitrotropone (50 μg/ml) and glutaraldehyde (.005%) to the apical solution reduced the conductance of the skin by 50 to 80%. The effects of the amino reagents were also apparent when ^{36}Cl fluxes were measured; the reduction in the partial Cl^- conductance estimated from the isotope measurements closely matched the change in the electrically determined conductance. When the amino reagents were added to skins immersed in SO_4 solutions no effects on transepithelial conductance were observed. This finding further suggests a selective effect on chloride pathways. Moreover, in skins in which Na transport had not been blocked the addition of the amino reagents to the apical solution had minimal or no effects on the Na transport process. These findings suggest that the Cl pathway of the skin is regulated by amino groups that are selectively accessible from the apical surface of the epithelium. Supported by the N.Y. Heart Association.

M-AM-F3 IONIC REQUIREMENTS FOR cAMP RESPONSE IN BULLFROG SMALL INTESTINE. S. J. Youmans and W.McD. Armstrong, Ind. Univ. Sch. Med., Dept. Physiol., Indianapolis, In 46223.

Recently, we proposed a mechanism by which exogenous serosal (S) cAMP alters ion transport in the small intestine of the bullfrog (1). This mechanism is consistent with our earlier data (2) on short circuit current (I_{SC}) and Na and Cl fluxes in NaCl-based Ringer's solutions, with and without 25 mEq HCO_3, and with and without SITS, a compound known to inhibit Cl/HCO_3 exchange in many cells and tissues. Features of this model are a mucosal (M) 1:1 Na:Cl influx, known to exist in bullfrog intestine, which we suggest is inhibited by S cAMP, and an electrogenic Cl/HCO_3 exchange at the basolateral cell border. In the present experiments we measured I_{SC} across intestinal sheets, stripped of external muscle, and mounted between Ringer's containing 105/105/0/0 mEq Tris/Cl/Na/HCO_3. Control I_{SC} was S-positive, + 0.09 ± 0.07 μeq/cm^2/hr (mean ± SE, n = 5), and with 6 mM S cAMP, + 0.14 ± 0.08, a change of + 0.05 ± 0.09 ($p > 0.5$). In isoosmotic Ringer's containing 105/53/0/0 mEq $Na/SO_4/Cl/HCO_3$, control I_{SC} was + 0.09 ± 0.08 (n = 7). cAMP elevated this to + 0.36 ± 0.09, a change of + 0.27 ± 0.09 ($p < 0.025$). Control unidirectional M → S Na flux ($J_{ms}Na$) was 7.53 ± 0.69 and backflux, $J_{sm}Na$, was 7.32 ± 0.82. cAMP elevated $J_{ms}Na$ to 8.28 ± 0.84, a change of + 0.75 ± 0.28 ($p < 0.05$, paired exps.), without altering $J_{sm}Na$. Thus, in Na_2SO_4 Ringer's, the elevation in $J_{ms}Na$ exceeds the increase in I_{SC}. We reported earlier a cAMP-induced S-positive elevation of I_{SC} of + 1.50 ± 0.23 ($p < 0.001$, n = 12) in Ringer's containing 105/81/25 mEq $Na/Cl/HCO_3$. Thus, removal of Cl and HCO_3 from the medium attenuates the I_{SC} response by 80%, and removal of Na and HCO_3 (retaining Cl) abolishes it. (Supported by USPHS grant AM 12715.)

(1) S. J. Youmans and W. McD. Armstrong, Physiologist 21(4): 131, 1978.
(2) S. J. Youmans and W. McD. Armstrong, Physiologist 20: 104, 1977.

M-AM-F4 THE MECHANISM OF Na^+-DEPENDENT D-GLUCOSE TRANSPORT. U.Hopfer and R.Groseclose*, Case Western Reserve University, Cleveland, Ohio, 44106

The Na^+-dependent glucose transport system catalyzes the co-transport of Na^+ and D-glucose (glc) across small intestinal and renal brush border membrane. To obtain insight into the translocation mechanism, equilibrium exchange kinetics of Na^+ and glc were determined in purified membrane vesicles of rabbit brush borders. The affinity of the transport system for glc was $4.1\pm0.5\times10^{2}$ M^{-1} (all values are means±SD) in intestinal and $3.1\pm0.4\times10^{2}$ M^{-1} in renal membranes at 0.1 M Na^+. Decreasing $[Na^+]$ to 0.001 M slightly lowered the affinity, viz. to $2.1\pm0.5\times10^{2}$ M^{-1}. In contrast, the rate of glc transport was strongly Na^+-dependent and increased 38fold between 0 and 0.2 M Na^+.$[Na^+]$ above 0.2 M was inhibitory, e.g., at 1 M NaCl the glc transport rate dropped to 42% of the maximum. The presence of 1-5 mM glc stimulated Na^+ transport, while [glc] above 10 mM had no effect. The ratio of Na^+ transported via the glucose carrier to glc was >1 at 1-5 mM glc, and <1 above 10 mM glc. These findings are compatible with a kinetic model in which the translocation step across the permeability barrier is not rate limiting for solute transport, and in which the ligands Na^+ and glc add in an ordered manner to the carrier on one side of the membrane and dissociate in an ordered sequence on the other side (iso ordered bi bi mechanism). The order of addition on the cytoplasmic side is reversed from that on the extracellular side (glide rather than mirror symmetry). Glide symmetry of substrate binding is predicted by a conformational change of the carrier with a rocker type movement, but not by a mobile carrier.

MODEL:

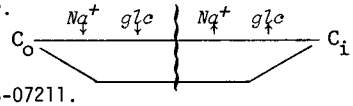

Supported by NIH Grant 2R01 AM 18265 and NSF Grant PCM78-07211.

M-AM-F5 MEMBRANE ELECTRICAL PARAMETERS IN GASTRIC MUCOSA MEASURED USING AC TECHNIQUES. C. Clausen, T.E. Machen and J.M. Diamond, UCLA Dept. of Physiology, Los Angeles, CA 90024.

The onset of HCl secretion in gastric mucosa is coupled with large morphological and conductance changes. We are interested in quantitating these changes by measuring the membrane conductances, areas, and morphological configurations using equivalent-circuit techniques in bullfrog gastric mucosa. We previously used techniques involving the analysis of voltage transients resulting from steps of constant current (Biophys. J. 21:169a). The electrical model used to represent the membrane conductances and areas consisted of "lumped" resistors and capacitors. The analysis of step response transients, however, suffers from several problems, notably the inability to extract unique sets of parameters when curve fitting, and the relative insensitivity to middle- to high-frequency effects. We therefore turned to the use of AC impedance measuring techniques, which are not subject to these problems. We found that (1) the lumped model was unable to accurately reproduce the measured impedance. We have shown earlier (Biophys. J. 17:21a) that membrane structures that border a narrow fluid-filled space (e.g., the lateral membrane) must be modeled electrically as distributed impedances. Hence we have developed a "distributed" model to represent these structures in gastric mucosa. The model accurately reproduces the impedance. (2) The changes in the circuit parameters follow the predicted physiological changes that accompany the onset of HCl secretion. (3) The circuit values determined by the distributed model are significantly different than those predicted by the lumped model. These differences are explained by the relative insensitivity of the transient method and the inadequacies of the lumped model. (4) The use of the distributed model allows one to quantitate the tubular comformation at the apical membrane and the tortuosity of the lateral spaces. Values obtained are validated by micrographs.

M-AM-F6 PERMEABILITY OF RAT GASTRIC MUCOSA TO ELECTROLYTES AND ETHANOL DURING HYPEROSMOTIC EXPOSURE. T.J. Sernka and R.E. Rollin*, Physiology Dept., Wright State Univ., Dayton, OH 45435.

The permeability of rat gastric mucosae was determined radioisotopically in the flux chamber from the unidirectional fluxes of electrolytes and ethanol during exposure to isosmotic and hyperosmotic Ringer solutions. The unmediated passive flux of Na^+ from submucosa (s) to mucosa (m) increased from 3.7 ± 0.2 μEq/cm^2h in isosmotic solution to 6.1 ± 0.4 μEq/cm^2h in 4-fold hyperosmotic solution. Similarly, the unmediated passive flux of urea from s to m increased from 0.034 ± 0.002 μmoles/cm^2h in isosmotic solution to 0.051 ± 0.003 μmoles/cm^2h in 4-fold hyperosmotic solution. In contrast, the carrier-mediated flux of Na^+ from m to s decreased from 6.4 ± 0.7 μEq/cm^2h in isosmotic solution to 4.1 ± 0.6 μEq/cm^2h in 4-fold hyperosmotic solution. Similarly, the carrier-mediated flux of Cl^- from s to m decreased from 17.1 ± 0.4 μEq/cm^2h in isosmotic solution to 8.9 ± 0.5 μEq/cm^2h in 2-fold hyperosmotic solution and to 9.2 ± 0.7 μEq/cm^2h in 4-fold hyperosmotic solution. The flux of ethanol from s to m decreased from 297 ± 20 μmoles/cm^2h in isosmotic solution to 199 ± 13 μmoles/cm^2h in 2-fold hyperosmotic solution. When isosmotic solution was replaced, the flux of ethanol from s to m rose back to 279 ± 14 μmoles/cm^2h. Hyperosmotic changes in ethanol flux from m to s were comparable. We conclude that the permeability of gastric mucosa is increased by hyperosmotic solutions to substances that are transported simply and passively but is decreased to substances that are transported by carrier mediation. By this criterion, ethanol permeation of the gastric mucosa is carrier-mediated. (Supported by USPHS, NIAAA Grant 5 ROI AA03210.)

M-AM-F7 ALTERATION OF FROG GASTRIC MUCOSA VOLTAGE TRANSIENTS DUE TO THE PRESENCE OF SCN^-. J. T. Tarvin,* H. A. Helms,* J. A. Pirkle,* and W. S. Rehm. Department of Physiology and Biophysics, University of Alabama in Birmingham, University Station, Birmingham, Alabama 35294

The time course of the voltage transient of the bullfrog fundus, resulting from the application of a step transmembrane current having a constant magnitude of 20 μA, was recorded under two sets of conditions: 1) standard amphibian solutions; 2) as in (1) with the addition of SCN^- to a final nutrient concentration of 15 mM. A total of 1024 data points were obtained for each transient, covering a time span of 0-650 milliseconds, via a microprocessor-controlled analog-to-digital converter. Previously, it has been shown that the transmucosal PD and total resistance both increase in the presence of SCN^-. Our present work confirms this result, the PD showing an average increase of 51%, and the total resistance showing an average increase of 104%. Using regression analysis, it was found that the transient data were accurately represented by a sum of 3 exponentials plus a linear background. Under control conditions, the resistance (ohm-cm^2) and time constant (msec) for each exponential were (34, 0.59), (48, 2.8), and (9, 47), respectively. Upon the addition of SCN^-, the resistances and time constants for the first two exponentials effectively doubled. The resistance for the third exponential increased by a factor of 6, while the corresponding time constant showed no significant change. Our primary orientation is that 1) total resistance measurements have been very important in advancing our knowledge about the frog gastric mucosa, and that 2) the present technique resolves the total resistance into four resistances, three of which are shunted by capacitors (the fourth resistance representing a pure ohmic series resistance). Interpretation of these results will be discussed. Also, similar experiments on the bullfrog antrum will be discussed. (NIH and NSF support.)

M-AM-F8 DOES INTRACELLULAR Ca^{2+} MODULATE THE RESPONSES OF THE AMPHIBIAN URINARY BLADDER TO SEROSAL HYPERTONICITY (SH)? M.A. Hardy and J.J. Bourgoignie* University of Miami School of Medicine, Miami, Florida 33101.

In urinary bladder of amphibia hypertonicity of the serosal bathing medium inhibits Na transport and elicits a hydrosmotic response. The following experiments were performed to determine the cationic requirements necessary for the development and maintenance of SH-induced water flow. Net water fluxes were measured across isolated toad urinary bladders at different concentrations of H^+, Na^+ and Ca^{2+} in the serosal Ringer solution. When the osmolality of the anuran Ringer was increased on the serosal side from 220 to 430 mOsm with mannitol, mean net water flux increased from 2.38±0.02 to 56.38±2.08 $\mu l.cm^{-2}.h^{-1}$ (n=22). This effect was completely prevented at pH 6.6 and was reversed by decreasing serosal pH from 8.2 to 6.6 when the response was already developed. Ca-free solutions or 2 mM serosal La^{3+} lowered the plateau response by 25%. The hydrosmotic response was completely inhibited by serosal amiloride (100 μM) or when Na was substituted by Tris. Na^+ and Ca^{2+} removal at the peak of the response inhibited the maintenance of the stimulated water flow. The inhibitory effects of pH 6.6, of Na-free or Ca-free solutions were completely reversible. Development of the response was enhanced by ouabain (100 μM) and A 23187 (5 μM). In conclusion: The hydrosmotic response to SH requires the presence of Na^+ on the serosal side of the membrane; maintenance of the plateau requires both serosal Ca^{2+} and Na^+. These ionic requirements are pH sensitive. We propose that SH increases a H^+-sensitive Na permeability at the basolateral membrane increasing intracellular Na concentration and resulting in Ca^{2+} release from intracellular pools. This increase in intracellular Ca^{2+} may be responsible for the hydrosmotic response and the inhibition of Na^+ transport by SH.

M-AM-F9 TRANSMEMBRANE POTENTIALS ACROSS TURTLE BLADDERS IN NA-RICH AND NA-FREE MEDIA. W. Nagel, J.H. Durham* & W.A. Brodsky. Mt. Sinai Sch. Med., Dept. Physiol. & Biophys., N.Y., N.Y. 10029

The transepithelial potential (PDsm), transmembrane potentials (PDcm and PDsc), the short-circuiting current (Isc) and fractional resistance of the apical membrane (Ra/Rt) were measured in the isolated turtle bladder epithelium. In Na rich media under short-circuiting conditions (PDsm=0), Isc= 60ua/cm^2, PDcm= −PDsc= −35 to −60mv and (Ra/Rt)=0.5 during control periods; After mucosal amiloride, Isc= −10ua/cm^2, PDcm= −80 to −90mv, and Ra/Rt= 0.95. Under open-circuit conditions (PDsm= 100mv), PDcm= +10mv, and PDsc=35 to 60mv during control periods. After amiloride, PDsm= 0 and PDcm= −90 to −110 mv. In Na-free media under short-circuiting conditions, Isc= −10ua/cm^2 and PDcm= −80mv during control periods. After substitution of SO_4 for Cl and HCO_3 in mucosal fluid, PDcm increased to −90mv. Under open-circuit conditions, PDsm= −40 to −60mv, PDcm= −120 to −140mv and PDsc= 80-90mv during control periods. After substitution of SO_4 for Cl and HCO_3, PD_{sm}= 0, PDcm= −80 to −90mv. When choline was substituted for Na in the mucosal fluid of short-circuited bladders, Isc decreased from 60ua/cm^2 to 0 and PDcm decreased from −45 to −75mv; then choline Ringer (with ouabain) was substituted for Na in S and PDcm increased from −75 to −30mv. Electrogenic anion (HCO_3 and Cl) pumps in the apical membrane and an electrogenic Na pump in the basal-lateral membrane would account for these changes.

M-AM-F10 EFFECTS OF MUCOSAL Cl SUBSTITUTIONS ON THE ELECTRICAL PARAMETERS OF TOAD URINARY BLADDER: MICROELECTRODE STUDIES. Javier Narvarte* and Arthur L. Finn, UNC School of Medicine, Chapel Hill, N.C. 27514.

The electrical potential across the tissue (V_{MS}), the cell membranes (apical:V_{MC}; basolateral:V_{CS}), and the electrical resistances of the tissue (R_T), the cell membranes (R_A, R_B), and the shunt (R_S) were measured before and after changes in mucosal Cl concentration ($[Cl]_M$). We could compute the equivalent electromotive forces (EMF's) for the apical (V_A) and basolateral (V_B) membranes from the measured transmembrane potentials and resistances. A decrease in $[Cl]_M$ (Gluconate or Sulfate substitutions) resulted in a reversible depolarization of all potentials and EMF's, which could not be explained by a reduction in mucosal Ca activity. At 12 mM $[Cl]_M$ the mean changes were 15 $\pm$ 1.4 mV for V_A and 10 $\pm$ 1.3 mV for V_B. There was a 20% to 100% increase in R_S, with no significant changes in R_A or R_B. On the other hand, Iodide-for-Cl substitutions resulted in hyperpolarization of V_{MC}, V_{CS}, V_A and V_B. These results confirm previous observations in this tissue (AJP: 221:1019, 1971) and suggest an effect of mucosal Cl replacement on Na transport, that is a function of the main anion in solution. To investigate the effect of mucosal anion replacements on Na permselectivity of the mucosal membrane, Na reductions (K replacement) were performed in Cl free media. The changes in EMF's brought about by lowering $[Na]_M$ were smaller than the changes observed in Cl media. This observation can be explained by the lower baseline values of EMF's in Cl-free media as compared to Cl Ringer, since a direct relationship between the baseline V_{MS} and the change in V_{MS} brought about by Na reductions (previously described in Cl Ringer) was also found in Cl-free media. Thus, the transport potential is partly determined by mucosal Cl, but this control is not exerted via an apical conductance for Cl. Supported by NIH grant AM17854.

M-AM-F11 EFFECTS OF TRIAMINOPYRIMIDINE ON ELECTRICAL PATHWAYS OF GALLBLADDER EPITHELIUM. L. Reuss and T.P. Grady*, Dept. of Physiology and Biophysics, Washington Univ. School of Medicine, St. Louis, MO 63110.

The protonated form of 2,4,6-triaminopyrimidine (TAP^+) has been shown to block selectively paracellular sodium conductance in gallbladders of rabbit and other species. In frog gallbladder, the resulting increase in transepithelial electrical resistance (R_t) is accompanied by an increase in transmural potential (V_{ms}) which was taken as an indication of electrogenic Na transport (Moreno, J.H., Nature 215: 150, 1974). To study the mechanism of the latter effect, the action of TAP^+ on Necturus gallbladder was studied with microelectrode techniques previously described (Reuss, L. and Finn, A.L., J. Membrane Biol. 25: 115, 1975). Transepithelial and cell membrane potentials, and cell membrane and paracellular resistances were measured. From these data, equivalent electromotive forces (emf) at the cell membranes and the paracellular pathway were calculated under control conditions and during exposure to TAP^+ (total concentration 10 to 20 mM) either on the mucosal or on both sides. Mucosal solution ionic substitutions were performed under the two conditions. TAP^+ reduces paracellular Na and K conductances. In addition, it reduces the K permeability of the luminal membrane, therefore decreasing total membrane conductance, equivalent emf and dependence of the apical membrane potential and emf on external K activity. This effect and the increase in paracellular resistance, account for the increase of V_{ms} observed during exposure to TAP^+, without the need to postulate an electrogenic Na transport mechanism. Supported by NIH Grant AM 19580.

M-AM-F12 AN IMPROVED MODEL FOR LITHIUM PHARMACOKINETICS IN MANIC-DEPRESSIVE PATIENTS. B.E. Ehrlich, C. Clausen, J.A. Maga*, J.M. Diamond and L. Gosenfeld*, UCLA Department of Physiology and Brentwood VA Hospital, Los Angeles, California 90024.

Lithium (Li^+) is the drug of choice for treating manic-depressive (MD) illness. Doses required to achieve therapeutic plasma levels vary nearly 6-fold among individuals, yet the toxic level is only twice the therapeutic level. Because, for any drug, individuals may vary in the rate constants for gut absorption, plasma-cell transport and equilibration, drug metabolism, and renal excretion, a pharmacokinetic model for Li^+ was developed and tested using single-dose kinetic experiments. We administered one 600 mg dose of Li_2CO_3 to MD patients and to normal controls. Changes in $[Li^+]$ over the next 24 hours were measured in 16 plasma and erythrocyte (RBC) samples. Excreted Li^+ was measured in the urine. Since Li^+ is not metabolized, we are able to extract rate constants for gut absorption, plasma-cell equilibration, and renal excretion, and volumes of distribution, by curve fitting a three-compartment open model to all data simultaneously. From the rate constants determined from a single Li^+ dose, we are able to predict Li^+ fluctuations during multiple dosing, and hence the optimal therapeutic dosage, for each individual. Li^+ kinetics were found not to differ between untreated MD patients and controls. The most marked differences among individuals are in gut absorption and renal excretion rates. From our measurements and model, we estimate the Li^+ distribution rate and flux in inaccessible compartments. This estimated distribution ratio agrees well with direct measurements for muscle, probably the major inaccessible compartment.

M-AM-Po1 CRYOPRESERVATION OF THE MOTILE CYTOSKELETON OF NITELLA. N. Strömgren Allen* and G.R. Ruben* (Intr. by R.D. Allen), Dartmouth College, Hanover, N.H. 03755.

A motile cytoskeleton consisting in part of subcortical fibrils and branched endoplasmic filaments of F-actin is part of a system that delivers the motive force responsible for the rapid rotational cytoplasmic streaming and saltatory movements in characean cells (N.S. Allen and R.D. Allen, Ann. Rev. Biophys. Bioeng. 7:497, 1978). Freeze-fracture and etching of Nitella cells preserves endoplasmic filaments throughout all regions of the endoplasm; many filaments are closely associated with organellar membranes as is observed in vivo. Since conventional chemical fixation preserves filaments and their associated organelles (e.g. spherosomes) very poorly in large, highly vacuolated plant cells (see also Mercy and McCully, J. Microscopy 114:49, 1978), it is evident that rapid cryopreservation of cells can preserve cytoskeletal structures as well as their relationship to membranes and organelles. The freeze-fracture results provide direct confirmation of the light microscopic observations of numerous endoplasmic filaments and their association with saltating particles (N.S. Allen, J. Cell Biol. 63:270, 1974). (Supported by NIH grant GM 22356)

M-AM-Po2 CHANGE IN ARRANGEMENT OF CORTICAL MICROFILAMENTS ASSOCIATED WITH CHANGE IN CELL LOCOMOTOR ACTIVITY. Wen-Tien Chen* (Intr. by Shaw-Chen Chen), Department of Biology, Yale University, New Haven, CT 06520.

Movement of embryonic chick heart fibroblasts in culture involves a cycle of protrusion of lamellipodia and microspikes into the medium, their attachment to the inanimate substratum or to other cells, and their retraction, resulting in either rupture of the attachment or formation of long, taut retraction fibers. Since lamellipodia, microspikes, and retraction fibers are very thin (0.1-0.2 μm thick), the arrangement of their microfilaments (MF) can be observed in critical point dried whole mounts with TEM at 80 kv. Individual fibroblasts were filmed with time-lapse, using phase contrast, polarizing, and interference reflection optics, before and during fixation, in order to record the locomotor activity of each living cell at the time of its fixation. Unattached lamellipodia and microspikes are very weakly birefringent, but, significantly, immediately after attachment to the substratum and upon retraction, they become strongly birefringent, with an average retardation of 1.9 nm. Strong birefringence persists as long as tips of microspikes and retraction fibers remain adherent, but fades as they detach and retract. MF in weakly birefringent extending and retracting protrusions free of the substratum are arranged in a meshwork. In contrast, in strongly birefringent extensions under stress, such as retraction fibers and portions of lamellipodia in contact with the substratum or other cells, the meshwork of MF is aligned to varying degrees to form "bundles" oriented in the direction of stress. Retraction fibers artificially induced by application of Ca^{++} and serum-free medium also show strong birefringence and MF arranged in "bundles". These observations suggest that a meshwork of MF is oriented to form "bundles" when tension is applied to the system. Supported by an NIH grant (USPHS-CA 22451) to J.P. Trinkaus.

M-AM-Po3 A STUDY OF THE MOBILITIES OF LABELLED COMPONENTS IN CYTOPLASMIC GELS BY FLUORESCENCE PHOTOBLEACHING RECOVERY. F. Lanni* and B. R. Ware, Department of Chemistry and J. Birmingham* and D. L. Taylor, Department of Biology, Harvard University, Cambridge, MA 02138

The sol-gel transition in the cytoplasm of certain motile eukaryotic cells has been shown to be an important feature of the mechanism of the generation of the motive force. Using cytoplasmic extracts prepared from Dictyostelium discoideum, we have monitored the mobility of labelled particles throughout the sol-gel transition to study the gelation process and the structure of the final gel. Measurements have been performed using the technique of fluorescence photobleaching recovery, in which fluorescence intensity from a small volume in the sample is monitored before and after an intense bleaching pulse. The time dependence of the return of fluorescence after the bleaching pulse is a measure of the diffusion coefficient of the labelled particles. For passive fluorescent probes we have used small dye molecules (fluorescein) and covalently labelled macromolecules, viruses, and polystyrene microspheres. Experiments have also been performed in which the fluorescent label is carried on actin, the major cytoplasmic gel component. Extensions of this method include the possibility of real-time monitoring in situ of the mobility of cytoplasmic gel components during the contractile process.

M-AM-Po4 PROPERTIES OF ACTIN FROM PORCINE BRAIN. J. Weir* and D. Frederiksen (sponsored by R. Post), Department of Biochemistry, Vanderbilt University, Nashville, TN 37232

Highly purified brain actin has been prepared by a procedure involving DEAE-cellulose chromatography, a polymerization-depolymerization step, and gel filtration chromatography. Electrophoresis on polyacrylamide gels in the presence of SDS shows a single band corresponding to more than 95% of the applied protein and migrating with the relative mobility of skeletal muscle actin. Brain actin activates the low ionic strength Mg^{++}-ATPase activities of both skeletal muscle and brain myosins; this non-muscle actin polymerizes or depolymerizes under conditions similar to those which elicit these phenomena in skeletal muscle actin. Although similar to its skeletal muscle counterpart, brain actin is distinctly different. Isoelectric focusing experiments indicate that brain actin consists of two species each of which are more basic than the α-fraction of skeletal muscle actin. The polymerization of brain actin was followed by viscometry and sedimentation techniques as a function of protein concentration, temperature, and ionic milieu. These experiments indicate higher critical actin concentrations for the brain protein than for muscle actin under all conditions tested. (Supported by a Basil O'Connor Starter Research Grant from the National Foundation and by NIH Research Grant HL 18516).

M-AM-Po5 PARTIAL CHARACTERIZATION OF MYOSIN FROM PORCINE BRAIN. D. Hobbs* and D. Frederiksen. Department of Biochemistry, Vanderbilt University, Nashville, TN 37232.

A highly purified myosin has been isolated from porcine brain. This protein has a Mg^{++}-ATPase activity of 4 nmoles/mg·min at low ionic strength and 25°C; skeletal muscle actin and porcine brain actin activate this activity about six-fold. The brain myosin has a high specific K^{+}(EDTA)-ATPase activity, 700 nmoles/mg·min, at pH 8.0 and high ionic strength in the presence of 2.0 mM EDTA. Sedimentation velocity studies on brain myosin at 20°C in 0.6 M KCl-2mM EDTA-50mM Tris-Cl (pH 8.0) give an intrinsic sedimentation coefficient of 4.98 S, and the data indicate that aggregation of myosin occurs under these conditions. This observation is in contrast to that with skeletal and smooth muscle myosins which are monomeric under these conditions. Diffusion analysis also indicates aggregation of myosin and gives an intrinsic diffusion coefficient of 1.0×10^{7} cm^2/sec. Thus, brain myosin has a monomeric molecular weight of 456,000 daltons. The frictional ratio of the protein, f/f_0, is 3.40, assuming 0.2 gms of bound water/gm myosin. Comparison of these values with those reported for skeletal and smooth muscle myosins indicates that brain myosin may be more resistant to translation through a viscous solvent than its muscle counterparts. (Supported by a Basil O'Connor Starter Research Grant from the National Foundation and by NIH Research Grant HL 18516).

M-AM-Po6 IS SPECTRIN A MYOSIN? F. H. Kirkpatrick, Department of Radiation Biology and Biophysics, University of Rochester, Rochester, N.Y. 14642

Crude spectrin fractionated on large-pore gel chromatography columns displays three peaks: a void volume "network" fraction, and two trailing peaks (spectrin tetramer and dimer). The network fraction contains spectrin and actin, in approximately stoichiometric ratio, while the tetramer and dimer fractions contain only spectrin. Under certain conditions of preparation, which appear to include lysis and washing of red cell membranes in 15mM or greater salt (NaHCO3), the network fraction contains an ATPase. This ATPase is stimulated by high concentrations of monovalent salts (1M), NH4Cl>KCl (no activity with NaCl) in the presence of EDTA, or by CaCl2 (100mM). Activity is also stimulated by MgCl2 (5mM). Average specific activities are 1.5μ mol/mg.hr (NH4), 0.5 (K or Ca) and 0.1 (Mg), but maximum observed velocities are over three times these values. The NH4, K or Ca ATPase activities are inhibited by MgCl2 (10μM for NH4 or K, 10mM for Ca) and then display the low level of ATPase seen with MgCl2 alone. The pattern of ATPase activity resembles that of myosin. Activation by added actin is not observed, presumably because the active spectrin is already saturated with actin. Non-erythrocytic myosins and other enzyme systems (kinase-phosphatase, pyrophosphatase) have been excluded. The non-physiological ATPase activities are not present in red cell ghosts, but appear during dialysis against low-ionic strength media, and in conjunction with a substantial loss of total Mg-ATPase activity. The K or Ca ATPase of spectrin-actin network fragments may reflect a partial denaturation of an acto-myosin-like network responsible for maintaining red cell membrane flexibility; and purified spectrin tetramer and dimer might be entirely denatured species. A possible mode of operation of this system will be illustrated.

Supported by NIH and DOE (Report #UR-3490-1497)

M-AM-Po7 SEQUENCE, INTERACTION AND FUNCTIONAL STUDIES OF EQUINE PLATELET TROPOMYOSIN. G.P. Cote*, W.G. Lewis* and L.B. Smillie, M.R.C. Group on Protein Structure and Function, Department of Biochemistry, University of Alberta, Edmonton, Canada T6G 2H7.

Amino acid sequence studies of horse platelet tropomyosin (plTm) although incomplete have demonstrated that the NH_2- and COOH-terminal sequences are markedly different when compared with muscle tropomyosin (mTm). This can be correlated with the relative inability of the protein to polymerize end-to-end. The plTm also binds poorly to muscle troponin even though the amino acid sequence in the central region of the structure including residues 197-217 (the hypothetical troponin binding site) is very similar to mTm. The major deletion dictated by its smaller molecular length when compared with muscle tropomyosin must lie near its NH_2-terminal end which is acetylated. The effects of plTm on the ATPase activity of a skeletal myosin S-1:skeletal actin (molar ratio 1:2.5) system have been examined. Under the assay conditions used (30 mM KCl, 5 mM $MgCl_2$, 2 mM ATP, 2 mM Tris, 2 mM DTT, 1 mM EGTA, pH 7.8) mTm inhibits the ATPase up to 60% while plTm has no effect. The potentiating effect of mTm on the inhibition of ATPase activity by muscle troponin-I (Tn-I) (90% inhibition at molar ratios of mTm:Tn-I:actin = 2:1:7) is less effective with plTm (60% inhibition at molar ratios of plTm:Tn-I:actin = 3:1:7). This inhibition in the presence of plTm can be increased to 90% by elevating the ratio of Tn-I:actin to 3:7. Similar results were found using whole muscle troponin instead of Tn-I. Under these assay conditions the binding of plTm to F-actin was found to be weak but was markedly increased by the addition of Tn-I or whole troponin. While the inhibition of the actin- S-1 ATPase in the presence of mTm and muscle troponin is released on addition of Ca^{++}, the corresponding inhibition in the presence of plTm is only partially (40-50%) released by Ca^{++}. (Supported by MRC of Canada)

M-AM-Po8 DEGRADATION OF SQUID NEUROFILAMENT PROTEINS BY A CALCIUM ACTIVATED PROTEASE. H.C. Pant and H. Gainer* NIMH, NIH, Bethesda, Md. 20014.

There have been several reports in the literature of Ca^{2+}-activated proteases found in various nervous tissues. However, due to the nature of the biological material, it was neither possible to evaluate the cellular origin of the protease (i.e., glial or neuronal), nor the endogenous substrates upon which it acted. Squid giant axons provide a unique model system for such a study. Some of the special features of this experimental preparation for biochemists is that the sheath which consists of the plasma membrane and surrounding satellite cells can easily be separated from the axoplasm by extrusion, and thus provides a unique opportunity for studying the properties of Ca^{2+}-activated endogenous proteases and substrates in this isolated system. In this presentation we have provided evidence for a protease in squid axoplasm which is selectively activated by Ca^{2+}, and blocked by SH-inhibitors and leupeptin. There appear to be two Ca^{2+}-activated proteases in the axoplasm, one in 100,000 x g supernatant and the other in the pellet. The protease present in the pellet degrades the 200,000 dalton neurofilament protein but also extensively degrades various other major protein components in the axoplasm. However, the protease present in the supernatant selectively degrades the 200,000 dalton neurofilament protein. Properties of this protease will be discussed and compared with other Ca^{2+}-activated proteases from other systems.

M-AM-Po9 SQUID NEUROFILAMENT PROTEINS. P. F. Roslansky* and R. V. Rice, Carnegie-Mellon Univ., Pittsburgh, PA 15213 and MBL, Woods Hole, MA 02543.

Neurofilaments can be physically separated from the rest of the axoplasm of the squid Loligo pealei by sonication and Millipore filtration. The neurofilament-rich retentate has been examined by SDS gel elecrophoresis and transmission electron microscopy. Using 5.6% Fairbanks gels, two major proteins with molecular weights of 63,000 and 200,000 were seen. Two other proteins with higher molecular weights were also consistently seen. Better resolution of the higher moleuclar weight proteins has been achieved using 4% Fairbanks gels. Axoplasm was electrophoresed alone and co-electrophoresed with the molecular markers flagellar dynein and spectrin. The calibration curve relating R_f to molecular weight was determined using albumen, ovalbumen and an extract of the anterior byssus retractor muscle of Mytilus edulis containing myosin, paramyosin and actin. Using 4% gels, the 200,000 dalton protein separated into two bands with molecular weights corresponding to 240,000 and 220,000. These comigrated with the bands of spectrin and had a distinctly lower R_f than the myosin of the standard solution. Dynein comigrated with a set of 3 or 4 bands having an approximate molecular weight of 380,000 to 420,000. The molecular weight of the heaviest polypeptide was 540,000 to 580,000. These high molecular weight polypeptides and the 63,000 D polypeptide have been isolated and tryptic peptide maps have been prepared using thin layer chromatography and high voltage electrophoresis. Electron microscopy of neurofilaments negatively stained with 2% uranyl acetate suggests the existence of more than one protein.

M-AM-Pol0 THE PURIFICATION AND CHARACTERIZATION OF TUBULIN FROM HUMAN LEUKEMIC LYMPHOID TISSUE. L. Liebes, D. Zucker-Franklin* and R. Silber*, New York University School of Medicine, New York, NY 10016.

Chronic lymphocytic leukemia (CLL) lymphocytes show a markedly increased sensitivity to the lethal effects of colchicine. Since tubulin is the principal, if not sole target site for this drug, we decided to purify, characterize and quantitate this protein from leukemic lymphocytes. Tubulin was purified to homogeneity from human leukemic spleen by a modification of the procedures of Eipper and Luduenna et al. (Eipper, B.A., P.N.A.S., 69:2283, 1972; Luduenna et al., J. Biol. Chem., 252:7006, 1977). Like its counterpart in other tissues, it is a dimeric molecule with the α and β subunits migrating with molecular weights respectively of 63,700 and 59,400 as compared to values of 60,000 and 56,500 for the α and β subunits of human brain tubulin. Under conditions which promote efficient in vitro assembly of neuronal tubulin, purified lymphocyte tubulin polymerized into microtubules as assessed by turbidity measurements at 350 nm and electron microscopy. Partial cross reactivity was observed between human lymphoid tubulin and human brain tubulin with rabbit antibody raised against human brain tubulin. The level of tubulin in normal and CLL lymphocytes was determined by a colchicine binding assay and found to be respectively 1.13 ± 0.33 to $1.42 \pm .87$ g x 10^{-2} tubulin/g soluble lymphocyte protein. These studies show the following: 1) Tubulin is approximately 1% of the total soluble lymphocyte protein; 2) Certain properties and some antigenic determinants are shared with human brain tubulin; 3) The similar level of tubulin in normal and CLL lymphocytes suggests that factors other than the level of this cytoskeletal protein must account for the sensitivity of CLL lymphocytes to colchicine.

M-AM-Pol1 A HIGH SENSITIVITY DIFFERENTIAL SCANNING CALORIMETRIC STUDY OF THE POLYMERIZATION OF CALF BRAIN MICROTUBULES. S. A. Berkowitz, G. Velicilebi* and J. Sturtevant*, Dept. of Chemistry, Yale University, New Haven, CT 06520.

The specific heat associated with the polymerization of microtubules in a buffer system containing 2M glycerol, 100mM PIPES, 2mM EGTA, 1mM $MgSO_4$ and 1mM DTE at pH 6.9 was measured using a differential scanning microcalorimeter. Data gathered indicate that there are two irreversible exothermic reactions accompanying the assembly of microtubules. The assignment of both reactions to microtubule assembly was based on the correlation between calorimetric scans and plots showing the amount of inorganic phosphorus and turbidity produced during polymerization as a function of temperature (where the temperature was scanned at rates similar to those used for calorimetric experiments). The assignment was further supported by correlating the effect of Ca^{++} on calorimetric scans and on scans of turbidity versus temperature. In both cases scans were shifted to higher temperatures on increasing the concentration of free Ca^{++} (1.5-10.0mM). In addition, the shapes and positions of the two exothermic peaks were found to be dependent upon both the molar ratio of GTP to tubulin and the scan rate. The main conclusion drawn from our data is that the reversibility of the assembly-disassembly process of microtubules is only apparent since microtubule polymerization is coupled to the irreversible cleavage of GTP. Hence, the van't Hoff enthalpy for microtubule polymerization determined from temperature studies on the equilibrium constant associated with this process is also an apparent quantity which does not necessarily equal the enthalpy determined directly by calorimetry. (Supported by NIH grant GM04725)

M-AM-Pol2 NOCODAZOLE LENGTHENS LIVING STENTOR. Victor Kai-Hwa Chen and Greg Cooper* Case Western Reserve University, Cleveland, Ohio 44106

Nocodazole, methyl[5-(2-thienylcarboyl)-1H-benzimidazol-2-yl]carbamate,R17934 , a new synthetic microtubule inhibitor lengthens living Stentor.The increase in the body length of the cone shaped free-swimming cell was proportional to the Nocodazole concentration added to the medium. The cell lengthened by 150% in 30uM Nocodazole. The minimum concentration of Nocodazole to produce a statistically significant cell lengthening was 0.1pM. Aside from their increased lengths the treated cells looked and behaved like naturally long cells found normally in cultures. This treatment did however alter the response of the cells to stimulation in two respects. 1) The magnitudes of mechanical and electrical stimuli needed to elicit cell contraction was greatly reduced. 2) The rate of habituation of the cell to mechanical stimulation was increased. The degree of alteration both responses were proportional to the concentration of Nacodazole present. Cells treated for a few second with Triton-X100 or saponin nolonger responded to Nacodazole. Cells lengthened in 10mM EGTA+(0.5-3)mM $MgSO_4$were not furthered effected by Nacodazole. However 10mM EGTA+(0.5-3)mM $MgSO_4$shortened the Nocodazole treated cells to their normal lengths. Calcium levels neither very low nor very high had any effect on the length or the excitability of Nacodazole treated cells. The theory in which Mg^{++}ions were the sole control of microtubule ribbon overlap in km fibers for cell extension appears inadaquate to explain our observations. We speculate 1)that "labile" microtubules depending on their length or number hold the ribbons of "stable" microtubules apart to differing degrees 2)that these "labile" microtubules are in contact or very near the cell membrane,are responsible for controlling the degree of cell extension.

M-AM-Pol3 EFFECTS OF SWIMMING SPEED, SHAPE AND HEAD ROTATION FREQUENCY OF SPERMATOZOA ON ELECTRIC FIELD AUTOCORRELATION FUNCTIONS OF SCATTERED LASER LIGHT. F. R. Hallett and T. C. Craig,* Department of Physics, University of Guelph, Guelph, Ontario N1G 2W1

Earlier quasielastic light scattering investigations on suspensions of live spermatozoa indicated that one could analyze the electric field autocorrelation function, $g^{(1)}(\tau)$ from the relationship

$$g^{(1)}(\tau) = 4\pi \int_0^\infty \frac{\sin(kv\tau)}{kv\tau} P_s(v)\, dv \qquad (I)$$

Such an analysis yielded swimming speeds for bull spermatozoa which were comparable to those observed by other techniques. However, equation (I) above assumes that the spermatozoa are point sources travelling on straight lines for times comparable to the measurement time. Such assumptions are difficult to rationalize for spermatozoa which have a large elliptical head, a long fairly rigid tail and a non-linear swimming trajectory. Recently we have calculated numerically the electric field autocorrelation function for ellipses over a range of axial ratios, a range of swimming speeds and a range of head rotation frequencies. Comparison of these functions to real data indicates that spermatozoa behave as ellipsoids with an axial ratio of about 12:1. The functions appear to be more sensitive to head rotation frequency than to linear velocity.

M-AM-Pol4 LACK OF CORRELATION OF ELECTROPHORETIC MOBILITY WITH ADHESION OF LEUKOCYTES TO ENDOTHELIAL CELLS INDUCED BY CHEMOTACTIC FACTORS. R. L. Folger* and B. R. Ware, Department of Chemistry, Harvard University, Cambridge, MA 02138 and R. L. Hoover* and M. J. Karnovsky*, Department of Pathology, Harvard Medical School, Boston, MA 02115 (Intr. by D. F. Englert)

During an inflammatory response, circulating polymorphonuclear cells (PMN's) adhere to the endothelial lining of vessels in the immediate area of inflammation. Prior studies *in vivo* and *in vitro* have shown that chemotactic factors such as bacterial filtrate, C5-a, and zymosan-activated serum enhance the specific adhesion of PMN's to the endothelial cells. It has been proposed that the increased adhesion is due at least in part to a reduction in the surface charge density of one or both types of cell. The experimental parameter most closely related to surface charge density is the electrophoretic mobility. Using the laser Doppler technique of electrophoretic light scattering (ELS), we have measured the electrophoretic mobilities of PMN and endothelial cells before and after incubation with chemotactic factors (bacterial filtrate, C5-a and zymosan-activated serum) and controls (C5 and normal serum). Both active and control factors induced a reduction in the electrophoretic mobilities of both types of target cell. However, in most cases significant differences between adhesion promoting factors and control factors were not observed. We conclude that surface charge reduction is not an essential feature of PMN's adhesion to endothelium. Supported by NIH grants HL-09125 and GM-23788.

M-AM-Pol5 ON THE GENERATION OF TORQUE IN THE FLAGELLAR MOTOR OF BACTERIA. Charles L. Stevens, Department of Biological Sciences, University of Pittsburgh, Pittsburgh, PA 15260.

Bacteria swim by rotating flagella about their long axis. It is likely that torque for the rotation is generated by an apparatus embedded in the cell wall and plasma membrane, consisting of several discs arranged in pairs and mounted coaxially on a rod. The rod is connected to a hook which in turn is attached to the flagellum. It is believed that the apparatus constitutes a motor which utilizes as a source of power, a gradient in electrochemical potential existing across the plasma membrane. It has been proposed that ion-conducting channels exist which can conduct protons only when those on opposing faces of the discs are superimposed. I wish to propose a model in which torque is generated by electrostatic repulsion of anionic groups located in these surface channels. At the appropriate rotational positions, the groups bind a proton and become buried in an apolar surface region on the opposite disc. By suitable arrangement of channels, anionic groups and apolar surfaces the model will produce a torque of constant sign over a full rotation. Calculations show that it is also large enough to propel the bacterium. The prototype for such surface groups are the anionic groups in protein from tobacco mosaic virus which bind a proton at a pH far above the intrinsic pK of the group, then become buried in a protein environment upon polymerization.

This work was supported by a research grant, GM 22558, from the National Institutes of Health, Bethesda, Maryland.

M-AM-Po16 Fe-BLEOMYCIN, A COMPLEX RESEMBLING HEME OXYGENASES.

R. M. Burger*, J. Peisach, W. E. Blumberg, and S. B. Horwitz,* *Albert Einstein College of Medicine, Bronx, N. Y. 10461, and Bell Laboratories, Murray Hill, N. J. 07974.*

Bleomycin (BLM) is a low molecular weight (~1550 dalton) glycopeptide antibiotic which contains no obvious prosthetic group such as porphyrin. It can bind an equimolar amount of Fe(II) yeilding a complex with a characteristic optical signature (λ_{max} = 476 nm). The formation of this complex is required for efficient, oxygen-dependent degradation of DNA by BLM.* CO alters the optical spectrum of the Fe(II)-BLM complex (λ_{max} = 384 nm) and also inhibits DNA degradation. NO binds to Fe(II)-BLM to form a paramagnetic complex (λ_{max} = 470) having an EPR spectrum exhibiting magnetic coupling to the NO (A_N = 24 gauss) similar to that observed for various NO-hemoproteins. Thus, Fe(II)-BLM has many of the properties of ferrous heme-containing oxygenases and might be considered to mimic this class of enzymes. Fe(II)-BLM autoxidizes at neutral *p*H to form a low spin ferric complex (λ_{max} = 365, 384 nm) the EPR of which has properties (g = 2.45, 2.18, 1.89) that resemble those of ferric myoglobin and other ferric hemoprotein hydroxides. At *p*H less than 3.8, BLM forms a high spin ferric complex (λ_{max} = 430 nm) of the rhombic type (g = 9.5, 4.3) since BLM contains no rigid prosthetic group to impose axial symmetry, such as the porphyrin that is found in heme-containing oxygenases. It is suggested that the ligands of Fe(II) in the BLM complex play a role in the activation of O_2, similar to that of porphyrin in heme-containing oxygenases.

---

*E. A. Sausville, *et al.* (1978) *Biochemistry* 17, 2740 and 2746.

M-AM-Po17 POSSIBILITY OF A μ-OXO BRIDGE BETWEEN IRON AND COPPER IN CYTOCHROME *c* OXIDASE.

W. E. Blumberg and J. Peisach, *Bell Laboratories, Murray Hill, N.J. 07974, and Department of Molecular Pharmacology, Albert Einstein College of Medicine, Bronx, N.Y. 10461.*

Cytochrome *c* oxidase is a multisubunit protein which contains both iron and copper. One of the subunits, designated cytochrome a_3, contains one iron atom bound in a molecule of heme *a* and is associated with one atom of copper. In the fully oxidized state the iron and copper atoms are usually considered to be ferric and cupric, respectively, but the paramagnetic properties of these metal atoms are not observed in EPR experiments because of strong antiferromagnetic coupling between them. From the magnitude of the coupling, one concludes that the iron and copper atoms are separated by no more than a few atoms. EPR experiments show that the iron is ligated to an imidazole group in both partially reduced and fully reduced redox states of the enzyme. One can envision three cases for the bridging group: (1) the imidazole group; (2) an endogenous group from the protein located on the side of the heme *a* distal to the imidazole; (3) an exogenous group. Case (1) can be discounted as the EPR of ferric heme *a* in partially reduced preparations shows that the imidazole is deprotonated, *i.e.* it lacks H^+, Cu^{2+} or any other cation on the uncoordinated nitrogen atom. Case (2) would hypothesize either an imidazole or carboxyl function to bridge the metal atoms. One would have to postulate that this group would be readily displaced by hydroxide, hydrosulfide, azide, and cyanide to give the observed EPR spectra in partially reduced states. It would also have to be displaced by O_2, CO, and NO in the fully reduced state. The most likely bridge in case (3) would be a single oxygen atom providing a μ-oxo linkage which would be jettisoned and regenerated during each enzyme turnover cycle. This hypothesis can be shown to be consistent with all known chemistry of cytochrome a_3 and leads to several experimental tests. Infrared stretching frequencies for both $Fe-O$ and $Cu-O$ should be observable in the oxidized enzyme, and these would be labelled by isotopically variant O_2 under *single turnover* conditions. Analysis of the EXAFS of the iron and copper x-ray absorption edges would show a $Fe-Cu$ distance of about 3 Angstrom.

M-AM-Po18 LINKAGE BETWEEN OXYGENATION AND SUBUNIT DISSOCIATION IN HEMOGLOBIN KANSAS.

D.H. Atha and A. Riggs, Dept. of Zoology, University of Texas, Austin, Tx. 78712, and M.L. Johnson, Clinical Endocrinology Branch, National Institute of Arthritis, Metabolism and Digestive Diseases, National Institutes of Health, Bethesda, Md. 20014.

Measurement of the concentration dependence of the oxygen binding equilibria of hemoglobin Kansas (a variant human hemoglobin with a substitution at the $\alpha_1\beta_2$ interface) was made with an automated Imai apparatus (Imai et al., Biochim. Biophys. Acta. 200:189, 1970) and a Gill cell (Dolman and Gill, Anal. Biochem. 87:127, 1978). Measurements were made at 20° in Tris/HCl buffer, pH 7.5, containing 0.1 M NaCl, 1 mM EDTA. The oxygen affinity of the hemoglobin decreases greatly when the concentration is increased from 0.36 μM to 6.2 mM heme: the P_{50} value increases from 4.7 to 32 mm Hg. The Hill coefficient is about 1.5 at all concentrations. The data were analyzed by a least squares computer program with the linkage relations of Ackers and Halvorson (Proc. Nat. Acad. Sci. USA 71:4312, 1974) to yield changes in the intersubunit contact and ligand binding free energies of the dimer and tetramer at successive oxygenation steps. These results show that a small degree of cooperativity exists in the successive steps of oxygen binding by hemoglobin Kansas. The β subunit, known to have an intrinsically low affinity for oxygen, (Riggs and Gibson, Proc. Nat. Acad. Sci. USA 70:1718, 1973), contributes a pseudo negative cooperativity to the oxygen binding by both the dimers and the tetramers. The free energy change for the tetramer dimer dissociation appears to decrease linearly with each oxygenation step, so that the dissociation constant for fully ligated hemoglobin Kansas is about 200 times greater than that for hemoglobin A. (Supported by a Robert A. Welch Foundation grant F-213 and NSF grant PCM-76-06719 to A. Riggs.)

M-AM-Po19 PROTEIN CONFORMATION AND NITRIC OXIDE BINDING TO HUMAN HEMOGLOBIN-A_0.
D. Bartnicki, and H. Mizukami, Dept. of Biol., Wayne State Univ., Detroit, Mich. 48202
Cassoly and Gibson (J. Mol. Biol., 19:301, 1975) have previously reported that the association constant for the first NO-ligand with deoxy-hemoglobin is 71 x 10^6 $M^{-1}s^{-1}$. Using stopped-flow, we have observed that a subsequent optical transition follows ligand binding. We have assigned this optical change to a conformational rearrangement of the protein within the R- or T-state. Solutions of deoxy-hemoglobin in 0.05M Bis-Tris plus 0.1M NaCl were mixed with NO-saturated buffer at 10°C in an Aminco-Morrow stopped-flow apparatus coupled to a transient recorder. Kinetic difference spectra were compiled with a minicomputer from both the UV and visible regions. The initial kinetics proceeded as a first order reaction, with $t_{1/2}$ = 25.0 ms. This reaction was followed by a slower one, dependent on the concentration of hemoglobin. The kinetic difference spectrum obtained between dead time and 100 ms does not coincide with the equilibrium difference spectrum, but resembles instead the spectrum obtained by Cassoly for the optical changes found after NO-binding to the hybrid $\alpha_2(NO)\beta_2(deoxy)$ (J. Mol. Biol., 98:581, 1975). Experiments performed in the presence of IHP at pH6.8, where nitrosylhemoglobin remains locked in the T-state, show a similar kinetic difference spectrum for the initial rapid phase. This rapid phase precedes the well characterized spectral changes that occur with IHP-bound nitrosylhemoglobin.
(This study was supported in part by the B-Haley Award, Sum.78 WSU)

M-AM-Po20 SOLUBILITY AND OXYGEN BINDING OF HEMOGLOBINS A AND S IN THE PRESENCE OF POLYETHYLENE GLYCOL,
W.A. Tisel*, R.N. Haire*, B.E. Hedlund*, A. Rosenberg and E.S. Benson, University of Minnesota, Minneapolis, MN 55455.

Polyethylene glycol (PEG, m.w. 6000) decreases the solubility of proteins primarily by volume exclusion. A linear relationship is obtained when the logarithm of protein solubility is plotted against the concentration of PEG in the supernatant. Experiments with hemoglobin (Hb) have shown that the water content of the solid phase decreases with increasing total concentrations of PEG. Furthermore, we have evidence that PEG is excluded from the solid phase while salts appear to equipartition between the two phases when the pH is near the isoelectric point of protein. PEG does not affect the oxygen binding parameters of Hb A and S in the absence of solid phase. However, at sufficiently high PEG concentrations, i.e. when the deoxygenated form of both Hbs are partially precipitated, both Hbs exhibit apparent decreased oxygen affinities. The effect is more pronounced for Hb S. The differential solubilities of the various forms of Hb A and S and their oxygen binding parameters in the presence of PEG will be discussed in terms of protein activities and the application to a potential linkage scheme between solubility and ligation. Supported by NIH Grant HL 16833 and the Minnesota Medical Fouccation.

M-AM-Po21 ASSOCIATION-DEPENDENT ABSORPTION SPECTRA OF β^{SH}(OXY) SUBUNITS OF HEMOGLOBIN.
M. L. Adams, J. S. Philo, and T. M. Schuster, Biochemistry and Biophysics Section, Biological Sciences Group, University of Connecticut, Storrs, CT. 06268.

Absorption spectra of purified human β^{SH} (oxy) subunits (0.1M TRIS, 0.1M NaCl, 1mM EDTA, pH 7.4, 10°C) reveal concentration dependent changes corresponding to a blue shift in the visible and Soret regions as the concentration is increased from 1 to 1000 μM heme. The maximum differences occur at 583, 571, 531 and 420 nm and an isosbestic point occurs at 577.3 nm, near the absorption maximum of the protein. Control measurements of human oxyhemoglobin A (0.1M HEPES, 1mM EDTA pH 7.0, 5°C) do not reveal concentration dependent spectral changes over a range of dimer/tetramer concentrations. The variation of ϵ_{583} with concentration is consistent with a monomer-tetramer equilibrium with an association constant of 1x10^{16} M^{-3}. This value is similar to that obtained by direct molecular weight measurements [Valdes & Ackers, Proc. Natl. Acad. Sci. USA 75, 311-314 (1978)]. The ϵ_{583} for the monomer is about 9% greater than that of the tetramer. These results imply that spectral changes associated with α and β subunit recombination are expected to be concentration dependent.
Supported by NIH-HL 17494 and NSF-PCM76-20041.

M-AM-Po22 KINETIC LIGHT-SCATTERING STUDIES ON LAMPREY HEMOGLOBIN. Lei-Ting Tam*, Lawrence J. Parkhurst, and Warner E. Love, Department of Chemistry, University of Nebraska, Lincoln, NE. 68588, and Biophysics Department, Johns Hopkins University, Baltimore, MD. 21218.

The kinetics of CO binding by the hemoglobin of the sea lamprey, Petromyzon marinus, have been followed in absorbance and light-scattering stopped-flow devices as well as by flash- and laser-photolysis. Lamprey hemoglobin is largely dissociated in the liganded form into monomers and is associated to dimers, and, at high concentration, tetramers in the non-liganded form. The deoxy protein is aggregated ($K_{2,1} \sim 0.5$ μM) at low pH (5.6) and largely dissociated at pH 8.8. In order to describe the kinetics of ligand-binding, a kinetic scheme was proposed (M. E. Andersen and Q. H. Gibson, J. Biol. Chem. (1971) 246, 4790) which involved the 5 forms of the protein in ligand-binding and in protein association -dissociation reactions. These latter processes occur on the same time scale as the ligand-binding reactions and rate constants for all reactions were obtained by Andersen and Gibson by fitting the extensive data obtained from the kinetic traces for absorbance changes. We have recently repeated these measurements and find good agreement with the absorbance changes. In addition, we have measured the light-scattering changes which occur following a sudden drop (pH 8.8 to 5.6) in pH and find second-order kinetics with an association rate constant ∿ one-fifth of that deduced by Andersen and Gibson from their curve-fitting operations. Other reactions associated with changes in protein aggregation show similar discrepancies and point to the utility in being able to make both light-scattering and absorbance change measurements in dissecting a complex ligand-binding mechanism.
(Grant Support: NIH HL 15284-07, NIH Biomedical Sciences Support Grant from the Research Council, University of Nebraska-Lincoln, and the Research Corporation.)

M-AM-Po23 AN ELECTRONIC INTERACTION MODEL FOR HEMOGLOBIN COOPERATIVITY: I. EVIDENCE FROM RAMAN DIFFERENCE SPECTROSCOPY. D. L. Rousseau, J. A. Shelnutt and J. M. Friedman, Bell Laboratories, Murray Hill, N. J. 07974, and S. R. Simon,* State University of New York, Stony Brook, N. Y. 11790.

Raman Difference Spectroscopy measurements were carried out on a series of chemically modified deoxyhemoglobins which could be stabilized in either the R or T quaternary structure. Frequency differences are observed in the oxidation state marker lines but not in the line sensitive to the pyrrole nitrogen-to-heme center distance. These data are consistent with extensive NMR and EXAFS data in which no changes in structure within the coordination sphere of the iron are observed. Although there is no evidence in our data for nuclear rearrangements in the porphyrin macrocycle between the two quaternary structures, the observed differences in the oxidation state marker lines indicate that the R structure has an effective increase of 0.1 electrons in the $e_g(\pi^*)$ orbital of the porphyrin rings. We interpret these data as evidence for a charge transfer interaction between the hemes and nearby aromatic residues and propose an electronic interaction model for hemoglobin function.

M-AM-Po24 AN ELECTRONIC INTERACTION MODEL FOR HEMOGLOBIN COOPERATIVITY: II. THE ELEMENTS OF THE MODEL. J. A. Shelnutt, D. L. Rousseau and J. M. Friedman, Bell Laboratories, Murray Hill, N. J. 07974, and S. R. Simon,* State University of New York, Stony Brook, N. Y. 11790.

In this new model for hemoglobin cooperativity, the R quaternary structure is stabilized by a charge transfer interaction between the porphyrin rings and aromatic residues of the globin. Through this interaction, charge from the filled π orbitals of the aromatic residues near the heme is transferred to the $e_g(\pi^*)$ orbital of the porphyrin macrocycle resulting in a stabilized complex. Since the O_2 binding has been shown to deplete the $e_g(\pi^*)$ orbital by the same amount as on oxidation, the sensitivity of this orbital to the quaternary structure provides a link between ligation and protein structure. In the model the heme aromatic complex is stabilized in the R structure with respect to the T structure and the stabilization energy of oxyhemoglobin is greater than it is in deoxyhemoglobin. The difference in stabilization energy between oxy and deoxyhemoglobin may be calculated by determining the charge density in the $e_g(\pi^*)$ orbital which may be inferred from resonance Raman data. This difference in stabilization is large enough to account for the free energy difference for binding O_2 in the two quaternary structures.

M-AM-Po25 HEME PROTEIN REACTIONS AT HIGH PRESSURE AND LOW TEMPERATURE. N. Alberding, D. Beece*, L. Eisenstein, H. Frauenfelder, D. Good*, M. Marden*, L. Reinisch*, A. H. Reynolds*, L. B. Sorensen*, and K. T. Yue*, Department of Physics, University of Illinois at Urbana-Champaign, Urbana, IL 61801.

Using flash photolysis, we have studied the dynamics of the binding of ligands such as oxygen and carbon monoxide to heme proteins over wide ranges in both temperature (40 K - 300 K) and pressure (0.1 MPa - 190 MPa). These experiments provide detailed insight into the molecular steps in heme protein reactions. At low temperatures recombination is intramolecular and controlled by a free energy barrier at the heme. In addition the binding is not exponential in time so the barrier must be described by a distribution. This distribution is most easily explained by the existence of different conformational substates of the protein, each with its own energy barrier for recombination. These conformational substates are frozen at low temperatures. However, at high temperatures, each molecule changes rapidly from one conformational substate to another (conformational relaxation) and the binding becomes exponential. Pressure applied to a set of conformational substates can have two different effects on the kinetics. (1) The kinetics of each substate can be changed by the activation volume term ($\Delta V^{\ddagger}$) for that substate. (2) The initial distribution of substates can be changed by pressure, those conformations with smaller volume being favored with increasing pressure. The two contributions can be studied and separated by measuring the kinetics as a function of the pressure and temperature. The results for oxygen and carbon monoxide binding to myoglobin will be presented. Supported in part by HEW Grant GM-18051 and NSF Grant PCM 76-81025.

M-AM-Po26 PRELIMINARY X-RAY CRYSTALLOGRAPHIC STUDY OF A ROOT EFFECT HEMOGLOBIN, J. A. Tainer, E. D. Getzoff*, J. S. Richardson, and D. C. Richardson*, Duke University Medical Center, Department of Biochemistry, Durham, North Carolina, 27710.

Since the single hemoglobin (Hb) present in the fish Spot shows extreme pH sensitivity in both CO and O_2 equilibria, Spot Hb was chosen as a prototype for investigating the Root effect. The α and β chains of Spot Hb have the same molecular weight and COOH-terminal residues as in human Hb; however, the NH_2-termini of the α-chains appear to be blocked and therefore incapable of contributing to the pH dependence of O_2 binding. Large, well-ordered crystals of CO-bound Spot Hb have been grown at a concentration of 35mg/ml from 0.01M phosphate buffer pH 7.8 containing 15% PEG 6,000. X-ray precession photographs indicate that the space group is C2:a=89Å, b=76Å, c=69Å and ß=141° with one αß dimer per asymmetric unit. As the exact molecular twofold axis is incorporated in the crystal symmetry and the approximate twofold axes are also present, we expect to phase these crystals from the known Hb structure using rotation and translation functions. Work is in progress on obtaining suitable crystals at pH 6.5 so that the three-dimensional structures of the high and low affinity forms of Spot Hb can be compared in detail and provide a model for checking current hypotheses on the basic mechanism of the Bohr effect.

M-AM-Po27 THE ASSIGNMENT OF REDUCED CYTOCHROME OXIDASE RESONANCE RAMAN BANDS TO CYTOCHROMES a and a_3. I. Salmeen and G.T. Babcock+(Intr. by L. Rimai), Ford Motor Co. Dearborn, MI 48121 (I.S.) and Michigan State University, East Lansing, MI 48824 (GTB).

Cytochromes a and a_3 are expected to contribute about equally to the 441.6 nm excitation resonance Raman spectrum of reduced cytochrome oxidase because the Soret band maxima, extinction coefficients, and band shapes for the two cytochromes are about equal. We have shown previously that bands at 215, 364, 1230, and 1670 cm^{-1} can be assigned to cytochrome a_3^{+2}. To further assign reduced oxidase Raman bands to the two heme components, we have studied heme a in detergents without added ligands, heme a-2-methyl imidazole, and heme a-bis imidazole. The two former heme complexes are high spin, the latter low spin and are models for cytochrome a and a_3 respectively as evidenced by MCD and optical absorption spectra. The Raman spectra of the high spin models show a resonance enhanced C=O vibration at 1650 cm^{-1} whereas the low spin model spectrum does not show a carbonyl vibration, thus supporting our previous assignment of the 1670 cm^{-1} reduced oxidase band to cytochrome a_3. Most of the bands in the reduced protein spectrum can be attributed to either of the two heme types, thus suggesting assignments of the protein bands to its component cytochromes. However, some protein bands between 200 and 500 cm^{-1} have no obvious counter parts in the model spectra, suggesting they may be iron-axial ligand vibrations. (+Research supported by a Cottrell grant from the Research Corp. and an MSU Biomedical Research Support Grant)

M-AM-Po28 BIOLOGICAL ELECTRON TUNNELING: ENERGY DEPENDENT RATE EFFECTS. Martha H. Redi and John J. Hopfield, Princeton University, Princeton, N.J. 08540.

An apparent discrepancy in measured photoassisted and thermal electron transfer rates for three pairs of electron transfer biomolecules is resolved. All previous estimates of electron transfer distances between biomolecules have assumed the transfer matrix element T_{ab} to be independent of the energy of the transferring electron. We have included this energy dependence. Photoassisted electron transfer elicits an infrared charge transfer absorption band which is characterized by a peak intensity proportional to the square of the tunneling matrix element and a width due to vibronic coupling. The thermal electron transfer rates predicted from infrared charge transfer absorption band measurements were found to exceed those observed by factors of 48, 43 and 318, when the electron was transferred between cytochrome c and $Fe(CN)_6$, bacteriochlorophyll and cytochrome c peroxidase. The energy dependence of the tunneling matrix element was investigated using weakly coupled square wells and the Bardeen transition current formulation of the transfer hamiltonian. The experimental rates were obtained with this simple picture in the high temperature gaussian spectral function limit. We assume that the absolute redox energy for cytochrome c is -2 eV. Otherwise the theory depends only on the experimentally determined relative redox energies, Stokes shifts and transfer band parameters. R = 10, 12, and 10Å are the edge to edge transfer distances. The width of the square well drops out of the equation for the ratio of the tunneling matrix elements and does not affect the estimate of R. Since the transfer distance may be temperature dependent, the combination of photo-assisted and thermal electron transfer experiments leads to a more accurate determination of R than possible by temperature-dependent measurements alone.

M-AM-Po29 PHOSPHORESCENCE SPECTROSCOPY OF COPPER CYTOCHROME c.
P.Glatz*, B. Chance, and J.M. Vanderkooi (Intr. by C.S. Owen), The Johnson Research Foundation Dept. of Biochem. and Biophys., Univ. of Pennsylvania, Philadelphia, Pa. 19104

The luminescence emission of a metal-substituted cytochrome (copper cytochrome c) has been studied below 80 Kelvin. The observed spectra and the microsecond time-resolved emission showed temperature-dependent characteristics, such as spectral shifts and non-exponential decay modes. By comparison with the emission data of free porphyrin derivatives (Gouterman and coworkers) we determined intramolecular rate parameters, i.e. the decay rates of the tripdoublet and the quartet level. We studied copper cytochrome c in the presence and absence of mitochondrial membranes. The significant difference of bound to free cytochrome c is explained with a model of differential energy transfer between cytochrome c and its mitochondrial binding site. The proposed model is also applied to cytochrome c in the presence of isolated (soluble) cytochrome c oxidase in freeze-trapped conditions. Upon binding of cytochrome c its tripdoublet decay time (determined at 77 K) increases from (13.2±.9) μs (unbound) to (15.4±.9) μs (bound); this result indicates an interaction but not a resonance energy transfer from Cu cytochrome c to its binding site. (Ref.: M. Gouterman, in: Excited states of matter (C.W. Shoppee, ed.), Grad. Studies, Texas Tech. Univ., 2:63-103 (1973))
Acknowledgment: This work was supported by the USPHS GM 12202. J.M.V. is supported by Career Development Award NIH GM 0053.

M-AM-Po30 RESONANCE RAMAN STUDIES OF CHROMATIUM FLAVOCYTOCHROME c_{552}. M. R. Ondrias*, G. T. Babcock, and G. E. Leroi*, Michigan State University, E. Lansing, MI 48824.

Resonance Raman spectroscopy has been shown to be a powerful tool for the elucidation of the structure and function of biological molecules, in particular those proteins which contain a heme moiety. We have used this technique to examine flavocytochrome c_{552} obtained from Chromatium vinosum, a photosynthetic purple sulfur bacterium. This cytochrome, which contains two c-type hemes and one covalently bound flavin (FAD) per molecule, has been postulated to be involved in the organism's H_2S oxidation pathway. Its multicomponent nature provides an excellent opportunity for the study of intramolecular interactions between similar (heme/heme) and dissimilar (heme/flavin) redox centers.

Resonance Raman spectra of oxidized and reduced c_{552} and its flavin-free, diheme apoprotein (prepared by treating the protein with 8M urea) have been obtained with both α-β and Soret excitation. The protein did not exhibit photoreduction; however, intrinsic flavin fluorescence with an emission maximum at 525 nm was evident. The high frequency (1000-1700 cm^{-1}) bands corresponding to in-plane macrocycle streches were strongly indicative of a low spin c-type heme in the ferrous forms of both apo- and holoprotein, differing only slightly from the high frequency regions of cytochrome c. The spectra of the oxidized protein, however, displayed a deviation from "normal" heme c behavior in both the high and low (200-800 cm^{-1}) frequency regions. Frequency shifts of 3-10 cm^{-1} were evident in both depolarized and anomalously polarized bands in the high frequency region obtained with α-β excitation. The low frequency spectra obtained with Soret excitation showed atypical polarized band intensities. The implications of such anomalous spectral behavior will be considered in the context of intramolecular interactions between the multiple redox centers of c_{552}.

M-AM-Po31 MERCURIMETHANES: ELECTRON DENSE REAGENTS FOR BIOLOGICAL STRUCTURE DETERMINATION. J.J. Lipka[1]*, H. Bazari[2]*, C. Levinthal[2], and S.J. Lippard[1], Departments of Chemistry[1] and Biological Sciences[2], Columbia University, New York, N.Y. 10027.

The polymetallic reagent tetrakis(acetoxymercuri)methane, $C(HgOAc)_4$ (TAMM), has been shown to bind to the 4-thiouridine residue of *E. coli* $tRNA^{Val}$ without forming intramolecular crosslinks (K.G. Strothkamp, J. Lehmann, and S.J. Lippard, Proc. Natl. Acad. Sci. U.S.A., 75, 1181 (1978)). We have synthesized an analogous reagent tris(acetoxymercuri)-methane, $HC(HgOAc)_3$ (TRAMM), and have studied its binding to human hemoglobin (Hb). Methods will be discussed for preparing TRAMM, solubilizing it in biological buffers, and keeping the resulting solutions stable. TRAMM has been used to label the sulfhydryl residues of Hb. Electron micrographs of Hb and the Hb·Hp (Hp = haptoglobin) complex, both labelled with TRAMM, exhibit characteristic black dots of unusually high intensity, corresponding to individual trimercurimethane units. This high contrast is due to the very high electron density of the label. Mercurimethane reagents are stable both to the high vacuum conditions and to the electron beam of commercial electron microscopes. These studies further suggest the potential utility of TAMM and TRAMM for both EM and X-ray crystallographic biological structure determinations requiring specific electron dense labels at reactive molecular sites.

M-AM-Po32 INTERACTION OF ELECTRON DONORS AND SOLUABLE CYTOCHROME OXIDASE AT INTERMEDIATE-LOW TEMPERATURES. A. Waring, E.K. Yang, and B. Chance, Johnson Research Foundation, University of Pennsylvania, Philadelphia, PA 19104.

Isolated beef heart cytochrome oxidase was solubilized using 2% cholate in 20mM phosphate buffer pH 7.4 and suspended in a solution having a final ethylene glycol concentration of 30% v/v for low temperature oxygen trapping. Oxidase was reduced with varying concentrations of reductant-mediator, ligated to CO, and the extent of reduction followed using a dual wavelength scanning spectrophotometer. The kinetics of oxidation at intermediate-low temperature (-40° to -80° C) was then initiated by flash photolysis, and monitored at appropriate wavelength pairs using a Johnson Foundation time-sharing multichannel spectrophotometer. When the kinetics were examined as a function of mediator concentration at -60° C, a rapid initial absorbance decrease at 608 nm indicative of peroxy-cytochrome oxidase (Compound B)[1] was observed which was followed by apparent re-reduction. A close correlation is found between the half time of this re-reduction and the mediator level. The initial rate of absorbance change at 655 nm which is taken as an index of a_3 redox state change also depended on the mediator concentration. At lower temperatures, the effect of mediator became less and less pronounced. These observations suggest that the flow of electrons through oxidase can in part be manipulated by temperature and relative reductant-mediator level.

1. Chance, B. et al.: These abstracts.

Supported by USPHS grants HL-17826 and GM-12202.

M-AM-Po33 CYTOCHROME c INTERACTION WITH CYTOCHROME b_2: USE OF LUMINESCENT DERIVATIVES TO DETERMINE HEME DISTANCES. J.M. Vanderkooi and G.W. Woodrow III*, Dept. of Biochem. & Biophys. Univ. of Pennsylvania, PA 19104.

Fluorescent derivatives of cytochrome c were prepared by replacing the heme iron with closed-shell metals such as zinc or tin. These derivatives bind to yeast lactate dehydrogenase (cytochrome b_2) stoichiometrically and with high affinity and are competitive with natine cytochrome c. Spectral overlap exists between the fluorescence emission of Zn (II) cytochrome c or Sn (IV) cytochrome c and the absorption of cytochrome b_2; therefore dipole-dipole interaction is possible as predicted by Forster' theory of energy transfer. The oxidized form of cytochrome b_2 is more effective in quenching the fluorescence of the metallocytochrome c derivatives than is the reduced form; this is attributed to the favorable spectral overlap of the oxidized form. Using assumptions made by Forster, the distance between the hemes of cytochrome c and cytochrome b_2 is estimated to be around 30 A. It can be argued that due to the symmetry of the metalloporphyrins, the relative orientation of the two hemes do not introduce a significant uncertainty in the calculation. The problem of energy transfer between chromphores which are large compared to the intermolecular distance will be discussed.

(Supported by NIH grant GM 12202. J.V. is supported by NIH Career Development Award· GM00059.)

M-AM-Po34 X-RAY ABSORPTION EDGE AND EXTENDED FINE STRUCTURE (EXAFS) STUDIES OF CYTOCHROME *c* OXIDASE. L. Powers, W. E. Blumberg, Y. Ching, P. Eisenberger,* *Bell Laboratories, Murray Hill, N.J. 07974,* B. Chance, C. Barlow,* J. S. Leigh, Jr.,* J. C. Smith, T. Yonetani, *Johnson Research Foundation, Univ. of Penn., Phila., Pa. 19174,* J. Brown,* T. Spiro,* *Department of Chemistry, Princeton Univ., Princeton, N.J. 08540,* J. Peisach, *Albert Einstein College of Medicine, Bronx, N.Y. 10461,* S. Vik,* *Univ. Oregon, Eugene, Or. 97403,* J. Hastings,* and M. Perlman,* *Brookhaven National Lab., Upton, N.Y. 11973.*

X-ray absorption spectroscopy has been used to study the local environment of the copper atoms and the iron in heme *a* groups of cytochrome *c* oxidase. Low temperature trapping and on-line optical assays were used to ensure the redox state of the copper and iron atoms in these highly concentrated (~1 m*M*) samples. At room temperature, x-irradiation alters the redox state but not the enzymatic activity of the reoxidized protein. These studies indicate that the copper associated with cytochrome a_3 is a Type I or "blue" copper similar to stellacyanin but not necessarily having the same ligating groups, and the copper of cytochrome *a* has an environment that is more covalent, where changes observed on reduction can be interpreted as either formal valence or ligand changes.* Major structural changes in the environment of the iron atoms is observed upon oxidation/reduction. In the reduced state in the presence of CO, both iron atoms are 6-coordinate low-spin, having an average first shell Fe-ligand distance of 1.98 Angstrom (similar to *bis*-imidazole heme). Using *bis*-imidazole heme as a model for the heme *a* of cytochrome *a*, an average distance of 2.05 Angstrom is observed for the first coordination shell of iron in cytochrome a_3 with mixed valence state prepared in the formate. These results are consistent with a μ-oxo structure of the oxidized enzyme, and these data constitute the first EXAFS measurements at concentrations of ~1 m*M*.

---

*Powers, L. *et al. Biochim. Biophys. Acta* (in press).

M-AM-Po35 REACTION MECHANISMS FOR LOW TEMPERATURE ELECTRON TRANSFER IN OXY AND PEROXI-CYTOCHROME OXIDASE (COMPOUNDS A AND B). Chance, B., Waring, A., Yang, E. The Johnson Research Foundation, University of Pennsylvania, Philadelphia, PA 19104.

The existence of heme iron and Type I stellacyanin-like copper in a near neighbor binuclear complex affords the site for a variety of unique oxygen intermediates and electron transfer reactions.[1] Current results verify and extend electron tunnelling mechanisms and indicate the role of Fe^{4+} and Fe^{5+} in peroxidase-like intermediates of cytochrome oxidase and oxygen. At -120° oxy- and at -80° peroxy-intermediates are quasi-stable and their electron transfer reactions can be studied without detectable function of cytochrome a and Cu_{a_3}.[2]

$$c^{2+} + a_3^{3+} - O\,O^{=} \; Cu_{a_3}^{2+} + 2H^{+} \rightarrow c^{3+} + H_2O + a_3^{3+} - O^{=} - Cu_{a_3}^{2+}$$

The oxidation of reduced cytochrome c is monitored at 550 nm and the appearance and disappearance of Compound B at 608 nm and the appearance of a^{3+} and $Cu_{a_3}^{3+}$ at 655 and 790 nm respectively. The reduced oxygen atom may be retained in the oxidized enzyme as a μ-oxo bridged configuration.* The reaction may involve the peroxidase compounds II and I respectively. A general equation for Compound B function may be in step-wise reduction by aromatics as well as by cytochromes c and a:

$$AH_2 + a_3^{5+} - O^{=} \leftrightarrow A + H_2O + a_3^{3+} \; Cu_{a_3}^{2+}$$

The non-adiabatic nuclear-controlled electron tunnelling over large distances may be the principal electron transfer mechanism.[3]

1. Powers, L. These abstracts. 2. Chance, B. et al: Proced. JASCO 1978 (in press).
3. Chance, B.: Biophys. J. 17 241a 1977 * Blumberg, W. and Peisach, J.; Personal Corres.
USPHS GM-12202, HL-17826, HL-05611

M-AM-Po36 ANOMALOUS X-RAY SCATTERING STUDIES FOR THE LOCATION OF REDOX CENTERS IN MEMBRANES. J. Stamatoff, P. Eisenberger,* G. Brown,* J. Pachence, L. Dutton, J. Leigh and K. Blasie. University of Pennsylvania, Philadelphia, PA, 19104, Stanford Synchrotron Rad. Lab., Stanford, CA. 94305 and Bell Telephone Labs., Murray Hill, N. J. 07974.

The effect of anomalous X-ray scattering from the metal ions associated with redox centers (Fe, Cu, etc.) on the X-ray diffraction from hydrated oriented membrane multilayers can in principle accurately determine the positions of these metal ions within the membrane protein components both in the membrane profile and in the membrane plane. These anomalous X-ray scattering effects on such diffraction would be expected to be small, on the order of a few per cent based on model calculations. However, since these effects would be small and since the phase problem can generally be solved for the diffraction independently of the anomalous scattering experiments, such small anomalous scattering effects determined to only moderate accuracy should be sufficient to determine the positions of the metal ions within the membrane structure. We have recently undertaken a study of the anomalous X-ray scattering effects from Fe on the lamellar diffraction from hydrated oriented multilayers of reconstituted lecithin/reaction center membranes and membranous cytochrome oxidase utilizing the intense tunable synchrotron radiation source at the Stanford Synchrotron Radiation Laboratory, the focused EXAFS beam line and diffractometer methods. The anomalous X-ray scattering effects observed are on the order of those expected and progress toward the determination of the distribution of Fe atoms within these membrane profile structures will be reported.

M-AM-Po37 GATING EFFECTS IN HALOBACTERIUM HALOBIUM MEMBRANE TRANSPORT. J.K. Lanyi, NASA-Ames Research Center, Moffett Field, CA 94035.

The transport of sodium via a proton/sodium antiporter and of aspartate and serine via sodium/amino acid symporters was studied in envelope vesicles. Gradients for protons were produced by illuminating the bacteriorhodopsin-containing vesicles, and the rate and extent of sodium and amino acid transport were followed as functions of the electrochemical potential difference for protons. The gradients of sodium and protons at different light-intensities were coupled to one another in the ratio 1.8:1, suggesting a translocation stoichiometry of 2 protons/sodium for the antiporter. The rate of sodium transport increased steeply with the electrochemical gradient of protons above a threshold value of - 130 to - 155 mV, but was very low below this value. Since the electrical potential and the chemical potential of protons at the threshold point varied greatly with the experimental conditions, while the sum of these potentials was approximately constant, it would appear that the gating of the sodium transport is caused by the entire electrochemical gradient of protons. Another kind of gating was observed for the amino acid transport systems of this organism. The sodium/amino acid stoichiometry was determined to be 4 and 2 for aspartate and serine, respectively at low electrical potentials, but 2 and 1 at electrical potentials more negative than - 35 mV. This finding is consistent with a previous report (Lanyi, J.K., 1978, Biochemistry, 17, 3011-3018) on the lack of correspondence between transport driven by electrical potential and by concentration difference for sodium ions. It appears from these results that the gradients of protons and sodium ions have two superimposed functions: to energize proton/sodium antiport and sodium/amino acid symport, and to modulate the properties of the transport carriers.

M-AM-Po38 ^{31}P-NUCLEAR MAGNETIC RESONANCE OF PROTON GRADIENTS IN INTACT PLATELETS. R.G. Johnson, B.D.N. Rao, and A. Scarpa, Dept. Biochem.-Biophysics, School of Med., Univ. of Pa., Phila., PA 19104, and Dept. Physics, Ind. Univ. Purdue at Indianapolis, Indianapolis, IN.

^{31}P-NMR spectra of intact platelets were obtained at 145.7 MHz. Analysis of the spectra revealed the characteristic resonances of the three phosphates of ATP. However, splitting of the γ-P and β-P peaks was observed. Given that the dense granules of the platelet, which contain a large amount of ATP, maintain an intragranular pH of 5.5 (Johnson et al., J. Biol. Chem. 253:7601, 1978), and that the γ-P and β-P resonances of ATP are pH dependent, it was proposed that this splitting originated from the existence of two pools of ATP within the platelet; one a cytosolic pool at pH 7.4, and the other an intragranular pool at pH 5.5. In order to test this hypothesis, the chemical shifts of the phosphate resonances of ATP were measured at these pH values and in various media. The results, when compared with the spectrum of intact platelets, gave a qualitative agreement, and therefore the γ-P and β-P peaks at the higher chemical shifts were assigned to the more acidic (intragranular) pH values. To further evaluate the apparent pools of ATP, reagents were added which would deplete ATP and perturb pH gradients. In the first experiment, the addition of 2-deoxyglucose and rotenone resulted in the disappearance of the peaks assigned to the cytosolic ATP without affecting the resonance peaks of the intragranular ATP, suggesting that two pools exist and that the ATP within the granules acts as if it were metabolically inert. In the second, 35 mM ammonium chloride administration produced a shift in the intragranular ATP peaks to a lower chemical shift,indicating a more alkaline intragranular pH. These results suggest that ^{31}P-NMR is an excellent non-destructive technique for the simultaneous and quantitative measurement of H^+ and ATP within the cytosol and the dense granules of platelets. (Supported by AHA-77-675 and HL-18708).

M-AM-Po39 MEASUREMENTS OF ΔpH AND $\Delta\Psi$ IN CHROMAFFIN GRANULES WITH FLUORESCENT INDICATORS. G. Salama,* R.G. Johnson, and A. Scarpa. Dept. Biochem.-Biophys., Univ. of Pa., Phila.,PA 19104.

ΔpH and $\Delta\Psi$ across the membrane of isolated bovine chromaffin granules were simultaneously and quantitatively measured using the dyes diS-$C_3(5)$ and 9-aminoacridine (9-AA), respectively. The excitation (400 nm) and emission maxima (440 nm) of 9-AA were not shifted by granules. However, the addition of granules suspended in a medium at pH 6.8 resulted in a large quenching of the fluorescence which could be reversed by the addition of large concentrations of NH_3. The internal pH was calculated from the fluorescence quenching as described by Shuldiner et al. (Eur. J. Biochem. 25:64, 1972) and found to be pH 5.5-5.8, which is consistent with values obtained through [^{14}C]methylamine distribution (Johnson and Scarpa, J. Biol. Chem 251:2189, 1976). The ΔpH could be collapsed quantitatively by NH_4Cl or K^+ and nigericin as calculated by both fluorescence and radiochemical methods. The addition of 5 mM ATP,which has been previously shown to generate a 40-60 mV transmembrane potential,positive inside (Johnson and Scarpa, J. Biol. Chem.253:7061, 1978), resulted in a decrease in the fluorescence of diS-$C_3(5)$ bound to the granules (670-690 nm). The addition of the uncoupler FCCP produced a large dose-dependent fluorescence increase corresponding to the establishment of a 60-90 mV potential (negative inside) with no detectable change in ΔpH. The diS-$C_3(5)$ fluorescence was linear with respect to positive and negative potentials as determined by two methods: a) as a function of external pH in the presence of valinomycin, e.g. the Nernst potential for K^+; b) as a function of external pH in the presence of FCCP, e.g. the Nernst potential for protons. Fluorescence changes in the supernatant were opposite to the fluorescence changes from dye bound to the granules, thus diS-$C_3(5)$ binding to the granules appears to be potential dependent. The wavelengths of the two dyes are sufficiently apart to use a double-beam spectrophotometer and a fluorometer to measure ΔpH and $\Delta\Psi$ simultaneously, quantitatively and kinetically in isolated chromaffin granules.

M-AM-Po40 DETERMINATION OF THE MITOCHONDRIAL PROTON-MOTIVE FORCE IN INTACT HEPATOCYTES. J. B. Hoek,* D. G. Nicholls,* and J. R. Williamson (Intr. by T. Ohnishi), Univ. of Pennsylvania, Philadelphia, Pa. 19104 and Dundee Univ., U.K.

The mitochondrial proton-motive force ($\Delta\bar{\mu}H^+$) in intact isolated hepatocytes was estimated from the intracellular accumulation of the lipophilic cation triphenylmethylphosphonium (TPMP) and the weak acid 5,5-dimethyloxazolidine-2,4-dione (DMO). TPMP was concentrated 150-200 fold in response to potential differences across the plasma membrane ($\Delta\Psi_{c-e}$) and the mitochondrial inner membrane ($\Delta\Psi_{m-c}$). The mitochondrial concentration factor of TPMP was estimated by two approaches: a) by comparing the distribution of [^{3}H]-TPMP with that of $^{86}Rb^+$ and Cl^-, which respond to the plasma membrane potential, b) by the determination of TPMP associated with the particulate cell fraction after selective disruption of the plasma membrane with digitonin (0.1 mg/mg d. w.) followed by rapid (2 sec) separation of soluble and particulate components. The mitochondrial accumulation of TPMP under standard conditions indicated a $\Delta\Psi_{m-c}$ of - 145-160 mV at an estimated $\Delta\Psi_{c-e}$ of -40 mV. The $\Delta\Psi_{m-c}$ was not affected by oligomycin, nigericin, or ouabain, slightly increased on incubation in a high K^+ medium, and collapsed on addition of uncoupler or valinomycin. Similar approaches were used to estimate the pH difference (ΔpH) across the mitochondrial membrane from the distribution of DMO in intact disrupted cell preparations. Disruption experiments demonstrated a relatively higher concentration of DMO in the particulate fraction, that was not released by digitonin treatment. In contrast, methylamine was concentrated in the cell, was released on treatment with digitonin (0.4 mg/mg d. w.) and was presumably accumulated largely inside lysosomes. From these experiments a ΔpH across the mitochondrial membrane in intact hepatocytes of 0.4-0.7 units is obtained, corresponding to a total proton-motive force of 180-200 mV. Supported by grants AM 19525, AM 22141 and HL 14461.

M-AM-Po41 FUNCTIONAL SEPARATION OF THE H^+-PUMPING AND ATP SYNTHETASE ACTIVITIES OF THE CHLOROPLAST CF_O-CF_1 COMPLEX. Cheryl Underwood* and J. Michael Gould, Dept. of Chemistry, Univ. of Notre Dame, Notre Dame, Indiana 46556

The rate of photosynthetic electron transport measured in the absence of ADP and P_i is stimulated by low levels of Hg^{++} (1 Hg^{++}/40 chlorophyll) or Ag^+ (1 Ag^+/20 chlorophyll) to a plateau equal to the electron transport rate obtained under normal, phosphorylating conditions (i.e. +ADP, +P_i). This stimulation of basal electron transport by Hg^{++} and Ag^+ is reversed by the CF_1 inhibitor phlorizin, by the CF_O inhibitor triphenyltin chloride, and can be further stimulated by uncouplers such as methylamine. The Hg^{++} stimulation, but not the Ag^+ stimulation, is completely reversed by below substrate levels of ADP (2 μM), ATP (2 μM) and P_i (400 μM). Variations in the pH of the medium affect both Hg^{++} and Ag^+ stimulation of basal electron transport in the same manner as the ADP + P_i stimulation of basal electron transport, with the maximum stimulation in each case at pH 8.2-8.5. Concomitant with the stimulation of electron transport by Hg^{++}, Ag^+ or ADP + P_i, there is a decrease in the magnitude of the transmembrane pH gradient (Δ pH), which can be effectively reversed by triphenyltin chloride. Results similar to those described above for Hg^{++} are also obtained with chloroplasts in which the γ-subunit of CF_1 has been modified in situ with N-ethylmaleimide (NEM). These results suggest that modification of CF_1 SH residues by Hg^{++}, Ag^+ or NEM leads to the loss of intra-enzyme coupling between the ATP synthesis and the transmembrane H^+-transferring activities of the CF_O-CF_1 complex. The modified enzyme can apparently turnover normally, at least in its H^+ transferring function, despite the absence of substrates for the ATP synthesis reaction. Supported by USDA Grant A-FY79-4-10.

M-AM-Po42 MEASUREMENT OF FREE Ca^{2+} AND Mg^{2+} CONCENTRATIONS IN HEPATOCYTES AND MITOCHONDRIA. J. R. Williamson, B. E. Corkey* and E. Murphy*, Univ. of Pennsylvania, Philadelphia, Pa. 19104.

A new approach has been developed which makes feasible measurements of free Ca^{2+} and Mg^{2+} in separate cytosolic and mitochondrial spaces of isolated cells. Free Ca^{2+} in solution is measured spectrophotometrically using the metallochromic indicators Arsenazo III (675-685 nm) for Ca^{2+} below 60 μM, and Antipyrylazo III (720-790 nm) for higher Ca^{2+} (see Scarpa et al, Biochemistry 17:1378, 1978). Free Mg^{2+} is measured in the presence of Ca^{2+} chelators using Antipyrylazo (620-655 nm). The dye indicators measure cations in the cell incubation medium. The plasma membrane of isolated hepatocytes is made permeable to ions (but not to enzymes) by addition of low concentrations of digitonin (0.01 mg/mg cell protein). Cells are incubated in the presence of known Mg^{2+} and Ca^{2+} concentrations in the medium and the initial rate of cation uptake or release from the cells is measured after addition of digitonin. For Ca^{2+} measurements, ruthenium red (30 μM) is included to prevent mitochondrial Ca^{2+} uptake, and low Ca^{2+} concentrations are achieved with Ca^{2+} buffers. The null point corresponding to zero cation flux is calculated from plots of flux versus external free cation concentrations. The cytosolic cation concentration is assumed equal to the external free Ca^{2+} or Mg^{2+} concentrations at the null point. Mitochondrial free cation concentrations are determined with similar null point measurements after addition of the divalent cation ionophore A-23187 to digitonin treated cells or isolated mitochondria. Preliminary data indicate values of approximately 0.7 mM and 0.3 mM for free Mg^{2+} in mitochondria and cytosol, respectively. Corresponding values for free cytosolic Ca^{2+} are in the range 0.2 - 1.0 μM while free mitochondrial Ca^{2+} is in the range of 60 - 100 μM for normal rat hepatocytes. Further studies with alterations of membrane potential and ΔpH are in progress to substantiate this approach. Supported by grants AM 15120 and AM 19525.

M-AM-Po43 THE PROPERTIES OF VDAC-A CHANNEL IN THE OUTER MITOCHONDRIAL MEMBRANE. E. Lynch,* M. Colombini, Albert Einstein Coll. of Med., Bronx, N.Y. 10461.

A voltage dependent anion-selective channel (VDAC) has been incorporated into planar lipid bilayer membranes. VDAC's characteristic properties include a distinct channel size, anion selectivity and a steep change in its conductance with voltage. VDAC's properties are independent of the source of the mitochondria, whether fungal, protozoan or mammalian. Each single VDAC channel displays a variety of conductance states. For example, the channel from rat liver mitochondria conducts at 1000, 400, 200, and 45pS in 0.1 M $CaCl_2$. The highest conducting state (the open state) occurs at low transmembrane voltages while at higher voltages, in both positive and negative directions, lower conducting states (closed states) become occupied. This voltage dependent transition occurs between 10 and 30mV transmembrane potential. The large pore, which VDAC produces in the membrane, allows the passage of ions such as succinate, fumarate, citrate and the $(Ca\text{-}EDTA)^{--}$ complex. The anion selectivity is most dramatic when divalent ions are compared: Ca^{++} is very poorly permeable while the 100X more massive $(Ca\text{-}EDTA)^{--}$ complex is much more permeable. VDAC's large size and its location in the outer mitochondrial membrane makes it a good candidate for the pathway that allows this membrane to be permeable to small molecules. The voltage dependence of VDAC raises the possibility that cells may activate or shut down mitochondria by controlling VDAC's gate thus controlling the access of substrates to the inner membrane.

M-AM-Po44 OSMOTIC SWELLING AND CONTRACTION OF POTATO MITOCHONDRIA - ABSENCE OF MONOVALENT CATION/H^+ EXCHANGE ACTIVITY. D. W. Jung* and G. P. Brierley. Dept. Physiol. Chem., Ohio State Univ., Columbus, Ohio 43210.

Non-energized mitochondria from most mammalian sources swell spontaneously in isotonic acetate salts and upon addition of tripropyltin (TPT) in chloride or an uncoupler in nitrate media. This swelling appears to depend on an endogenous cation/H^+ exchanger (C^+/H^+) with a selectivity of $Na^+ > Li^+ > K^+ \approx 0$ and optimum activity at pH 7.3. Well coupled potato mitochondria (PoM) do not swell passively in Na^+, Li^+ or K^+ salts under any of these conditions and it appears that C^+/H^+ may be missing or inactive in PoM. However, respiring PoM swell spontaneously in Na^+ and K^+ acetate and in chloride salts following addition of TPT. Swelling in respiring mitochondria appears to depend on electrophoretic cation uptake via a uniport pathway (see Brierley et al. Arch. Biochem. Biophys. 190: 181-192, 1978), and therefore the uniport seems to be present in PoM. Respiration-dependent contraction of beef heart mitochondria appears to depend on C^+/H^+ (Brierley et al. J. Biol. Chem. 252: 7932-7939, 1977). PoM swollen passively in hypotonic (50 mM) chloride salts contract when respiration is initiated with NADH. The rate, extent and efficiency of contraction in PoM is poor relative to the reaction in heart mitochondria. Contraction in PoM is sensitive to uncouplers, but differs from that in heart mitochondria in that it shows little cation specificity, little pH dependency, and no respiratory control upon completion of contraction. These studies suggest that in the absence of C^+/H^+, the weak contraction may depend on extrusion of anions (in response to the interior negative potential) with secondary efflux of accumulated cations via the uniport. Supported in part by USPHS Grant HL 09364.

M-AM-Po45 EFFECT OF IN VITRO AGING ON ENERGY-LINKED PROPERTIES OF LIVER MITOCHONDRIA. C. Cunningham*, J. Parce*, and P. Spach* (Intr. by M. Waite), Wake Forest Univ., Winston-Salem, N. C. 27103

In a previous study [Parce et al., Biochemistry 17, 1634 (1978)] changes in mitochondrial phospholipid metabolism and energy-linked functions were monitored as coupled mitochondria were aged in isotonic sucrose at 18°C. The sequence of events that occur in mitochondrial aging under the above conditions have been established more completely. Decline in respiratory control, which occurs early during the aging process, is due primarily to a loss in state 3 respiration. State 3 respiration is also more sensitive to temperature perturbation than is state 4 respiration. The observation that loss in state 3 respiration is accompanied by lowered ADP and ATP translocation suggests that the sensitivity of state 3 respiration to in vitro perturbation is related to the stability of the adenine nucleotide translocation system. Mitochondrial ATPase activity does not increase significantly until state 4 respiration has increased appreciably. At the time of loss in respiratory control the ATPase activity then increases to levels equal to uncoupler stimulated activity. The H^+/O ratio and P/O ratios do not decrease appreciably until respiratory control is lost. Likewise, permeability of the membrane to proton back diffusion increases only after respiratory control is lost. These observations reinforce our earlier conclusion that there are two main phases in mitochondrial aging. The first phase is characterized by a loss of adenine nucleotide translocation capability. The second is characterized by a decline in the ability of the mitochondrion to conserve energy (maintain a respiration driven proton gradient) and to synthesize ATP. (Research support: NIAAA AA02887 and NIH AM11799)

M-AM-Po46 INHIBITION OF K^+ FLUX INTO RAT LIVER MITOCHONDRIA BY DICYCLOHEXYLCARBODIIMIDE. Lynn Gauthier* (Intr. by W. H. Johnson), Biology Dept., Rensselaer Polytechnic Institute, Troy, New York 12181.

The oxidative phosphorylation inhibitor, dicyclohexylcarbodiimide (DCCD) binds to a subunit of the mitochondrial ATP synthase which is involved in proton translocation (Glaser et al., in Packer et al., eds., Bioenergetics of Membranes, 1977, p. 513). The effect of DCCD on ^{42}K flux into rat liver mitochondria has been examined under conditions of approximately steady-state K^+ content in the presence of the respiratory substrate, succinate. DCCD, at a concentration (40 nmoles/mg. prot.) sufficient to block stimulation of respiration by ADP plus P_i, decreases the rate of unidirectional K^+ influx. In contrast, oligomycin (0.5 μg/mg. prot) does not affect K^+ influx. The dependence of the reciprocal of the initial rate of K^+ influx from a pH 7.5 medium on the reciprocal of the external K^+ concentration (K^+ range 0.75-14 mM) remains linear in the presence of DCCD. The apparent K_m for K^+ is increased from 7.2 ± 2.8 mM for control samples to 15.4 ± 5.0 in the presence of DCCD (average values from 10 expts. ± standard deviations). The V_{max} of K^+ influx remains approximately constant at 3.3 ± 1.0 and 3.1 ± 1.1 μmoles/g. prot./min. in the absence and presence of DCCD. Thus DCCD appears to decrease the affinity of the transport mechanism for K^+. At constant external K^+ concentration (2-3 mM), DCCD consistently decreases the stimulation of K^+ influx with increasing external pH, over the range from pH 6.8 to 8.0, both in the presence and absence of the P_i/OH^- exchange inhibitor, N-ethyl maleimide. These results agree with the conclusion that the mechanism of K^+ transport in mitochondria is closely associated with the mechanism of energy transduction. A direct coupling of K^+ and OH^- (or H^+) fluxes via an energy-linked mechanism has been postulated previously (Diwan & Lehrer, Membrane Biochem. 1:43,1978). Supported by NIGMS Grant Gm-20726.

M-AM-Po47 RESOLUTION OF THE DICYCLOHEXYL-CARBODIIMIDE BINDING PROTEOLIPID FROM BOVINE HEART MITOCHONDRIA. G. A. Blondin, University of Wisconsin, Madison, Wisconsin 53706.

The dicyclohexyl-carbodiimide (DCCD) binding proteolipid which is extractable from beef heart mitochondrial inner membrane with chloroform: methanol (2:1) has been resolved into two hydrophobic protein components (HPα and HPβ) by preparative reverse phase high pressure liquid chromatography on octadecylsilane treated microparticulate silica. Polyacrylamide gel electrophoresis of purified HPα and HPβ in sodium dodecyl sulfate-urea suggests molecular weights in the range of 9000 and 7000 daltons respectively, which is in agreement with the amino acid analyses of the individual purified components. HPα and HPβ bind added inorganic phosphate (100 to 200 nmoles per mg protein) and ADP (60 to 120 nmoles per mg protein) when the former are in solution in organic solvents. Moreover, this activity is lost in both components when they are isolated from membrane preparations previously labelled with DCCD; and, the binding of ADP by HPβ is stoichiometrically inhibited by the presence of atractyloside in the assay medium. These findings are in sharp contrast to the protonophoric activity of the DCCD binding proteolipid described by others (Criddle, R. S., Packer, L., and Shieh, P., (1977) Proc. Natl. Acad. Sci. USA, 84, 278-282), and suggests a more direct role for these components in the mechanism of oxidative phosphorylation.

M-AM-Po48 LOW LEVEL CHEMILUMINESCENCE IN HYDROPEROXIDE-SUPPLEMENTED MITOCHONDRIAL MEMBRANES. A. Boveris, R. Reiter*, E. Cadenas* and B. Chance. Johnson Research Foundation, University of Pennsylvania, Philadelphia, PA 19104.

Submitochondrial particles from beef heart in the presence of substrate, hydroperoxides and oxygen show low level chemiluminescence (Seliger, Photochem.Photobiol.4:1199 (1975) with emission of 1.2-2.5 x 10^3 photons/sec per mg of protein. NADH was more effective (50%) than succinate as substrate and antimycin (Boveris & Chance, BJ: 134: 707 (1973) had an enhancing effect (35%). tert-Butyl, ethyl and cumene hydroperoxides were effective in the range 0.5-10 mM, with half-maximal effect at about 2 mM. Oxygen profiles were biphasic (Km values = 30 and 500 uM O_2). Superoxide dismutase was an effective inhibitor of chemiluminescence (maximal inhibition: 65%); moreover, it acted as competitive inhibitor respect of hydroperoxide for chemiluminescence. Catalase was much less effective. Different singlet oxygen quenchers such as β-carotene and dimethylfuran partially inhibited chemiluminescence. Other active inhibitors were azide, α-tocopherol and cyanide which also produced incomplete inhibition. DABCO and dimethylpiperazine, which enhance singlet oxygen dimol emission (Deneke & Krinsky, Photochem.Photobiol.: 25,299 (1977), increased the chemiluminescence of hydroperoxide-supplemented submitochondrial particles. The observed results are interpreted on the basis of a multiplicity of chemiluminescent reactions. Singlet oxygen appears to be generated as a consequence of the reaction between hydroperoxide and superoxide anion (Peters & Foote, JACS, 98: 873 (1976); it could be produced either (a) as a product of such reaction or (b) from the condensation (Howard & Ingold, JACS, 90: 1056 (1968) of ROO· generated through a lipid peroxidation process initiated by RO· or HO·.

Supported by USPHS-HL-15061.

M-AM-Po49 THEORY OF HYDROGEN BONDED CHAINS IN BIOENERGETICS. J.F. Nagle, M. Mille and H.J. Morowitz, Department of physics and Biological Sciences, Carnegie-Mellon University, Pittsburgh, PA 15213 and Department of Molecular Biophysics and Biochemistry, Yale University, New Haven, Conn. 06520.

The thesis that proton conduction across membranes is a central ingredient in bioenergetics is indicated by many experiments and from the emerging preeminence of the chemiosmotic hypothesis. Based on mechanisms of proton transport in low molecular weight crystals we have previously postulated a continuous chain of hydrogen bonds from protein side groups as the fundamental structure in proton conduction across membranes. In this presentation we show how such a structure can conduct protons against a chemical potential gradient of hydrogen ions. The kinetic equations for the motion of an excess proton injected onto a hydrogen bonded chain are set up and solved. The local free energy of the excess proton can be converted rapidly (10^{-3} - 10^{-6} sec) on a biological time scale into electrochemical or mechanical energy. Utilizing this result we construct a complete cycle for a molecular engine fueled by a proton injector such as ATPase. In the following paper this result is used to discuss possible mechanisms for the bacteriorhodopsin proton pump in Halobacterium halobium.

M-AM-Po50 RATE CONSTANTS FOR THE BINDING OF POTENTIAL-SENSITIVE PROBES TO MEMBRANES: IMPLICATIONS FOR FAST SPECTRAL PROBE RESPONSES. J. C. Smith, S. J. Frank*, and B. Chance (Intro. by P. Mueller), Johnson Research Foundation, Univ. of Penna. School of Medicine, Philadelphia

Dyes of the cyanine, merocyanine, and oxonol classes are able to respond by spectral changes to potential gradient formation across black membranes and those of excitable tissues with a half time of ∿10 μsec. A mechanism by which these rapid changes occur has been proposed by Waggoner, et al (J. Membrane Biol. 33, 109 (1977)) and involves the association/dissociation of the probe with the membrane from the volume of the bathing dye solution adjacent to the bilayer surface. The second order rate constants for the binding of the dyes oxonol V, oxonol VI, and diS-C_5-5 to soybean lipid vesicles or submitochondrial particles (SMP) have been obtained under pseudo first order conditions with the dye in excess. Values for the rate constants fall within the range (2-9) x $10^6 M^{-1}$ sec^{-1}. For a 10 μsec. half time, the effective dye concentration corresponding to these values can be calculated from

$$k_{app} = \ln 2/t_{\frac{1}{2}} = k_2 X_D \quad (1)$$

where k_{app} is the apparent first order rate constant, $t_{\frac{1}{2}}$ the half time, and X_D the reactant in excess, the dye in this case. The concentrations obtained from eq (1) fall in the range 7 - 35 mM, which greatly exceeds the bulk dye concentrations commonly used in membrane work. The mechanism described above is compatible with these results only on the assumption that a high local dye concentration exists near the membrane surface. Formation of such high concentrations may be possible by a diffusion polarization process dependent on dc bias or resting potentials in bilayer or excitable membranes, but in SMP or chromatophores where such potentials are unlikely to be present, the mechanism above is unlikely to be applicable nor are microsecond probe signals observed in such systems. This work was supported by U. S. P.H.S. grants NINCDS NS-10939, HL-18708, and HL-17826.

M-AM-Po51 INTERPRETATION OF THE SATURATION TRANSFER IN THE ^{31}P NMR SPECTRUM OF THE HUMAN RED BLOOD CELL. Raj K. Gupta, The Institute for Cancer Research, Philadelphia, PA 19111

Saturation of the βP resonance of intracellular ATP with radiofrequency energy in the NMR spectrum of oxygenated human red blood cells results in ∿10% decrease in the amplitude of the γP resonance (Gupta, R.K. (1978) Fed. Proc., Fed. Am. Soc. Exp. Biol. 37, 1713). This intracellular transfer of saturation was ascribed to an exchange of the β and γ phosphoryl groups via the adenylate kinase mechanism (ATPβ* + AMP ↔ ADPβ* + ADP ↔ AMP + ATPγ*) since reversible nucleotidyl and pyrophosphoryl transfers are negligible in red cells. A saturated ^{31}P nucleus starting at the β position of ATP has equal probability of ending up in the β or γ position after 2 cycles of the adenylate kinase reaction. In support of this interpretation, in vitro experiments with purified rabbit muscle adenylate kinase reveal a sizable intramolecular transfer of saturation from the βP to the γP of ATP and vice versa. In the NMR spectrum of a solution containing 12 mM ATP, 2 mM ADP, ∿0.2 mM AMP, 12 mM Mg^{2+} and 10,000 units/ml of adenylate kinase, radiofrequency saturation of the βP resonance of ATP results in (47 ± 3%) decrease in the amplitude of the γP resonance at 24°C and 40.5 MHz. In a reverse experiment, saturation of the γP resonance of ATP resulted in (56 ± 3%) decrease in the amplitude of the βP resonance. The somewhat greater transfer of saturation from the γP to the βP compared to the βP → γP saturation transfer effect may arise from an unavoidable direct radiofrequency saturation of the βP resonance of ADP which happens to be located in the vicinity of the γP resonance of ATP. These in vitro experiments with purified adenylate kinase reaffirm our hypothesis that the observed βP → γP saturation transfer effect in the human red cell arises from the reversible phosphorylation of AMP in the red cell via the adenylate kinase mechanism. (Supported by NIH Grants AM-19454, AM-13351 and USPHS RCDA AM-00231).

M-AM-Po52 THE CIRCULAR DICHROISM OF BACTERIAL CYTOCHROMES, M.A. Cusanovich and J.A. Watkins*, Department of Biochemistry, University of Arizona, Tucson, Arizona 85721

Although considerable progress has been made in recent years concerning the mechanism of electron transfer by c-type cytochromes, a number of important questions remain, including the origin of biological redox potentials. To address this problem we have been investigating the circular dichroism (CD) spectra of a variety of bacterial cytochromes with particular emphasis on the transitions in the 250-350 nm region. Our primary emphasis has been on the bacterial cyto. c_2 as they have a wide range of redox potentials (300-390 mV). Further, the structure of one example, Rsp. rubrum cyto. c_2, is known and the amino acid sequence of nine other examples of this class of cyto. have been reported. It is known from the structure of Rsp. rubrum cyto. c_2 that the bulk of aromatic amino acid in the protein are in close proximity to the heme and likely interacting to yield an induced asymetry. Further, cyto. c_2 from different sources has either the lack of or addition of aromatic groups at a number of sequence positions. With the above in mind, we have made a detailed study of the near-UV CD of several examples of cyto. c_2 acquiring the CD spectra for both the oxidized and reduced states. This data has been analyzed by a fitting procedure designed to yield the minimum number of Guassian curves required to describe each spectra. Based on the data analysis and the amino acid sequences of the cytochromes investigated, assuming structural homology to Rsp. rubrum cyto. c_2, the various transitions have been assigned. Finally, from the individual transitions and their rotational strength, correlations between the CD spectra and the measured oxidation-reduction potentials and the kinetics of reduction by potassium ferrocyanide have been investigated. Supported by research grants from the NSF (PCM 75-21009) and NIH (GM 21277).

M-AM-Po53 THE ROLE OF CHLORIDE ION IN PHOTOSYSTEM II. Patrick M. Kelley and S. Izawa (Intr. by Philip D. Morse II), Wayne State Univ., Detroit, Mich. 48202

Cl^- is known to be required for the evolution of O_2 in photosynthesis, but the mechanism of this cofactor action of Cl^- remains to be elucidated. Recently we found that the Mn-containing, O_2 evolving center of chloroplasts is more resistant to inactivation by NH_2OH in the presence of Cl^- than in its absence (Kelley and Izawa, BBA 502, 198, 1978). This indicates a direct relation between the Mn-containing water-splitting center and the function of Cl^-. We have extended this line of investigation and obtained the following results. (1) Heat-inactivation of the center is also markedly retarded by the presence of Cl^-, and to a lesser extent by Br^-, which is a slightly less efficient cofactor of O_2 evolution than Cl^-. Acetate, which is a totally inactive anion as a cofactor of O_2 evolution, had no effect. (2) Tris-inactivation of the O_2 evolving center, which is known to be reversible, is also abated by the pres- of Cl^-. Furthermore, the rapid inactivation in the absence of Cl^- leads to an irreversible destruction of the center. (3) In contrast, the inactivation of the O_2 evolving mechanism by low pH (4.3) or high pH (9.6) is independent of the presence or absence of Cl^-, which suggests that the site of pH inactivation may be different from the site(s) of inactivation by Cl^- removal, NH_2OH or Tris treatment.

Ion analysis of well-washed, highly Cl^--dependent chloroplasts by neutron activation (performed by J. Barber and H. Y. Nakatani of Imperial College) indicated that these chloroplasts were indeed deficient in Cl^- (2 Cl^-'s per reaction center as opposed to the 10-20 Cl^-'s per center in briefly washed chloroplasts that show little Cl^- dependence).

M-AM-Po54 DIVERSION OF OXIDIZING CHARGES ACCUMULATED IN PHOTOSYSTEM II OF CHLOROPLASTS. S. M. Theg,* R.T. Sayre,* and P.H. Homann, Inst. of Molecular Biophysics, Florida State Univ., Tallahassee, Fl. 32306.

Accumulated oxidizing charges in photosystem II of chloroplasts are assumed to be located in a Mn-enzyme and mediate the oxidation of water to molecular oxygen. Occasionally they are diverted into other reactions. Such diversion results in the direct oxidation of electron donors other than water. A special type of diversion is induced in the presence of certain anionic agents like CCCP which, under aerobic conditions, involves the consumption of oxygen with an associated oxidative destruction of carotenoids. In contrast to the general belief that the enzyme-associated Mn is EPR-silent, recent studies in Malkin's (Arch. Biochem. Biophys. 179 174-182, 1977) and Gribova's (Biofizika 22 651-655, 1977) laboratories have assigned light-induced changes of an asymmetric EPR signal to reactions of the Mn-enzyme in the water oxidizing reaction-complex. In repeating these EPR-studies, we have confirmed the presence of an asymmetric Mn-signal in chloroplasts which was reversibly lowered in the light. However, the signal disappeared when EDTA was added, and the change was not abolished by CCCP which is expected to efficiently remove oxidizing charges from photosystem II. Instead, CCCP accelerated the recovery of the signal in the dark. We interpret these findings with the well known light dependent oxidation by photosystem II of Mn non-functional in photosynthetic oxygen evolution. At least some of it appears to be bound to the thylakoid, and to take part in the CCCP mediated photodestructive reactions which we shall show to represent oxygen dependent, presumably radical propagated oxidations of components of membrane and suspension medium. (Supported by grant # PCM 76-16975 from NSF.)

M-AM-Po55 INVESTIGATION OF PRIMARY ACCEPTORS OF PHOTOSYSTEM II BY FLUORESCENCE. J.M. Bowes+*, A.R. Crofts+*, A. Joliot++*, P. Joliot++* and K.J. Kaufmann+* (Intr. by G. Weber), +Depts. of Physiology and Biophysics, and Chemistry, University of Illinois, Urbana, Illinois 61801; ++Institute de Biologie Physico-Chimique, Paris 75005, France.

Several reports have suggested that during a 5 μs flash, photosystem II undergoes a double hit, implying that some centers are associated with two acceptors--Q1,Q2. Important differences exist between these reports with respect to (a) postulated quenching properties; (b) redox potential of the second acceptor; (c) series or parallel reaction, and (d) stoichiometry of Q2. We have reexamined these effects and attempted to measure the turnover time of the double hit. The fluorescence yield of dark-adapted chloroplasts preincubated for 10 m with no additions, or with either ferricyanide or hydroxylamine and then inhibited by DCMU, was sampled with a weak detecting flash at 350 μs after a laser flash of duration 8 ps, 30 ns, or 1 μs. Under all the above experimental conditions, all flashes showed saturation, but the maximal change in fluorescence yield induced by the 8 ps flash was ~70% of that induced by the 1 μs flash. The low efficiency of the ps flash compared to that of the μs flash could be interpreted either as showing a double hit in the μs flash, or annihilation in the ps flash, or both. The slow reduction of P^+ in the presence of hydroxylamine makes a double hit seem unlikely and for this reason we favour an explanation in terms of annhilation under these conditions. Models of photosystem II compatible with these results will be discussed.

M-AM-Po56 INVESTIGATION OF SIGNAL II IN GREEN PLANT SYSTEMS. Brian J. Hales and Anupam Das Gupta, Department of Chemistry, Louisiana State University, Baton Rouge, Louisiana 70803.

The effects of pH and solvent deuteration on the esr spectrum of signal II in chloroplasts from spinach and collard greens have been investigated. Results from these studies as well as those reported earlier on model systems strongly suggests that signal II is due to a plastosemiquinone radical ionically bonded to a nonparamagnetic cation at the quinone oxygen ortho to the isoprenoid chain. Computer simulation of a radical in such an environment closely resembles that of signal II. The cation presumably stabilizes the plastosemiquinone possibly in the aprotic environment of the chloroplast inner membrane. Furthermore, an esr study of oriented chloroplast membranes can be interpreted in terms of the normal to the quinone plane making an angle of ca. 35° to the plane of the membrane. Signal II in these oriented systems not only shows a strong saturation dependency previously unobserved in powder samples but also the presence of additional fine structure in chloroplasts from collard greens.

M-AM-Po57 ELECTRON SPIN RESONANCE STUDIES OF PLASTOCYANIN IN SPINACH CHLOROPLASTS. J. R. Norris, K. W. Kinnally and J. T. Warden, Biochemistry Program, Dept. of Chemistry, Rensselaer Polytechnic Institute, Troy, N.Y. 12181 and Argonne National Laboratory, Argonne, IL 60439.

The copper-containing protein, plastocyanin, has been characterized both *in vitro* and *in vivo* by cryogenic electron spin resonance combined with potentiometric analysis. The midpoint potential (Em_8) for this Photosystem 1 electron carrier has been determined to be +370±10mV (n = 1). Quantitation against a standard *in vitro* plastocyanin sample suggests that each Photosystem 1 electron transport complex is associated with two plastocyanins. Electron spin echo envelope modulation spectra of isolated plastocyanin are consistent with the participation of more than one histidines in copper ligation at the active site. (Supported by U. S. D. A., Petroleum Research Corporation and BES of DOE)

M-AM-Po58 IS ELECTRON TRANSPORT IN PHOTOSYNTHESIS SWITCHED BY ATP LEVEL? A.B. Rubin* and Don DeVault. Lomonosov State University, Moscow, USSR, and University of Illinois, Urbana, Illinois 61801.

Cytochrome oxidation and reduction in whole cells of the photosynthetic bacterium *Chromatium* is altered by addition of the uncoupler m-chlorocarbonyl cyanide phenylhydrazone (CCCP) in several ways: Under anaerobic, dark-adapted conditions in which one normally observes photooxidation of the low-potential cytochrome C-553, the pulsed laser-induced oxidation is slowed from t 1/2 = 1μs to t 1/2 = 2μs; the amplitude of cytochrome oxidation by strong, steady illumination is reduced to 1/4 and in both cases the re-reduction was speeded many fold (from 10 or more seconds to tens of milliseconds). (The latter effect confirms earlier observations by Morita, Edwards & Gibson, BBA, 109 (1965), 45). The spectra of the cytochromes oxidized in the presence of CCCP corresponded to that of the high-potential cytochrome, C-555, especially in the case of steady illumination. CCCP also abolished the light-induced oxidation of cytochrome at liquid nitrogen temperature. These observations are consistent with an interpretation that CCCP causes the cytochrome photooxidized to switch from C-553 to C-555. It is suggested that in general when the level of ATP is low C-555 is the electron donor to the reaction center thereby activating the cyclic electron transport system in order to phosphorylate ADP, and that when the ATP level is high (via glycolytic system when dark and coupled) C-553 becomes the donor to take electrons from substrate and shove them to the CO_2 reducing system. A mechanism for the switching could be a redox equilibration between C-553 and the low-potential side of the energy transduction site in the cyclic system, the high-potential side being equilibrated to a redox potential sufficiently constant at the level of the midpoint potential of C-555 that the variations of phosphorylation potential will control the dark redox state of C-553. (Ref.: BBA 501 (1978) 440)

M-AM-Po59 SPIN LATTICE RELAXATION OF P700 REACTION-CENTER CHLOROPHYLL. Keith A. Rose and Alan Bearden. Donner Lab, University of Calif., Berkeley, Calif. 94720

A pulsed saturation EPR system has been developed capable of directly observing electron spin relaxation of weak but easily saturated EPR signals. A boxcar integrator is used to resolve spin relaxation over a time base of 100 microseconds to 5 milliseconds with a minimum time response of 10 microseconds. The cavity magnetic field is modulated at frequencies below 200 Hz, which avoids rapid passage effects in the sample. The system has demonstrated excellent relaxation signals from organic samples containing as few as 10^{16} spins. T_1, the spin-lattice relaxation time, has been determined for the oxidized P 700 reaction-center chlorophyll in spinach. The effects of temperature, chemical redox potential, and membrane fragmentation upon relaxation have been measured. Over the temperature region of 20 K to 80 K the relaxation time for P 700 exhibits a 1/T dependence indicating a direct lattice relaxation process. The commonly used oxidant ferricyanide forms a free radical species in D 144 chloroplast fragments with a T_1 five times shorter than that observed in D 144 control. This may indicate the presence of a radical species other than P 700. The mild reductant ascorbate has not demonstrated any effect on relaxation by this technique. Fragmentation of chloroplast membranes with the detergent digitonin to create D 144 PS I particles increases T_1 relative to P 700 in whole chloroplasts by approximately 50%. Incubation of the D 144 particles with plastocyanin restores P 700 relaxation to the value found in whole chloroplasts. As well as elucidating the mechanism of primary photochemistry in photosynthesis, this pulsed saturation technique has the sensitivity and time resolution necessary to examine relaxation of electron radicals in many other organic systems.

Supported by NSF Grant No. PCM76-02968 and DOE funds through Lawrence Berkeley Lab.

M-AM-Po60 TIME RESOLVED ELECTRON SPIN ECHO SPECTROSCOPY APPLIED TO PHOTOSYNTHESIS.† Marion C. Thurnauer and James R. Norris, Chemistry Division, Argonne National Laboratory, Argonne, Illinois 60439.

Time resolved magnetic resonance techniques provide a convenient probe of the primary photosynthetic reactions, particularly in systems which cannot be studied by optical techniques. Previous time resolved epr studies on these systems have been limited by lack of adequate time resolution, possible spectral distortions due to the use of field modulation, and an inability to positively identify the observed radical species. We are approaching the problem using time resolved electron spin echo spectroscopy. Our time resolution is superior (∿20 nsec), and we can fingerprint the observed radicals by their characteristic modulation patterns. We have observed signals showing CIDEP in several photosynthetic systems. In *S. lividus* ^{1}H, the rise time for P^+_{700} is 50 nsec, and the decay time of the polarization is ∿260 nsec. Two distinct spin polarized signals are observed in *S. lividus* ^{2}H. By comparing the results in the ^{1}H and ^{2}H systems we are probing the mechanism of CIDEP and hence the mechanism of primary photosynthesis.

†This work was performed under the auspices of the Division of Basic Energy Sciences of the Department of Energy.

M-AM-Po61 ELECTRON SPIN POLARIZATION IN PHOTOSYNTHESIS. O. Adrianowycz,* K. W. Kinnally and J. T. Warden, Biochemistry Program, Dept. of Chemistry, Rensselaer Polytechnic Institute, Troy, NY 12181.

Electron spin polarization (Chemically Induced Dynamic Electron Polarization) in photosynthetic reaction centers has been probed in the 0.2-10μs time domain by laser flash-photolysis electron spin resonance in the direct detection mode. Electron spin polarized components have been detected in spinach chloroplasts, Scenedesmus obliquus, Photosystem 1 subchloroplast preparations and reaction-center preparations from Rps. sphaeroides (R-26). The principal emissive feature in all systems arises from the reaction-center chlorophyll dimer (P_{700} or P_{870}), and exhibits a linewidth and g-factor indistinguishable from those of the "relaxed" cation. Spin lattice relaxation times (T1) for the cation chlorophyll dimer are estimated to be 200-300ns at 300K. In chloroplasts the lineshape and linewidth of the emissive Signal 1 is independent of the orientation of the chloroplast with respect to the external magnetic field. Orientation dependences similar to those reported by Dismukes et. al. (Biophys. J. 21, 239 (1978)) appear when conventional field-modulation detection techniques are utilized.

(Supported by the Research Corporation, American Cancer Society and the U. S. Department of Agriculture)

M-AM-Po62 EQUILIBRIUM AND KINETIC MEASUREMENTS OF THE pH DEPENDENCE OF THE REDOX POTENTIAL OF CYTOCHROMES c_2. C. Lindsay Bashford and Roger C. Prince*, Johnson Research Foundation, University of Pennsylvania, Philadelphia, PA 19104.

In vivo, cytochromes c_2 are usually tightly bound to the reaction center and show only a slightly pH dependent E_m in the range pH 5-11 (Prince and Dutton, BBA 459, 573). In contrast, Pettigrew *et al* (BBA 503, 509) have demonstrated that the equilibrium E_m *in vitro* has a strong pH dependence in alkaline solutions, ascribed to a pK on the ferricytochromes in the range pH 7.2-9.4. However, as with cytochromes *c* (Brandt *et al*, JBC 241, 4180, Davis *et al* JBC 249, 2624) this pH dependency may be due to a combination of a pK near pH 11, coupled with conformational changes, the altered form(s) of the cytochrome being responsible for the low E_m at equilibrium. When neutral ferricytochrome is mixed with alkaline $K_4Fe(CN)_6$ so that the final pH is 10, the ferricytochrome is rapidly reduced, and then slowly oxidized as the conformational change proceeds. We have titrated the E_m of the cytochrome at the time of mixing and 5 min later. With *Rps. sphaeroides* c_2 both values were 340 mV when the final pH was 7, but were 330 mV and 260 mV respectively when the final pH was 10. The kinetics of the transition are similar ($t_{\frac{1}{2}}$ 2-20 s) for a wide range of cytochromes *c* and c_2. The complexity of the alkaline transition (Kihara *et al*, BBA 430, 225) suggests that it may be premature to assign the equilibrium pKs to specific groups in the heme cleft. It is conceivable that the same group is responsible for the pK at pH ~11 in all cases, but that subtle differences in overall structure modify the rates of conformational change in the different species, and thereby yield the variety of apparent pK values in the pH 7-9 range at equilibrium.

Supported by NIH GM 12202 and NSF GB 14209.

M-AM-Po63 CYTOCHROME C_2-REACTION CENTRE COUPLING IN CHROMATOPHORES AND CELLS OF RHODOPSEUDOMONAS SPHAEROIDES Ga. J.R. Bowyer* and A.R. Crofts* (Intr. by W. Sleator), Department of Physiology and Biophysics, University of Illinois, Urbana, Illinois 61801.

Chromatophores prepared by French cell breakage contained one cytochrome c_2 haem per reaction centre (RC). In chromatophores in the presence of 5-n-undecyl-6-hydroxy-4,7-dioxobenzothiazole (UHDBT) and antimycin A (AA), ~70% of the cyt c_2 was oxidised within 5 ms of a single saturating light flash, and ~70% of the oxidised RCs were rereduced. The kinetics of RC rereduction and cyt c_2 oxidation matched well over the time range 50 μs-10 ms provided the level of redox mediators was low. In the presence of AA alone, 50% of the cyt c_2 was oxidised within 5 ms of a single flash, but 85% of the reaction centre was rereduced. The kinetics of RC rereduction and cyt c_2 oxidation did not match over this same time range. Redox titrations of the extent of cyt c_2 oxidation following a single excitation in the presence of AA alone and with AA plus UHDBT indicated that in the absence of UHDBT, a component J (E_m 7.0 -270 mV, n=1) rereduced part of the cyt c_2 in an AA insensitive fashion, enabling more extensive RC reduction. This cyt c_2 rereduction is responsible for the difference in apparent E_m for the first and second flash oxidisable cyt c_2 in comparison to the total kinetically viable cyt c_2 in the absence of UHDBT. J may be the Rieske FeS centre. Essentially similar results were obtained in Rps. capsulata except that <70% of the cyt c_2 was rapidly oxidised after a single flash in the presence of UHDBT and the slow phase of cyt c_2 oxidation was considerably slower. In cells of Rps. sphaeroides Ga, the kinetically viable cyt c_2:RC ratio was also about one. These results are in contrast to those of Dutton et al. [Biochim. Biophys. Acta (1975) 387, 536-556]. The stoichiometry of J:cyt b_{50}:cyt c_2:RC measured after eight saturating excitations of chromatophores in the presence of AA appeared to be 0.3-0.5: 0.3-0.5:1.0:1.0, assuming equal $\Delta\varepsilon_{red-ox}$ for cyt b_{50} and cyt c_2.

M-AM-Po64 REACTION CENTER $(BChl)_2^+$ INDUCED pK SHIFTS ON THE AGENTS RESPONSIBLE FOR PROTON BINDING AND RELEASE IN *Rps. sphaeroides* MEMBRANES. P. Leslie Dutton, Katie Petty, and J. Barry Jackson, Johnson Research Foundation and Department of Biochemistry and Biophysics, University of Pennsylvania, Philadelphia, PA 19104.

In *Rhodopseudomonas sphaeroides* two protons are incorporated into the chromatophore per light activated reaction center. One of the protons (H_I^+) is incorporated in a similar time ($t_{\frac{1}{2}}$ 50-400 μs; pH dependent) as the primary quinone of the reaction center reduces the secondary quinone to yield Q·H. The apparent pK of Q·H/Q^- is 8.5. The release of H_I^+ can occur in milliseconds in the interior of the chromatophore as cytochrome b_{50} is reduced; this is governed by the pK at 7.5 on the ferrocytochrome b_{50} (Petty and Dutton, ABB 172, 346, 1976). The agent (unidentified) which is responsible for the binding ($t_{\frac{1}{2}}$ 0.2-2 ms) of a second, and antimycin sensitive proton (H_{II}^+) has a pK at 7.5. However, when $(BChl)_2^+$ is present these pK values are altered: H_I^+ moves to pH 7.5; ferrocytochrome b_{50} becomes <pH 5 and H_{II}^+ also becomes <pH 5. Addition of ionophores has no effect on H_I^+ and cytochromes b_{50} but returns the pK of H_{II}^+ back to the value in the absence of $(BChl)_2^+$. In the former cases there may be a problem of accessibility of the ionophore in collapsing electric fields between the acid-base groups and the reaction center $(BChl)_2^+$. It is tentatively concluded that the charge on the $(BChl)_2^+$ within the dielectric influences the H^+ binding/release properties at the membrane-aqueous interfaces. A consequence of the pK shift on cytochrome b_{50}, where an equilibrium E_m and pK are known, is that in the presence of $(BChl)_2^+$ its operating E_m could be >150 mV. In functional terms these results demonstrate the possibility that biological electron transfer pathways in one protein complex may be steered by interactions from key components in another. Supported by NIH GM 12202 and NSF GB 14209.

M-AM-Po65 LIGHT-INDUCED QUENCHING OF ATEBRIN FLUORESCENCE IN UNIT-MEMBRANE VESICLES FROM GREEN BACTERIA. J. M. Olson and Z. Gromet-Elhanan*, Biology Department, Brookhaven National Laboratory, Upton, NY 11973 and Biochemistry Department, Weizmann Institute of Science, Rehovot, Israel.

Unit-membrane vesicles (Complex I, [Bchl a] ≈3 μM) from Chlorobium limicola f. thiosulfatophilum (Tassajara) mixed with atebrin (5 μM), $MgCl_2$ (3.8 mM), and KCl (75 mM)were irradiated with weak blue light (436 nm), and the atebrin fluorescence monitored at 500 nm. Strong actinic illumination ($\lambda > 555$ nm) provided by a 500-watt projection lamp in combination with a Corning 3-67 cut-off filter induced a ~50% quenching of fluorescence in the presence of PMS (50 μM) and ascorbate (2.5 mM). With valinomycin (1.5 μM) also present 70% quenching was observed. Nigericin (25 μg/ml) and CCCP (7.5 μM) inhibited the quenching 97% and 94% respectively. These results indicate that green bacterial membrane vesicles interact with atebrin so as to quench its fluorescence when the membrane is energized by light. A similar quenching of atebrin fluorescence has been shown to reflect the light-induced proton gradient coupled to photosynthetic electron transport in Rhodospirillum rubrum chromatophores [Z.G.-E. (1971) FEBS Lett. 13: 124-126; Z.G.-E. and M. Leiser (1973) Arch. Biochem. Biophys. 159: 583-589.] In green bacteria the inhibition of atebrin fluorescence quenching by CCCP or nigericin (+KCl), and its stimulation by valinomycin (+KCl) suggest that the energized state in these organisms is also associated with a light-induced proton gradient. (Supported by U. S. Department of Energy.)

M-AM-Po66 MAGNETIC PROPERTIES OF ELECTRON TRANSPORT COFACTORS IN PHOTOSYNTHETIC MEMBRANES OF RHODOPSUEDOMONAS VIRIDIS. C. Dismukes,* Department of Chemistry, Princeton University, Princeton, N.J. 08540; H. Frank, R. Friesner, and K. Sauer, Department of Chemistry and Lawrence Berkeley Laboratory, University of California, Berkeley, CA. 94720.

Different EPR signals are associated with the reduction of the two quinones in the ferroquinone complex in whole cells of R. Viridis. Both signals have g=1.82 but differ in linewidths. Under non-reducing conditions a linewidth of 230G is observed, which increases to 420G upon reduction with dithionite. These results suggest the following identities of the narrow and broad signals: $Q_AFeQ_B^-$ and $Q_A^-FeQ_B^=$, respectively. The similarity in g values indicates that the oxidation state of Fe is not changed upon reduction, and that the electron spin exchange interaction between the Fe and the quinones is roughly equal. When the cells are aligned, both signals display a marked dependence on the orientation of the EPR magnetic field. This dependence is similar for both signals and arises from the existence of a preferred orientation of the ferroquinone complex in the internal membranes. The origin of the linewidth differences and the orientation dependence will be discussed in terms of the interactions between the Fe and the quinones and the organization of the complex in the membranes.

Illumination in the presence of dithionite reduces the intermediary electron carrier, I, which can be trapped by cooling. The EPR spectrum of I^- appears as a split doublet centered at an effective g value greater than that expected for an isolated organic anion radical. The intensity and linewidths of the doublet show a marked dependence on the orientation of the membranes. These properties are predicted from a spin hamiltonian involving predominantly a weak isotropic exchange interaction between an organic radical, like bacteriopheophytin anion, and $Q_A^-FeQ_B^=$. The orientation dependence arises in part from the anisotropy of the ferroquinone complex and from dipolar or anisotropic exchange coupling with I^-.

M-AM-Po67 REACTION CENTRES IN HEXANE. M. Kendall-Tobias and A.R. Crofts*, Department of Physiology and Biophysics, University of Illinois, Urbana, Illinois 61801.

Reaction centres isolated from the R26 mutant of Rhodopseudomonas sphaeroides have been extracted into hexane by mixing a suspension of lipid and detergent solubilized reaction centres with hexane in the presence of divalent cations. The extraction was dependent on the presence of negatively charged phospholipids and cations. Phosphatidylserine and divalent cations (the order of effectiveness being Cd^{++}, Ba^{++}, Sr^{++}, Ca^{++}) gave the highest yields of about 80%. No detergent could be detected in the hexane phase of the preparation as measured by NMR or by colourimetric methods. The properties of the hexane preparation were not affected by prolonged storage over sodium metal, and no water could be detected in the sodium dried preparations by NMR or IR spectroscopy. Lipid was present in the hexane extract to about 100 mg/mg of protein. The reaction centres had the same absorption spectrum in hexane as in 0.1% LDAO solution. The photoactive bacteriochlorophyll dimer (P870) could be oxidised by tetrachlorobenzoquinone (0.1 mM) or by iodine and reduced by tetrachlorobenzoquinol, 5 hydroxy-1,6-Naphoquinol and DAD; of these, reduced diaminodurene (DAD) was the most effective (1 μM). The flash-induced difference spectrum over the range 400-620 nm was similar to that of detergent solubilized reaction centres. The bleaching at 601 nm produced by multiple flashes was increased by the addition of ubiquinone 10 (0.4 mM, RC 0.1 μM) or more efficiently by Duroquinone (0.2 mM, RC 0.1 μM).

M-AM-Po68 CYTOCHROME *c* INTERACTIONS WITH REACTION CENTER-LECITHIN VESICLES. J.M. Pachence, C.C. Moser*, J.K. Blasie, and P.L. Dutton, University of Pennsylvania, Phila., PA 19104.

Functional and structural details of membranous reaction center protein from *Rps. sphaeroides* can be systematically investigated by detergent isolation and subsequent reincorporation into a model membrane of known constituents. A technique to remove the detergent in the presence of lecithin was developed in order to prepare RC-lecithin membranes. Binding and trapping of mammalian cytochrome *c* have established that these membranes are vesicular. Furthermore, kinetic studies of the oxidation-reduction reaction between externally added cytochrome *c* and the photo-induced $(BChl)_2^+$ of the RC indicate that the vesicles are unilamellar, since cytochrome *c* added externally to RC-lecithin vesicles reduces up to 90% of the photo-induced $(BChl)_2^+$; this would also indicate that the RC incorporates into the membrane in an asymmetric manner. Binding of cytochrome *c* to RC-lecithin membranes was investigated using centrifugation to form multilayers at different ionic strength, pH, and lipid/protein ratios. An apparent binding constant of $\sim$ 1 μM was measured when the buffer consisted of 10 mM Tris-HCl at pH 8 for all lipid/protein ratios studied; the dissocation constant increased with ionic strength, with the highest K_d measured being $\sim$ 23 μM for 10 mM Tris-HCl and 100 mM KCl at pH 8. When the lipid/protein ratio was 100 or less, there appears to be three binding sites available; at a lipid/protein ratio of 200, there appears to be two. Cytochrome *c* binding studies with lecithin alone showed no significant binding, indicating that tight binding of cytochrome *c* is associated with the reaction center itself. Furthermore, in the multilayers of lecithin, RC, and cytochrome *c*, it is clear that cytochrome *c* is positioned so that it is kinetically coupled to the reaction center. Parallel binding and kinetic studies with cytochrome c_2 are being done. Supported by NSF GB 14209.

M-AM-Po69 A MODEL FOR THE AGGREGATION STATE OF CHLOROPHYLL a IN A MULTILAYER ARRAYS. C. Chapados*, D. Germain* and R.M. Leblanc, Université du Québec à Trois-Rivières, Trois-Rivières, Qué., Canada G9A 5H7.

The nature of the interaction between the chlorophyll a molecules in a mono- and multilayers obtained by the Langmuir-Blodgett technique is examined by electronic and infrared spectroscopies. The ketone bands in the infrared spectra showed a different aggregation state in single monolayer compared to the one present in multilayers. Following the deposition of the multilayers, a blue shift is observed in the electronic spectra. This effect is monitored by infrared spectroscopy. The intensity of the coordinated ketone band is decreased while the intensity of the free ketone band is increased. These modifications are explained by reorganization of the chlorophyll a molecules from an organized to a less organized one. The influence of H_2O, D_2O and SO_2 vapors on the chlorophyll a multilayers gave some information on the role of water molecules in the aggregation of chlorophyll a in this ordered system. From these observations, a model is proposed for the multilayer arrangement implying two molecules of water per molecule of chlorophyll a.

M-AM-Po70 ULTRASTRUCTURAL ASSOCIATIONS BETWEEN STATIONARY MITOCHONDRIA, ROUGH ER AND CORTICAL MEMBRANES IN TETRAHYMENA PYRIFORMIS. L.A. Hufnagel* (Intr. by K. Hartman), University of Rhode Island, Kingston, R.I. 02881.

Mitochondria of the ciliated protozoa fall into two classes: those which freely circulate in the fluid cytoplasm and those which are stationary and closely associated with the cell surface. During a thin section analysis of Tetrahymena pyriformis, strain GL-C, structural associations between the stationary mitochondria and cortical membranes, were examined. In Tetrahymena, the cell membrane rests upon a system of flattened cisternae, the alveoli, which, in turn, intimately contact a thin, fibrous layer, the epiplasm. Immediately subjacent to the epiplasm, an extensive system of rough ER cisternae occurs. Stationary mitochondria are closely associated with rough ER or epiplasm. Fibrous connectives, about 20 nm long, attach the mitochondria to the epiplasm or the rough ER. The rough ER is also attached to the epiplasm, via fibrous linkers about 20-30 mm in length. Ribosomes are present on surfaces of the ER cisternae which face toward the mitochondria and on surfaces directed toward the epiplasm. The close association of the rough ER system with stationary mitochondria and epiplasm may be related to transfer of nascent proteins to the mitochondria, epiplasm and alveolar membranes. An intriguing question is how constituents are added to the cell membrane, since the alveoli provide an almost continuous barrier to such transfer. Freeze-fracture studies on a related species, Tetrahymena thermophila (strain Mpr^+/mpr; 6 mp sens, IV) suggest that growth of the cell membrane may occur through vesicular intermediates transferred from outer alveolar membrane to plasma membrane.